8-2004

Molecular Dynamics Simulation of Aqueous Electrolytes Behavior in Nanochannels

Lingchen Liao
University of Tennessee - Knoxville

To the Graduate Council:

I am submitting herewith a thesis written by Lingchen Liao entitled "Molecular Dynamics Simulation of Aqueous Electrolytes Behavior in Nanochannels." I have examined the final electronic copy of this thesis for form and content and recommend that it be accepted in partial fulfillment of the requirements for the degree of Master of Science, with a major in Chemical Engineering.

Hank D. Cochran, Major Professor

We have read this thesis and recommend its acceptance:

Shengting Cui, David Keffer, Mary Leitnaker

Accepted for the Council:
Dixie L. Thompson

Vice Provost and Dean of the Graduate School

(Original signatures are on file with official student records.)

To the Graduate Council:

I am submitting herewith a thesis written by Lingchen Liao entitled "Molecular Dynamics Simulation of Aqueous Electrolytes Behavior in Nanochannels". I have examined the final electronic copy of thesis for form and content and recommend that it be accepted in partial fulfillment of the requirement for the degree of Master of Science, with a major in Chemical Engineering.

Hank D. Cochran

_____

Major Professor

We have read this thesis and
recommended its acceptance:

Shengting Cui

_____

David Keffer

_____

Mary Leitnaker

_____

Accepted for the Council:

Anne Mayhew

_____

Vice Chancellor and Dean of Graduate Studies

(Original signatures are on file with official student records.)

Molecular Dynamics Simulation of Aqueous Electrolytes Behavior in Nanochannels

A Thesis

Presented for

The Master of Science Degree

The University of Tennessee, Knoxville

Lingchen Liao

August 2004

DEDICATION

This dissertation is dedicated to my mother and father, Mrs. Junqing Gao and Mr. Yaohan Liao, and my grandmother and late grandfather, Mrs. Xingtao Zhu and Mr. Yuanshen Liao, who encouraged me to pursue a career in Chemical Engineering.

ACKNOWLEDGEMENTS

I acknowledge support from U.S. National Science Foundation through a Nanoscience Exploratory Research Initiative Grant, from the Division of Chemical Sciences, Geosciences, and Biosciences of the U.S. Department of Energy, and from Oak Ridge National Laboratory through a Laboratory-Directed Research project.

I would like to express my sincere gratitude to my advisor, Dr. Hank D. Cochran for his encouragement and guidance throughout my graduate program. His cheerful nature and analytical insights not only helped me attain my academic success, but also enabled me to develop as an independent person which should benefit me in the future. I feel indebted to Dr. Shengting Cui for his invaluable guidance during my research work. Dr. Cui was kind enough to share his time explaining the previously written software program and provided an immense source of inspiration. I am very thankful to Chunggi Baig, Jiandong Zhou, and Ke An for their helpful suggestions too.

Also, great thanks to Dr. David Keffer, who taught me classes of Che 505 and Che 548 and Dr. Mary Leitnaker, who advised me in class Stat 566, where I have applied the statistical method (JMP software) to this research. I would like to thank them for their assistance as committee members.

ABSTRACT

This thesis discusses the molecular dynamics simulation to determine the density distribution and diffusion coefficient of aqueous electrolytes ($CaCl_2$, NaF, NaCl, NaBr, NaI, KCl, CsCl, RbCl) within silica nanochannels at 298K. An atomistic wall model, charged Lennard-Jones models for the ions, and the SPC/E model for water have been used. The effect of different channel radius and wall charges on divalent $CaCl_2$ electrolytes solutions is discussed in comparison with the previously studied behavior of monovalent NaCl solutions. The comparison of (NaF, NaCl, NaBr, NaI) aqueous solutions in 1.0 nm nanochannel reveals the effects of different anion sizes. Likewise, the comparison of (KCl, NaCl, CsCl, RbCl) aqueous solutions shows the effects of different cation sizes. The effects of ions size were seen to be small compared with the effects of doubling the cation charge. The calculations demonstrate that charges on the wall surface exert an influence on the density distribution of water molecules and calcium ions. Divalent calcium ions also display a different diffusion characteristic from the Fickian behavior of the monovalent cations, in which the mean square displacement of calcium ions is proportional to the square root of time rather than to the first power of time.

Table of Contents

List of Tables

List of Figures

1. Introduction and Background

1.1 Introduction

DNA sequencing has been probed over the past decades. Achieving this goal has required around 30 years of efforts, following the initial "Plus and Minus" method introduced by Sanger[1], the approach depending on specific chemical degradation of the DNA proposed by Maxam and Gilbert[2], and other methods using DNA polymerase with chain-determining inhibitors[3], etc. Neither of these methods is completely accurate nor very efficient in sequencing DNA. Among all of these, the most efficient method can sequence ~30,000 bases per day per instrument, which costs ~$0.50 per nucleotide for a finished sequence[4]. For example, the functional analysis of each mammalian genome, which is the same size as the human genome, costs approximately $300 million[5] to sequence using the standard Sanger sequencing method[1]. So, although DNA sequencing has important medical applications, the present methods of sequencing polynucleotides are too slow, costly, inaccurate, and unrealistic[6]. The demand for faster and cheaper technology is responsible for spurring development of novel, fast, and inexpensive methods aimed at analysis of single macromolecules.

At present, the use of a new nanopore method to characterize DNA could potentially determine the base sequence in a single-stranded DNA (ssDNA) molecule at rates between 1,000 and 10,000 per second. The characteristic that the scale of the nanopore may be the same as the molecules of interest is the reason why nanochannels have been explored as the basis for ssDNA sequencing and analysis. For instance, the diameter of

ssDNA is approximately 1.3 nm, while the diameter of a nanoscale channel may be varied from 1.5 ~ 3.0 nm. When ssDNA passes through such a nanochannel, it must be straightened from its coiled native state and must enter and exit the nanochannel in a linear fashion. This serial progression of the molecules makes the nanoscale channel very attractive for fast ssDNA sequencing[5].

In principle, through electrophoresis, an electric field can cause individual DNA molecules to move through a single nanopore (~2 nm in diameter) on a microsecond or millisecond timescale, while each nucleic acid base generates a distinctive electrical signal as it enters and passes through the nanochannel. Because the channel is very narrow, when ssDNA molecules are drawn into the pore by electrophoresis, they pass through the nanochannel in a linear fashion. By recording the translocation, duration, and blockade current (magnitude of the reduced ionic flow through the pore), it may be possible to monitor the polynucleotide passage and sequence DNA.

Several efforts have been under the way to bring such a nanoscale channel to DNA application. Kasianowicz *et al*.[7] studied ssDNA passing through single ion channels in biological membranes. The discovery was that the single purine or pyrimidine nucleotide passing through the nanochannel would block the ion current in a manner that reflected the molecular size and chemical properties of each nucleotide in a polynucleotide chain. This demonstrated a possibility to partially characterize the DNA molecule by measuring the variation of electrical current and translation speed.

Similarly, Nakane, Akeson, and Marzili[5] have done much experimental work with nanopore detection of DNA in using an α-haemolysin (alpha-HL) ion-channel with a ~2 nm diameter pore, which allowed the translocation of ssDNA. By tracking and analyzing the induced ion current in the pore when individual DNA molecules with electrical charges are driven through the channel, properties of DNA molecules would be indicated including length and base compositions.

Another nanopore approach under development is to sculpt artificial, synthetic pores with nanometer-scale dimensions based on a microfabricated device. In 2001, Li *et al.*[8] fabricated a molecular-scale hole, or nanoscale hole in a thin insulating solid-state membrane. The authors called the method "ion-beam sculpting". They sculpted a single 5 nm diameter nanopore in a Si_3N_4 membrane, which served as a robust electronic detector capable of monitoring single DNA molecules in aqueous solution. Also, in 2002, Saleh and Sohn[9] used a micromolding technique to embed a nanoscale pore to sense single DNA molecules electronically.

However, further development of these strategies is impeded by several technological barriers. One is that these ionic measurement methods are not completely capable of achieving single-nucleotide resolution. New remedies have been proposed by coupling nanochannel technologies with other detection schemes such as electrical dipole measurement[10], and near-field spectroscopy[11].

Another problem arises from the pore structure itself. Transmembrane protein pores, which are composed of proteins embedded in a lipid bilayer, are intrinsically unstable. The instability of biological pores restricts the optimization of the experimental conditions and limits the standardization of testing techniques. With synthetic organic pores, there are also difficulties in creating an efficient pore or array of pores to stabilize for a long period of time. Nanoscopic channels manufactured from more robust material such as silica might circumvent this problem.

Further, the lack of molecular level information is also troublesome when DNA in ionic solution passes through a nanochannel. How and to what extent different nucleic acids block the aperture of pores and affect the electrical current are unknown, and methods to monitor the translocation rate need to be implemented.

1.2 Background

With growing emphasis on nanoscale science and technology, there have been more studies in nanoscale channels. Such devices may have very important potential applications in the separation of biological molecules such as ssDNA. There has been some prior work related to our interest. Marti and Gordillo[12] studied temperature effects on the static and dynamic properties of water inside carbon nanotubes. Brodka and Zerda[13] published the properties of acetone in silica nanopores. Nakane *et al*.[5] had analyzed the alpha-HL ion channel and its applications to single-molecule detection.

However, little attention has been paid to water and ions inside nanochannels, especially nanochannels made from silica. Lo *et al.*[14] simulated ions in a charged capillary, using a softly repulsive Lennard-Jones (L-J) interaction for the ion-wall interaction. Lynden-Bell and Rasaiah[15] investigated the mobility and solvation of ions in smooth nanochannels.

For DNA sequencing, it is important to understand the properties of DNA and proteins and the selective adsorption of metal ions in aqueous environment inside the nanochannel. Because of the nanometer size of the channel, the wall surface exerts forces upon all the liquid molecules inside the channel. The interfacial region may extend totally across the nanochannel, which may result in an obvious difference from bulk aqueous electrolytes, and this has not been entirely understood yet. To this end the molecular dynamics simulation with aqueous electrolytes in silica nanochannels has been undertaken.

In this regard, two years ago, Zhou [16] did a series of runs on (Na^+ and Cl^-) in silica nanochannels with radius ranging from 0.67nm to 1.5nm. In his research, he studied the effect of cutoff radius, r_c, on density distribution of water and ions and decided to select $5\sigma_{oo}$ (five times the oxygen-oxygen contact distance in the water model) for use in his production calculations, after taking into account the required calculation time and simulation accuracy. He also investigated the influence of a charged wall versus an uncharged wall on the fluid's density distribution. Thereafter, the effects were studied of nanochannel radius and wall charges on the radial density distribution and axial self-

diffusivities of water and ions. The wall charges were evenly distributed along the axial direction and around the circumference of the nanochannel. It was found that the discrete charges of the wall exerted little influence on the distribution of water and negative ions, while the strong adsorption of sodium ions was observed. This is because every sodium ion only has one positive unit charge so sodium ions were tightly adsorbed to the charge sites to neutralize the wall charges. The adsorbed sodium ions retarded the movement of water molecules and chloride ions and lowered self-diffusivities of unadsorbed sodium ions.

This research has continued the investigation of the properties of water with ions inside charged silica nanoscale channels. The effect of wall charges on the behavior of ions and water molecules has also been studied since ions are used to buffer and disentangle DNA, and a charged channel wall probably enables ssDNA to move electrokinetically through the channel. The effects of nanochannel radius ranging from 0.9 nm to 1.5 nm with a charged wall upon the radial density distribution and axial self-diffusivities of water molecules and additional ions beside NaCl ions have been studied. Every calcium ion has two positive unit charges, which gives rise to different density distributions and self-diffusivities from those of sodium ions as Zhou[17] found. To delve further into the mechanism of the (Ca^{2+} and Cl^{-}) aqueous electrolytes, the preliminary examination of spatial configurations among oxygen atoms, calcium ions and wall charges has been performed. In this work, the negative charges are located at the center of wall atoms. This center placement of wall charges differs from the arbitrary placement of charges relative to the wall atoms used in the previous work by Zhou[16, 17] and is likely a more realistic

wall model. In addition, a series of runs of monovalent cations and chloride [(Na^+ and Cl^-), (K^+ and Cl^-), (Rb^+ and Cl^-), (Cs^+ and Cl^-)] at fixed nanochannel radius have been performed and compared. Similarly and concurrently, simulations were performed of sodium and monovalent anions with [(Na^+ and F^-), (Na^+ and Cl^-), (Na^+ and Br^-), (Na^+ and I^-)] at fixed nanochannel radius.

2. Simulation Models and Methods

2.1 SPC/E water potential model

Many effective pair potentials have been used for the simulation of polar liquid water, such as the SPC (simple point charge) and the SPC/E (extend simple point charge) nonploarizable water models. The SPC/E model stems from the SPC model, but produces better agreement with experiment[18]. Water is treated as three point charges on the H-O-H atomic centers with L-J interactions between the oxygen atoms.[18] The model accounts for the effect of the polarizability of the water molecule at ambient conditions in an approximate way by reparameterizing the charges and non-bonded L-J interactions[19].

The SPC/E model has been extensively used in molecular simulation of transport properties of charged or uncharged solutes in water in the past few years[20]. The model is composed of 3 interaction sites with the OH bond distance of 0.1 nm and HOH angle equal to the tetrahedral angle, 109.47°. The charges on the oxygen and hydrogen are –0.8476e and +0.4238e (electronic charge units), respectively. The total potential between water molecules includes the Columbic potential between these charges and an L-J potential between the oxygen centers on different water molecules. The intermolecular interaction between a pair of water molecules is:

$$u_{pair} = 4\varepsilon_{oo}[(\frac{\sigma_{oo}}{r_{oo}})^{12} - (\frac{\sigma_{oo}}{r_{oo}})^{6}] + \frac{1}{4\pi\varepsilon_0}\sum_{i=1}^{3}\sum_{j=1}^{3}\frac{q_i q_j e^2}{r_{ij}}$$

The first term is the L-J potential energy of interaction between the oxygen sites, where the L-J core diameter $\sigma_{oo} = 0.3166\,nm$ and well depth $\varepsilon_{oo}/k_B = 78.168\,K$; r_{oo} is the oxygen-oxygen separation distance; and k_B is the Boltzmann constant. The second term is the sum of electrostatic potential energies of interaction between charges on sites i and j on different water molecules, where q_i is the charge on site i , q_j is the charge on site j, and r_{ij} is the distance between the sites i and j[19]. ε_0 is the dielectric constant of vacuum, and e is the unit charge.

2.2 S_iO_2 wall potential model

Because silica (SiO_2) is important geologically and technologically, a number of silica potential models have been suggested. There are several important models such as the two-body potential model developed by Tsuneyuki *et al.*[21], the BMH pair potential model proposed by Feuston and Garofalini[22], and the BKS model starting from *ab inito* calculations on small clusters[23]. However, a united-atom L-J model for the SiO_2 surface with σ = 0.3 nm and ε/k_B = 230K with discretely charged (-1e) sites has been applied in this research to approximate the effect of the silica surface on the liquids in contact with the wall. In this model, a single layer of close-packed L-J sites, each representing a SiO_2 unit, has been wrapped into a cylinder[17]. For the charged wall, the charges were first evenly distributed along the axial direction and around the radius of the nanochannel, then were moved to the center of the wall atoms nearest the charges.

The interactions between the particles and the wall were modeled as explicit atoms for the first layer in the wall interacting with the fluid molecules via the 12-6 L-J potential. The additional layers of the wall interact with the fluid particles via the Steele Potential[24] The first atomistic layer used in the wall model instead of the smooth wall is mainly to eliminate the effect of the smooth wall of the cylindrical symmetry leading to unrealistic structure for the fluid[25], which is not a concern in this research.

The Steele potential[24] is used to model the potential between particles and additional wall layers (the "particles" here referred to are the anions, cations, or solvent molecules), which is given by:

$$u_{wf}(r) = 2\pi\rho_w\varepsilon_{wf}\sigma_{wf}^2\Delta[\frac{2}{5}(\frac{\sigma_{wf}}{R-r})^{10} - (\frac{\sigma_{wf}}{R-r})^4 - (\frac{\sigma_{wf}^4}{3\Delta(R-r+0.61\Delta)^3})]$$

in which u_{wf} is the shifted L-J type wall potential[26]. σ_w and ε_w are the size and energy parameters in the L-J potential, where $\varepsilon_w / k_B = 230K$, and $\sigma_w = 3.0\,\mathring{A}$. The subscripts f and w present fluid and wall respectively. σ_{wf} and ε_{wf} are obtained in terms of Lorentz-Berthelot[27] combing rules as:

$$\sigma_{fluid-wall} = (\sigma_{fluid} + \sigma_{wall})/2$$

$$\varepsilon_{fluid-wall} / k_B = \sqrt{(\frac{\varepsilon_{fluid}}{k_B}) * (\frac{\varepsilon_{wall}}{k_B})}$$

Δ, the distance between two successive lattice planes of the solids, $= 0.2709\,nm$. R is the radius of the cylinder, and r is the radial position of a fluid molecule. ρ_w=42.76 nm^{-3} and k_B = 1.38066*10^{-16} erg/K.

2.3 Method

The molecular dynamics simulation numerically solves Hamilton's equation of motion for each particle:

$$\overline{v_i} = \frac{\partial H}{\partial \overline{p_i}} = \frac{\overline{\dot{p}_i}}{m_i}$$

$$\overline{\dot{p}_i} = -\frac{\partial H}{\partial \overline{r_i}} = \overline{F_i}$$

Where H = Hamiltonian;

$\overline{F_i}$ = force on molecule i;

$\overline{\dot{p}_i}$ = molecular momentum;

m_i = the mass of molecule;

$\overline{r_i}$ = molecule position;

U = total potential energy of molecule i

$\overline{v_i}$ = velocity of molecule i = $\overline{\dot{r}_i}$

The total potential energy:

$U_i = U(\text{interparticle}) + U(i, \text{wall})$

Where,

$$U(\text{interparticle}) = \sum_{i \neq j} U_{L-J}(i,j) + \sum_{i \neq j} U_{columbic}(i,j)$$

i, j represent either oxygen atoms, hydrogen atoms, cations, or anions. $\sum_{i \neq j} U_{L-J}(i,j)$ includes L-J potential between the oxygen atoms on different water molecules, L-J

potential between ions and oxygen atoms, and L-J potential between ions. $\sum_{i \neq j} U_{columibic}(i, j)$ is the electrostatic interaction among particles.

$$U(i, \text{wall}) = \sum U_{L-J}(i, \text{wall}) + \sum U_{columbic}(i, \text{wall})$$

$U(i, \text{wall})$ is the total energy the wall exerts on the particle *i*. Here *i* refers to oxygen atoms, hydrogen atoms, cations, or anions, as well. The potential interaction between a particle inside the nanochannel and the wall is the summation of the interaction between every wall site and the particle, including L-J potential ($\sum U_{L-J}(i, \text{wall})$) and Columbic interaction ($\sum U_{columbic}(i, \text{wall})$) between wall charges and electrolyte particles.

Canonical (N,V,T) ensemble molecular dynamics simulations (MD) have been carried out. The system, confined within volume, V, is composed of N particles, which is the total number of water molecules, anions, and cations. The temperature is maintained at 298 K by a Berendsen thermostat[28] through rescaling the kinetic energy to be constant after each time step. The Verlet method[27] for the ions and the "RATTLE" constrained dynamics method[29] for water molecules have been selected to solve Hamilton's equations of motion numerically for the ions and water molecules with a 2.5 *fs* time step.

All the systems simulated here include a cylindrical nanochannel with an atomistic wall in which water molecules, positive ions and negative ions are confined. It has been filled with water molecules so that the density of the fluid near the center of the nanochannel is close to 1g/cm^3. The initial configuration of the system is prepared by creating bulk water

at the density 1.0 g/cm^3. The ions are placed in the system by replacing water molecules at random. Periodical boundary conditions have been applied to the axial direction. Equilibration runs are between 7,000 and 12,500 *ps* in duration. Considering computation time and the required accuracy of the calculations, the intermolecular potential is truncated at $r_c = 5.0\sigma_{oo}$=1.583 nm (r_c: potential cutoff, beyond which intermolecular potential is set to zero). Because the radius of the nanochannel is very small, the value of r_c is set so large that it spans the diameter of the nanochannel in this research. Thus, the potential cutoff acts only in the axial direction of the nanochannel.

The charges are discretely distributed on the wall surface. Every three electric charges are placed on one ring at discrete locations with adjacent rings rotated by 60° to insure the discrete charges are distributed uniformly on the surface. Charges locations are determined by[30] :

$$x(i) = (R + 0.5)\cos\varphi$$

$$y(i) = (R + 0.5)\sin\varphi$$

$$z(i) = ((i-1)/3 \times L)/(n_q/3)$$

Where, n_q is the number of surface charges, R is the radius of the cylinder, and L is the length of the cylinder. Charges are set to positions slightly larger than the wall radius.

Where, $i = 1, 2, ..., n_q$,

$$\varphi = 2\pi(i-1)/3 + \mathrm{mod}(j,2)\pi/3$$
$$j = (i-1)/3$$

Then, these charges are moved to the center of wall surface atoms nearest the charges. The FORTRAN code "nearest.f" has been applied to this application and is listed in *Appendix1*.

The density, $\rho(r)$ is a function of the distance from the axis of the nanochannel, and is defined as[13]:

$$\rho(r) = \frac{< n(r + \Delta r, r) >}{\pi\ L[(r + \Delta r)^2 - r^2]}$$

Where $< n(r_1, r_2) >$ is the average number of molecules between cylindrical shells of radius r_1 and r_2, and L is the length of the cylinder.

The axial self-diffusion coefficient of water molecules and ions in silica nanochannel is calculated according to the Einstein relation[27] :

$$D = \frac{1}{2}\lim_{t\to\infty}\frac{d}{dt} < | \vec{r}(t) - \vec{r}(0) |^2 >$$

Where the brackets <…> denote the ensemble average of the mean-square axial displacement; D is the diffusion coefficient; t is time; and r is position.

For convenience in simulation, reduced units are adopted[27] using the water mass parameter m, distance parameter σ, and energy parameter ε, the reduced units are defined for temperature as $T^* = k_B T / \varepsilon$, time $t^* = (\varepsilon / m\sigma^2)^{1/2} t$, and density $\rho^* = \rho\sigma^3$.

3. Results and Discussion

3.1 Effects of channel radii in $CaCl_2$ aqueous electrolyte systems: -density distribution

In this section, the objective is to understand the mechanism of calcium and chloride ions density distribution as well as ion transport in silica nanochannels with radius varying from 0.9 to 1.5 nm while the other parameters are kept constant.

A series of runs with (Ca^{2+} and Cl^-) with a charged wall has been performed first to compare with the prior work of Zhou[16] on (Na^+ and Cl^-). The effects of silica nanochannel radius and charges on the wall have been investigated upon the radial density distribution and axial self-diffusivity of water and ions. Radius is studied at 0.9, 1.0, 1.1, 1.2, 1.3 and 1.5nm. The chloride density ($0.132/nm^3$) and surface charges concentration ($0.0957/nm^2$) are kept constant for all the systems. The fluid density (water molecules, positive ions, and negative ions) is ~1 $g.cm^{-3}$ in the core of the nanochannel.

Also, the nature of the charged surface deserves more careful consideration and may have significant effect on radial density profiles and self-diffusivity of water and ions. Unlike sodium ions, calcium ions have two positive unit charges. The degree of calcium ions adsorbed by the charged surface would be different from that of sodium ions. So is the self-diffusivity of calcium ions.

The parameters used in the simulation are listed in Tables1-3.

The radial density distributions of water molecules are displayed in Figures 1 through 6. The radial density distributions of calcium and chloride ions are shown in Figures 7 through 12. For different channel radii, the solvent water density distribution exhibits a typical behavior which is essentially same for each case. The profiles show that, within 0.35 nm from the wall, water structure is oscillatory, but near the center, it becomes more bulk-like. Further from the wall, the water structure becomes less pronounced and appears to be uniform. Because oxygen atoms denote the center of mass of the molecules, seeing the oxygen atom distribution, water molecules form a layer with a maximum in the probability density just 0.31 nm from the wall, and its height and position is basically unchanged as radii increases from 0.9 nm to 1.5 nm. There is room for other layers in the nanochannel with lower probability density. The number of distinct layers and the corresponding radial positions at different nanochannel radii are listed in Table 4. The number of layers of water molecules varies when radius changes. It is attributable to the free energy of the system which depends on whether the cylinder size is commensurate with the natural separation of the layers[15]. But this issue is not discussed further in this research.

The charges on the wall atoms of the nanochannel set up a static electrical field. The movements of the aqueous electrolytes inside the nanochannel are influenced to a differing extent. Because there are negative charges distributed discretely at the centers of

Table 1 L-J parameters for $CaCl_2$-H_2O-SiO_2

Pair	σ (nm)	ε / k_B (K)
Ca-Ca[30]	0.2895	50.32
Ca-Cl	0.3648	50.32
Ca-O	0.303	62.72
O-O[20]	0.3166	78.168
Cl-Cl[30]	0.4401	50.32
Cl-O[15]	0.3784	62.72
Ca-Wall	0.2948	107.6
Cl-Wall	0.3701	107.6
Wall-Wall	0.3	230

Table 2 Site charges for $CaCl_2$ aqueous electrolytes solutions

Ions	Ca^{2+}	Cl^-	O	H
Charge	+2e	-1e	-0.8476e	+0.4238e

Table 3 Calculation parameters for $CaCl_2$-H_2O-SiO_2 system

Radius (nm)	Length (nm)	Number of water	Number of Ca^{2+}	Number of Cl^-	Number of charges
0.9	11.087	563	4	2	6
1.0	6.651	470	3	2	4
1.1	6.047	523	3	2	4
1.2	6.929	717	4	3	5
1.3	6.396	772	4	3	5
1.5	6.652	1132	6	6	6

Table 4 Solvation layers of water molecules at different channel radii

Radius (nm)	Number of layers of water molecules	Radial positions (nm)
0.9	2	0.27, 0.60
1.0	3	0.00, 0.38, 0.70
1.1	3	0.14, 0.48, 0.80
1.2	3	0.22, 0.59, 0.90
1.3	3	0.31, 0.66, 0.99
1.5	4	0.24, 0.50, 0.87, 1.19

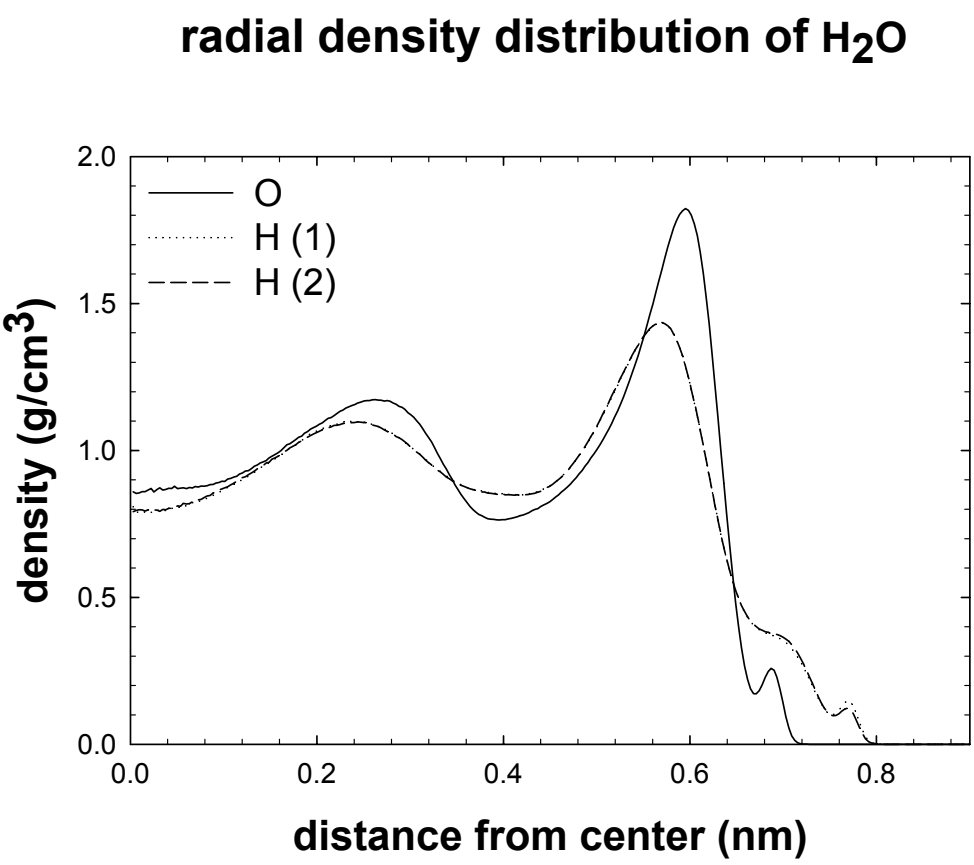

Figure 1: Radial density distribution of oxygen and hydrogen atoms when the radius of silica nanochannel is 0.9 nm ($CaCl_2$). The system consists of 563 water molecules, 4 calcium ions, 2 chloride ions. 6 negative charges are distributed on the wall surface. The channel length is 11.087 nm, while the concentration of chloride ions (0.132/nm^3) and density of charges on the wall (0.0957/nm^2) are kept constant.

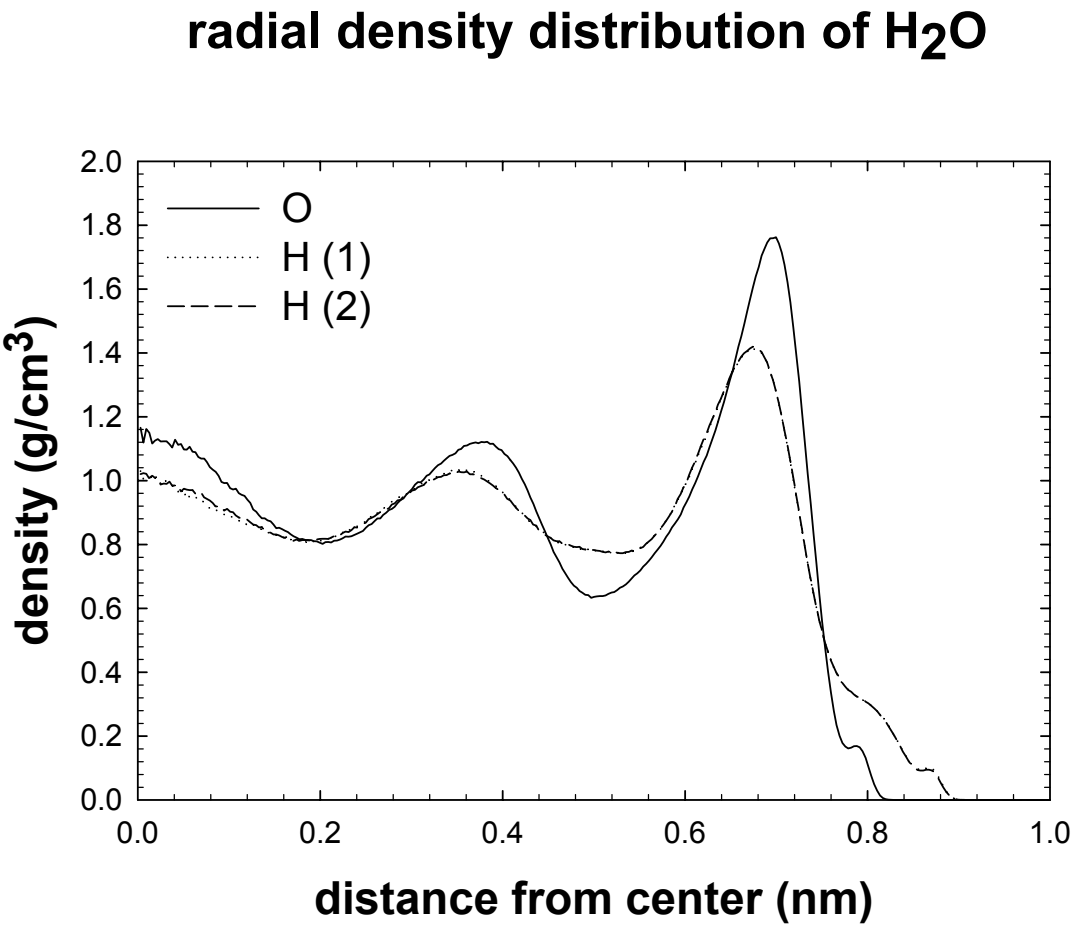

Figure 2: Radial density distribution of oxygen and hydrogen atoms when the radius of silica nanochannel is 1.0 nm ($CaCl_2$). The system consists of 467 water molecules, 3 calcium ions, 2 chloride ions. 4 negative charges are distributed on the center of wall atoms. The channel length is 6.651 nm, while the concentration of chloride ions ($0.132/nm^3$) and density of charges on the wall ($0.0957/nm^2$) are kept constant.

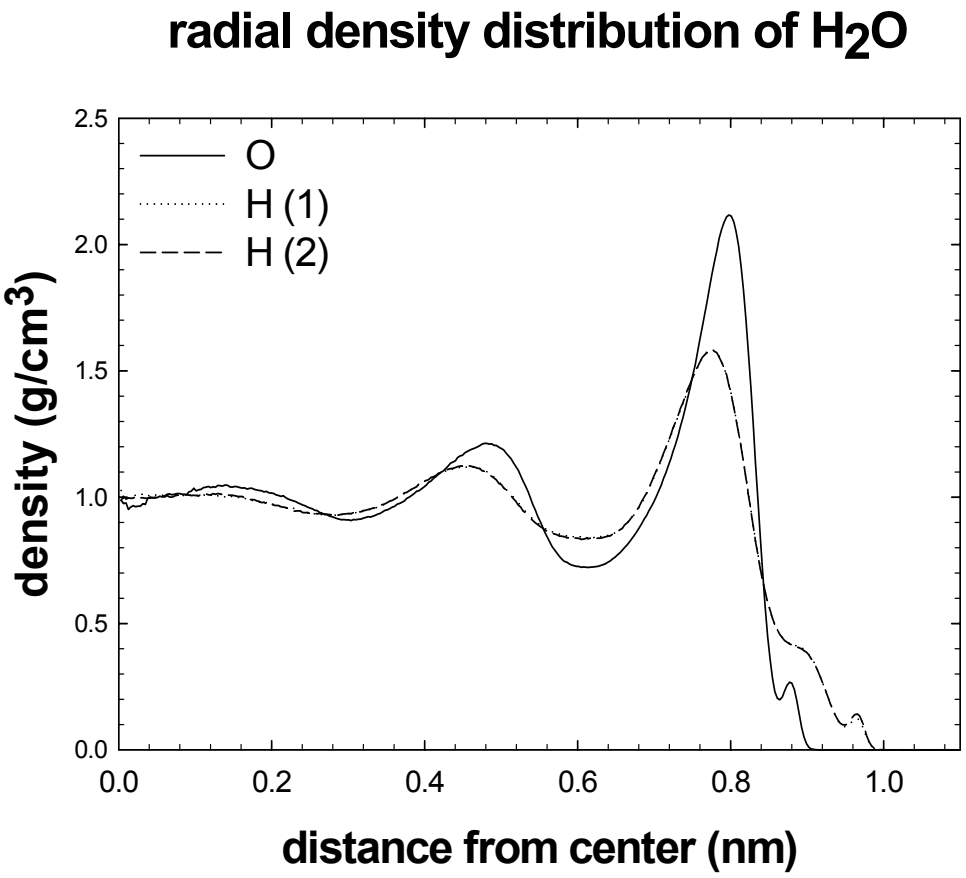

Figure 3: Radial density distribution of oxygen and hydrogen atoms when the radius of silica nanochannel is 1.1 nm ($CaCl_2$). The system consists of 523 water molecules, 3 calcium ions, 2 chloride ions. 4 negative charges are distributed on the center of wall atoms. The channel length is 6.047nm, while the concentration of chloride ions ($0.132/nm^3$) and density of charges on the wall ($0.0957/nm^2$) are kept constant.

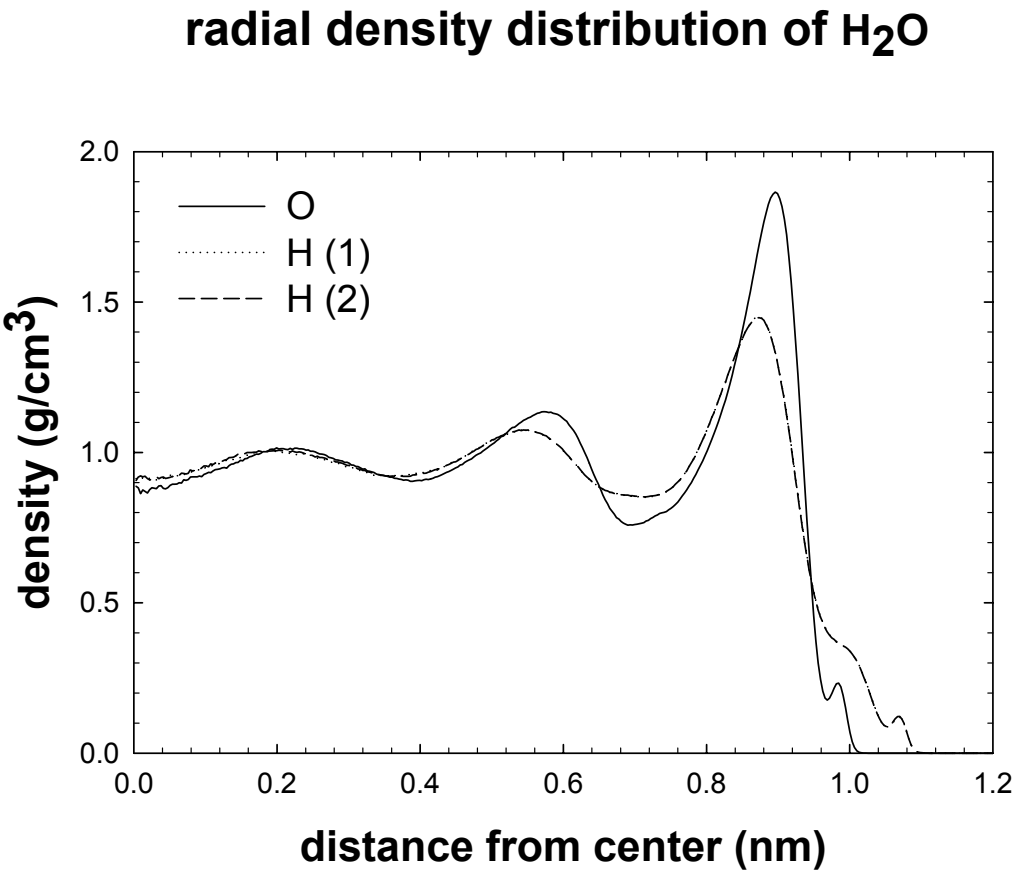

Figure 4: Radial density distribution of oxygen and hydrogen atoms when the radius of silica nanochannel is 1.2 nm ($CaCl_2$). The system consists of 717 water molecules, 4 calcium ions, 3 chloride ions. 5 negative charges are distributed on the center of wall atoms. The channel length is 6.929 nm, while the concentration of chloride ions ($0.132/nm^3$) and density of charges on the wall ($0.0957/nm^2$) are kept constant.

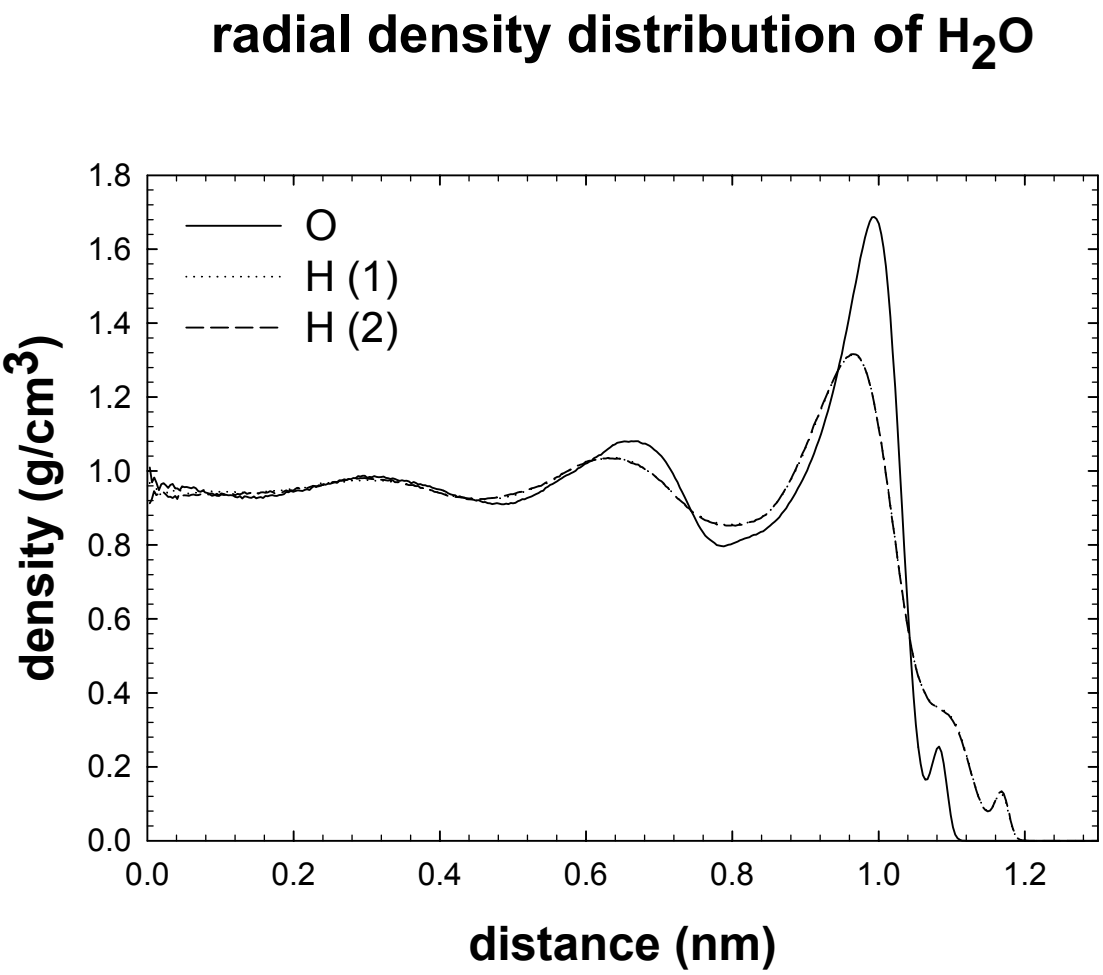

Figure 5: Radial density distribution of oxygen and hydrogen atoms when the radius of silica nanochannel is 1.3 nm ($CaCl_2$). The system consists of 772 water molecules, 4 calcium ions, 3 chloride ions. 5 negative charges are distributed on the center of wall atoms. The channel length is 6.396 nm, while the concentration of chloride ions ($0.132/nm^3$) and density of charges on the wall ($0.0957/nm^2$) are kept constant.

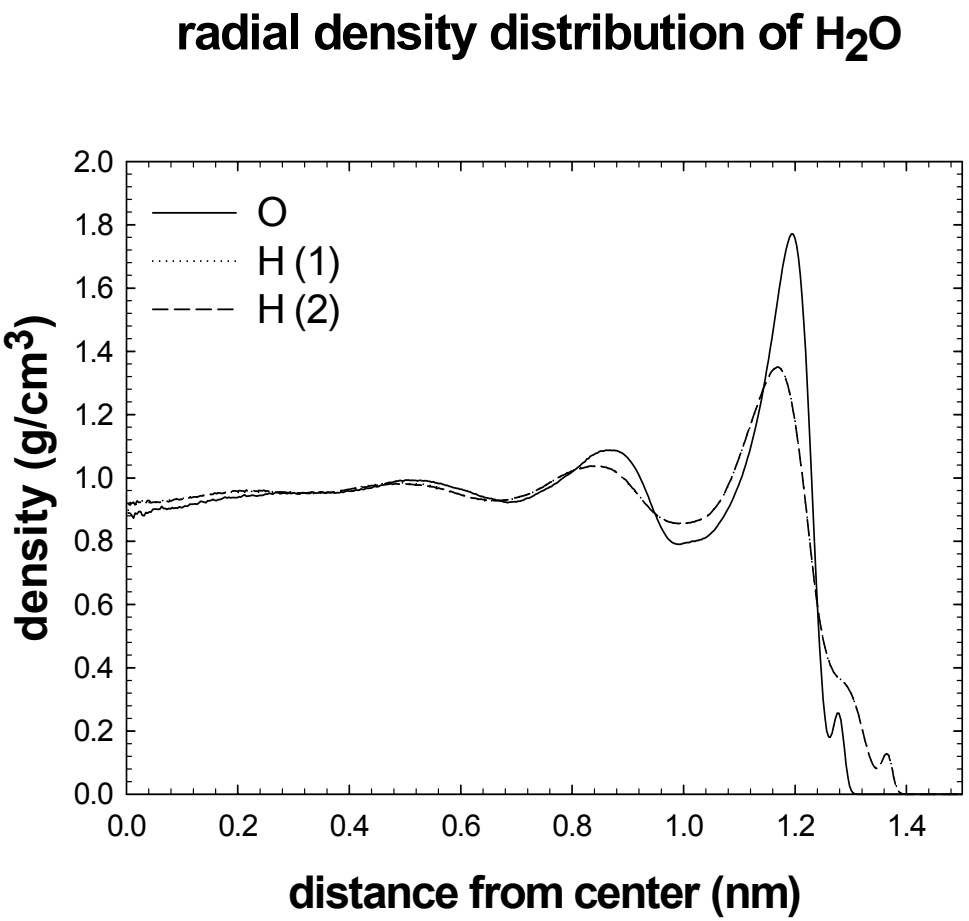

Figure 6: Radial density distribution of oxygen and hydrogen atoms when the radius of silica nanochannel is 1.5 nm ($CaCl_2$). The system consists of 1132 water molecules, 6 calcium ions, 6 chloride ions. 6 negative charges are distributed on the center of wall atoms. The channel length is 6.652 nm, while the concentration of chloride ions ($0.132/nm^3$) and density of charges on the wall ($0.0957/nm^2$) are kept constant.

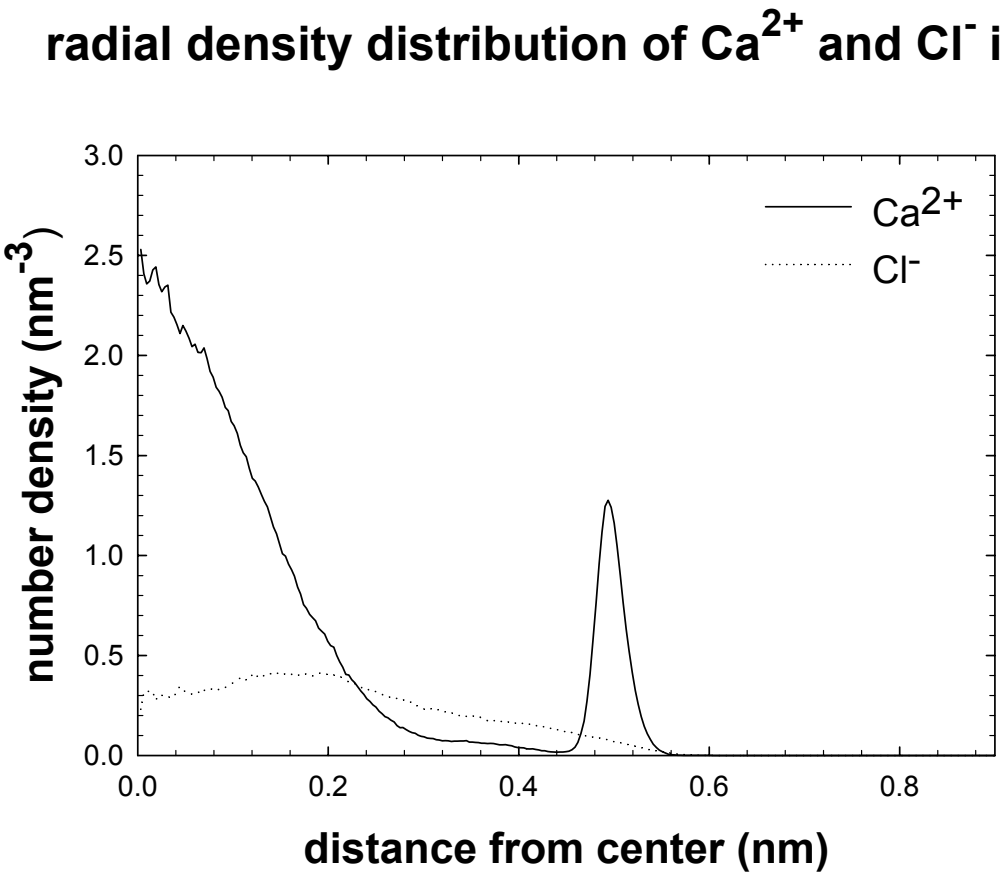

Figure 7: Radial density distribution of calcium and chloride ions when the radius of silica nanochannel is 0.9 nm. The system consists of 564 water molecules, 4 calcium ions, 2 chloride ions. 6 negative charges are distributed on the center of wall atoms. The channel length is 11.087 nm, while the concentration of chloride ions ($0.132/nm^3$) and density of charges on the wall ($0.0957/nm^2$) are kept constant.

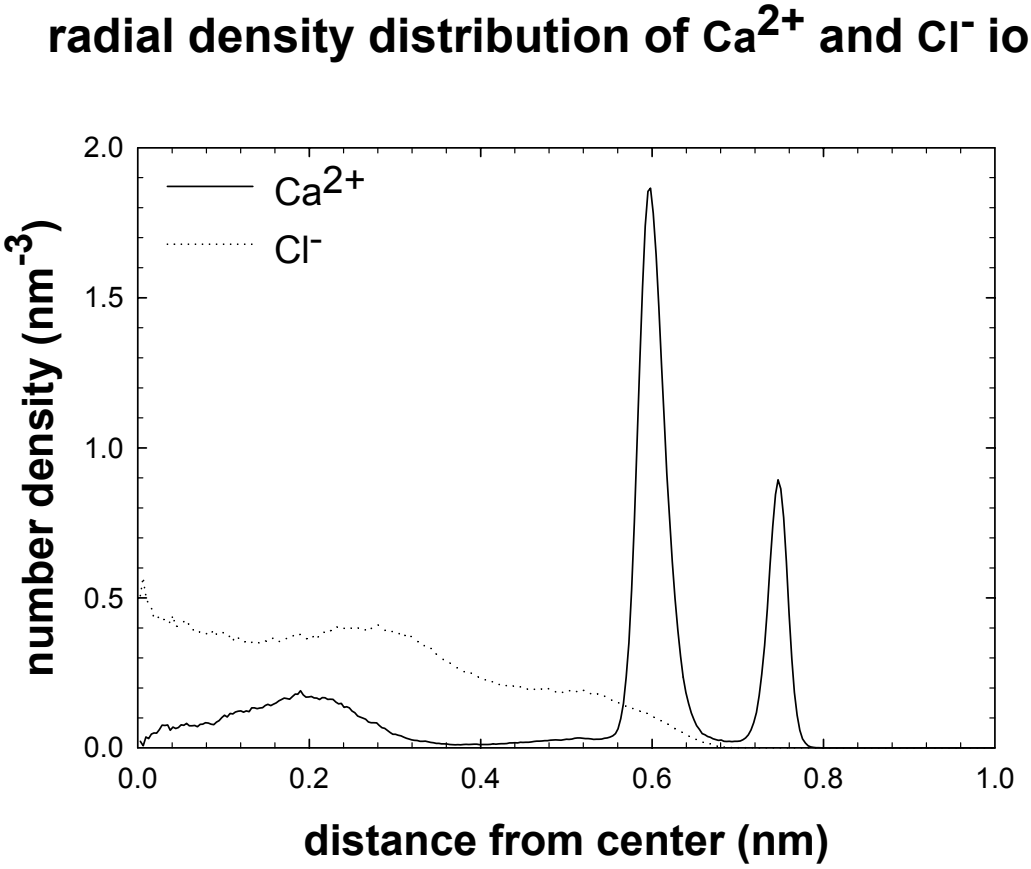

Figure 8: Radial density distribution of calcium and chloride ions when the radius of silica nanochannel is 1.0 nm. The system consists of 470 water molecules, 3 calcium ions, 2 chloride ions. 4 negative charges are distributed on the center of wall atoms. The channel length is 6.651 nm, while the concentration of chloride ions (0.132/nm^3) and density of charges on the wall (0.0957/nm^2) are kept constant.

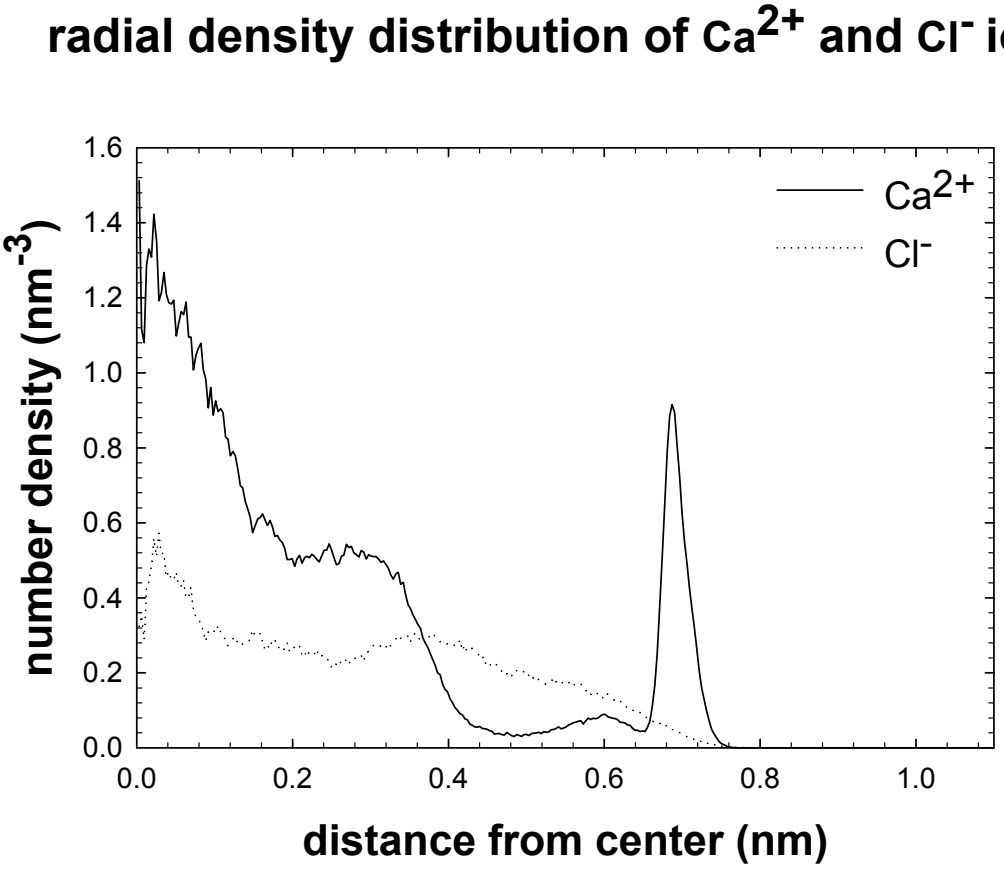

Figure 9: Radial density distribution of calcium and chloride ions when the radius of silica nanochannel is 1.1 nm. The system consists of 523 water molecules, 3 calcium ions, 2 chloride ions. 4 negative charges are distributed on the center of wall atoms. The channel length is 6.047 nm, while the concentration of chloride ions ($0.132/nm^3$) and density of charges on the wall ($0.0957/nm^2$) are kept constant.

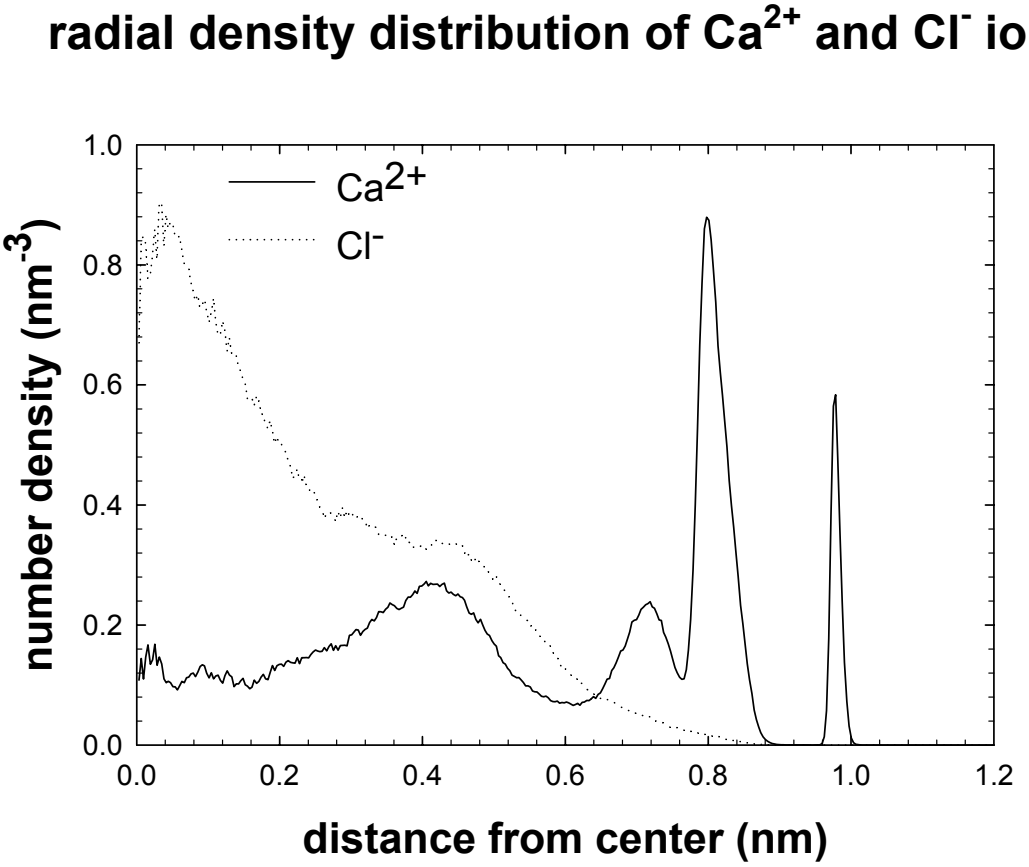

Figure 10: Radial density distribution of calcium and chloride ions when the radius of silica nanochannel is 1.2 nm. The system consists of 717 water molecules, 4 calcium ions, 3 chloride ions. 5 negative charges are distributed on the center of wall atoms. The channel length is 6.929 nm, while the concentration of chloride ions ($0.132/nm^3$) and density of charges on the wall ($0.0957/nm^2$) are kept constant.

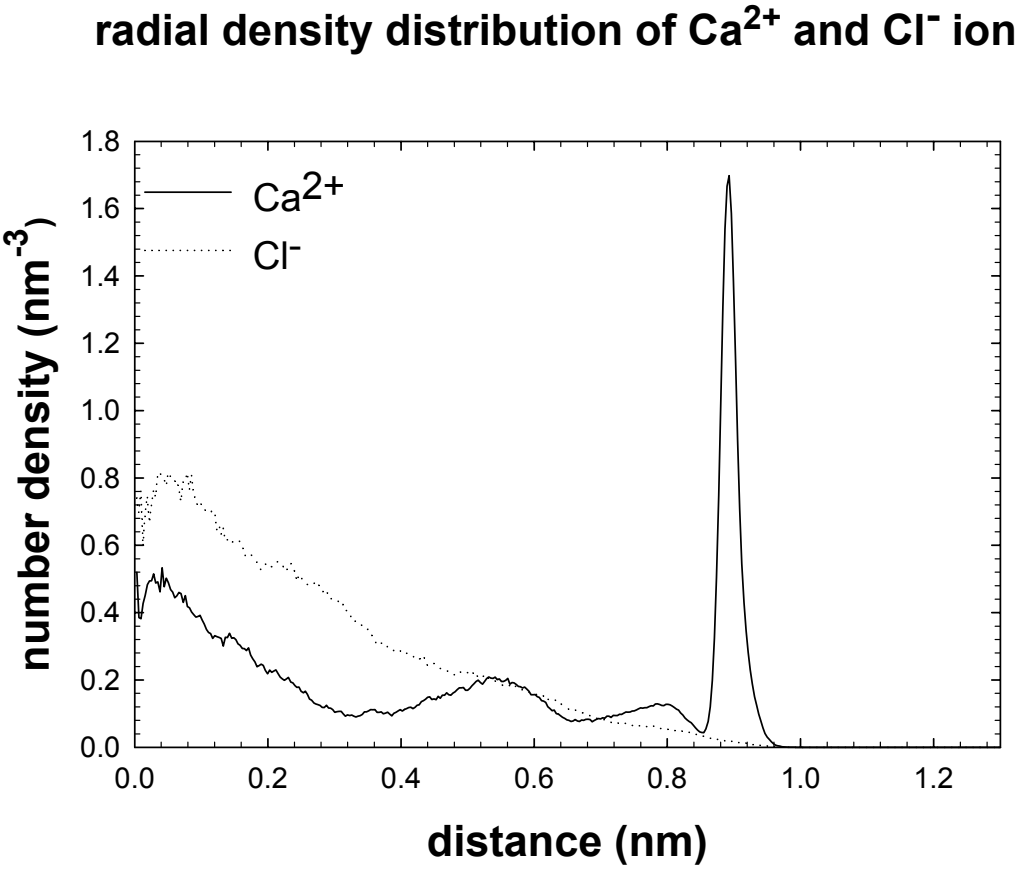

Figure 11: Radial density distribution of calcium and chloride ions when the radius of silica nanochannel is 1.3 nm. The system consists of 772 water molecules, 4 calcium ions, 3 chloride ions. 5 negative charges are distributed on the center of wall atoms. The channel length is 6.396 nm, while the concentration of chloride ions ($0.132/nm^3$) and density of charges on the wall ($0.0957/nm^2$) are kept constant.

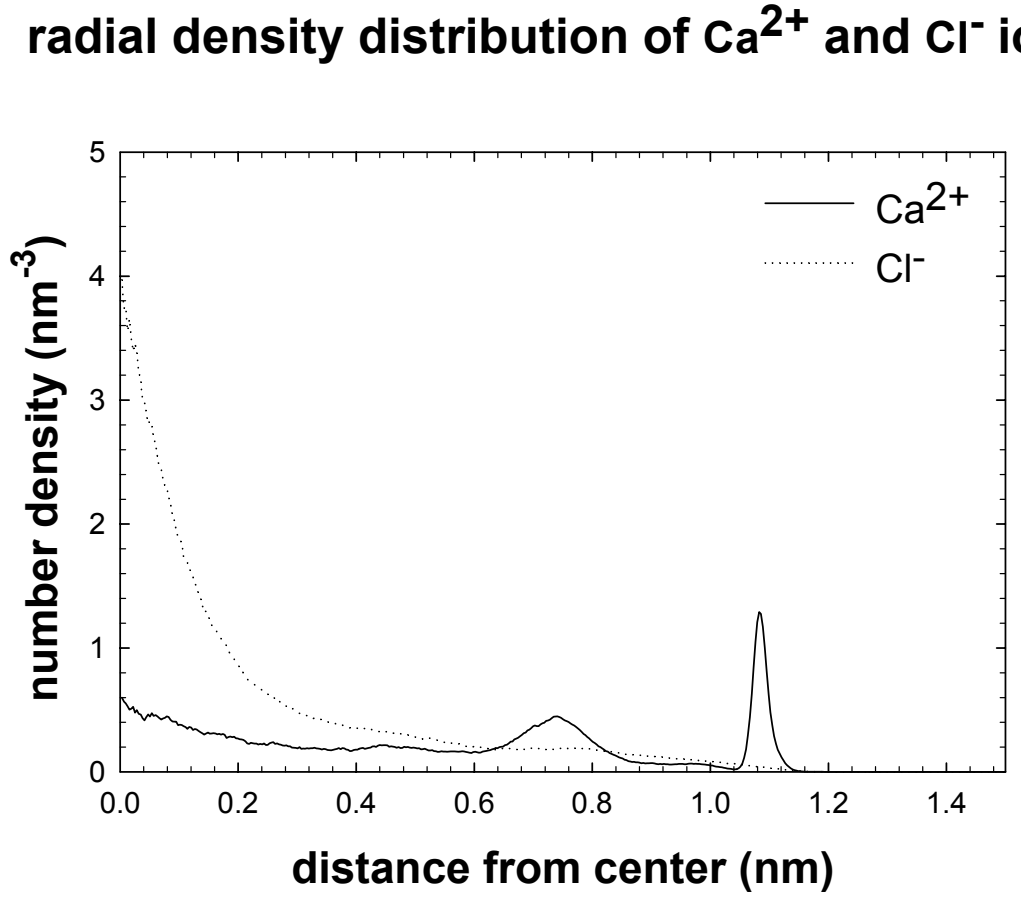

Figure 12: Radial density distribution of calcium and chloride ions when the radius of silica nanochannel is 1.5 nm. The system consists of 1132 water molecules, 6 calcium ions, 6 chloride ions. 6 negative charges are distributed on the center of wall atoms. The channel length is 6.652 nm, while the concentration of chloride ions ($0.132/nm^3$) and density of charges on the wall ($0.0957/nm^2$) are kept constant.

some wall atoms, hydrogen atoms are attracted closer to the wall, and oxygen atoms (water center) are slightly repelled further from the wall. The water structure is arrayed in a manner that hydrogen is closer to the wall than oxygen atoms. The number of water molecules increases as nanochannel radii increase. Water molecules in different layers continually exchange their positions and do not stay in the layer all the time.[16, 17]

The small hydrogen peak closest to the wall and the second peak slightly farther from the wall are features that were not apparent in previous simulations of monovalent cationic chloride (e.g., NaCl) solutions[16, 17]. Probably, previous simulations[16, 17] are results of the surface charges being randomly located with respect to the wall atoms, which would result in broadening such small peaks so much that they are not seen. (See sections 3.4 and 3.5 for monovalent density distribution with surface charges at the center of wall atoms.) The peak closest to the wall likely represents configurations in which hydrogen atoms are in the valleys between three surface sites (one charged) where they are attracted by the wall charge and the L-J interaction with three wall atoms. The second small peak, then, likely represents hydrogen atoms between a pair of wall atoms (one charged) where they are attracted by the wall charge and the L-J interaction with only two wall atoms. The spherical L-J repulsion between the water and each wall atom, then, creates two potential energy minima for hydrogen atoms of the first shell water molecules: The deeper minimum between three wall atoms, which is located closest to the wall, and the shallower one between two wall atoms slightly farther from the wall. This geometry is illustrated by the distances and angles between the wall charge, the Ca^{2+}, and the near-by hydrogen atoms from two representative configurations shown in

Figure 13 and 14. Of course the thermal motions of the atoms lead to the width of these peaks.

Similarly, the small peak in the water density curve is from the oxygen atom in the first shell water molecule.

By tracing the movement of calcium ions in the nanochannel, it is found that calcium ions are attracted and remain adjacent to the point where the wall charges are set. These calcium ions do not move freely; some are fixed without intervening water molecules by the attraction of charges; some are separated from the wall atoms by water molecules in the first hydration shell and just vibrate back and forth at a certain distance due to the less strong attraction force from charges. The examples of calcium ions activities are shown in Figure 15 and 16. Since there are more surface charges than calcium ions in this aqueous electrolytes system, it is always possible for calcium ions to find remaining charges to attract them. The adsorption of calcium counter ions on the wall neutralizes the charges on the wall surface so that the radial density distribution of chloride ions is hardly affected by wall charges. Excess chloride ions move freely in the system and are repelled a little bit further from the wall than calcium ions. The FORTRAN subroutine "location.f" to track the activities of calcium ions in aqueous solutions has been applied to this application and listed in *Appendix 2*.

The classical Stern theory describes an important concept called the electrical double layer, in which the ion distribution near the charge sites consists of an immobile layer of

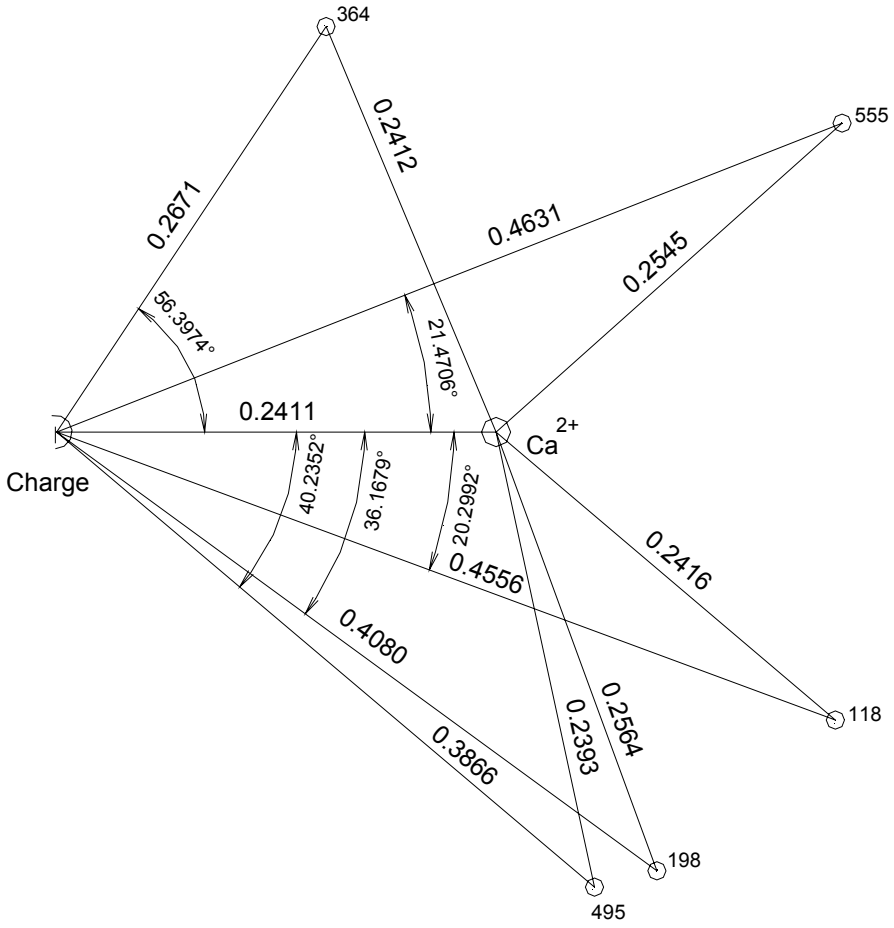

Figure 13: The spatial configuration of charge, calcium ion nearest this charge and oxygen atoms around calcium ion within the range of $1.2\sigma_{Ca\text{-}Ca}$ in 1.2 nm nanochannel. The distances between calcium ion and charge, between charge and oxygen, between oxygen and calcium, and the angle of oxygen-charge-calcium are shown. The system consists of 717 water molecules, 4 calcium ions, 3 chloride ions, 5 negative charges. This corresponds to Figure 15 where adsorbed calcium ion is fixed to the wall sites by the attraction of charges.

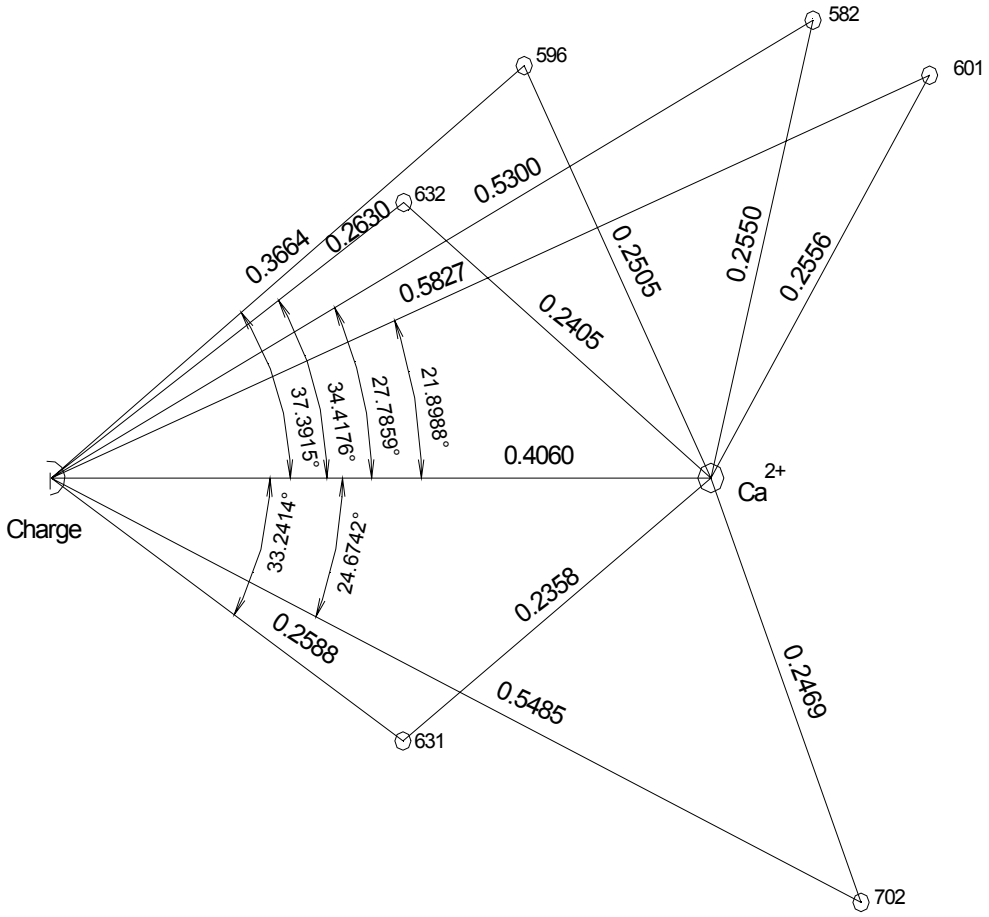

Figure 14: The spatial configuration of charge, calcium ion nearest this charge and oxygen atoms around calcium ion within the range of $1.2\sigma_{Ca\text{-}Ca}$ in 1.3 nm nanochannel. The distances between calcium ion and charge, between charge and oxygen, between oxygen and calcium, and the angle of oxygen-charge-calcium are shown. The system consists of 772 water molecules, 4 calcium ions, 3 chloride ions, 5 negative charges. This corresponds to Figure 16 where calcium ion is separated from the wall atoms by water molecules in the first hydration shell.

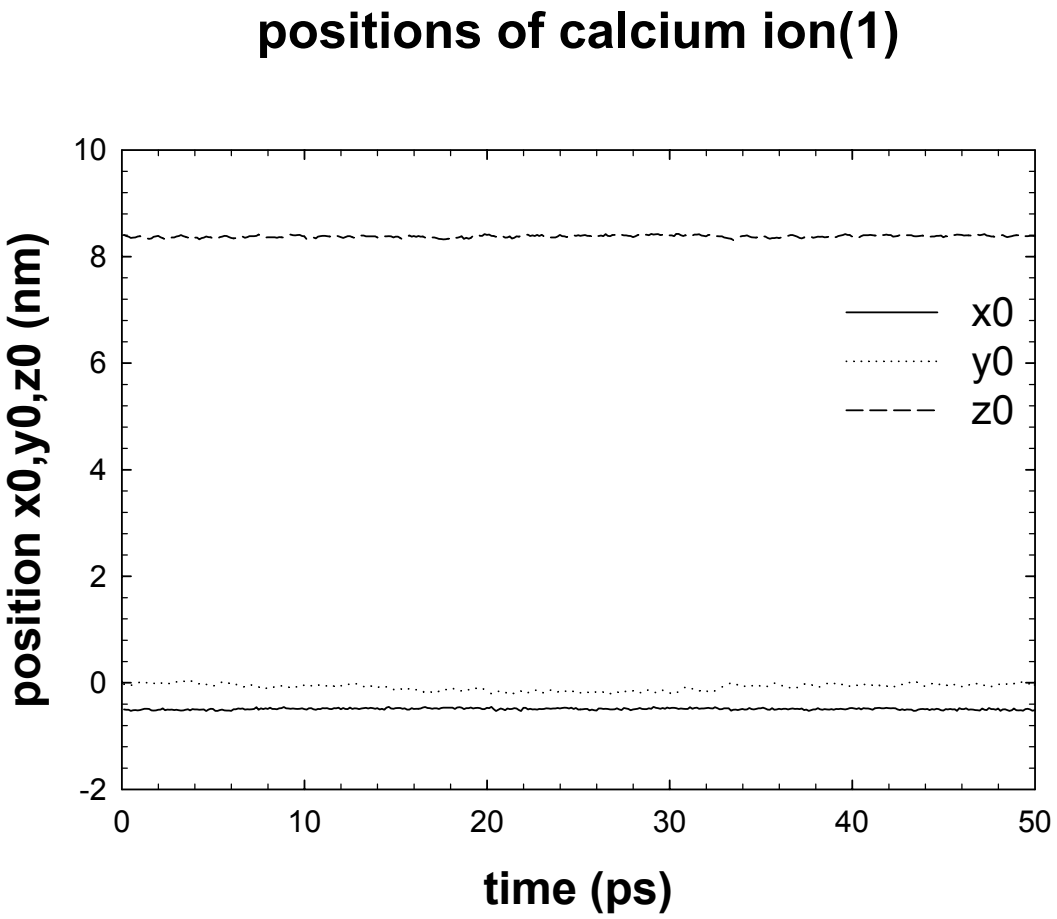

Figure 15: The positions of one calcium ion vs. time (1). This calcium ion is attracted by the wall charges and fixed on the surface wall of the nanochannel. This corresponds to Figure 13 where adsorbed calcium ion is fixed to the wall sites by the attraction of charges. Note: This is the sampling frequency which expresses frequency of Ca^{2+} vibration every 50 timestep.

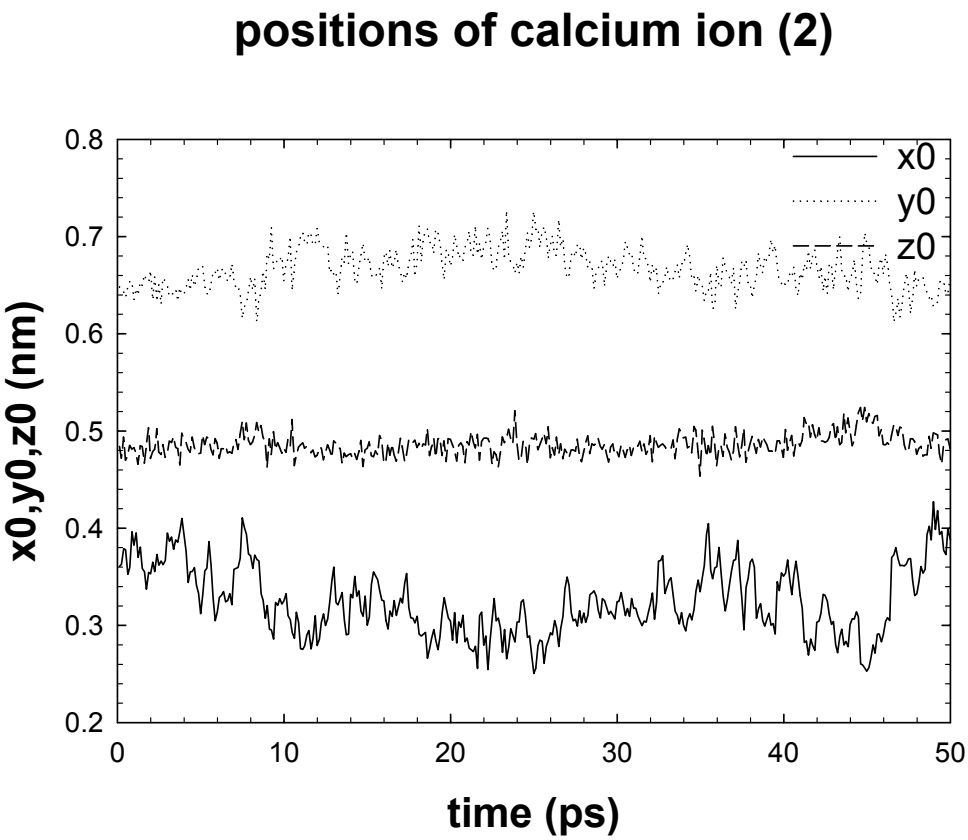

Figure 16: The positions of one calcium ion vs. time(2). This calcium ion vibrates back and forth at certain distance adjacent to the surface wall charges of the nanochannel. This corresponds to Figure 14 where calcium ion is separated from the wall atoms by water molecules in the first hydration shell. Note: This is the sampling frequency which expresses frequency of Ca^{2+} vibration every 50 timestep.

counterions (Stern layer) at the surface and a diffuse layer of more mobile ions, characterized by depleted ion concentration in the interfacial region with further distance from the wall[30].

As seen from the density distribution of ions in Figures 7 - 12, as radial position varies from near the wall to the center, there is an increased ion density (excepting the Ca^{2+} adsorption peak). It may be inferred that ions seem to avoid the region near the wall, which is preferentially occupied by layered water molecules[30]. The calcium ions are distributed closer to the oxygen sites and chloride ions are distributed closer to hydrogen sites of the layered water structure.

The calcium ion distributions, however, displays some interesting features. Take the calcium density distribution at radius 1.2 nm and 1.3 nm (Figures 10 and 11) as representative cases. In the 1.2 nm nanochannel, the highest peak occurs at 0.40 nm from the wall, which is expected for a hydrated calcium ion. (Because the diameter of calcium is 0.2895 nm, the diameter of water is approximately 0.30 nm, and the radius of the wall atom is 0.30 nm. (0.2895+0.30)/2 + 0.15 = 0.44 nm which basically coincides the hydration calcium peak position). Another smaller distinct peak occurs 0.22 nm from the wall, which is the effect of the charged sites on the wall, suggesting the direct adsorption of calcium ions to the charged sites, according to the classical Stern layer. Calcium ions are fixed on the wall charges by the attraction force and have a direct contact with wall atoms. The spatial configuration of calcium ions, charges, and water atoms is shown in Figure 13. Tracing back the radial density distribution for calcium ions at 1.3 nm radius,

the sharp peak occurs at 0.40 nm from the wall, indicating a hydrated calcium ion shell. The narrow width and the strong height indicate the nearly fixed positions of the hydrated ions. The spatial configuration of calcium ions, charges, and water atoms is shown in Figure 14. The FORTRAN subroutine "cawater.f" has been applied to this application and listed in *Appendix3*. However, these two structures illustrated by Figures 13 and 14, in which one represents hydrated calcium ions, another represents directly-adsorbed calcium ions, do not represent a real effect of the two of pore sizes; instead, they reflect two snapshots from a dynamic equilibrium between adsorption states.The radial distributions of chloride ions are very similar for each case in different nanochannel radii, which means the negative charges on the wall surface have been screened by the Ca^{2+} ions and associated waters and thus the wall charges have little effect on it.

In addition to the increased ion density at the radial position far away from the wall, the calcium density distribution displays peaks that coincide with the valleys of the water density distribution. The chloride density distribution is not affected by the water density oscillation. Again, density distributions with radius 1.2 nm and 1.3 nm are taken as examples (Figure 17 and 18). By sitting in the valleys between two peaks of the oxygen distribution, calcium ions increase their hydration number of water molecules and thus have a lower potential energy[25]. Because of the smaller-nearest approach, with the small size of a calcium ion ($\sigma_{Ca\text{-}Ca}$ = 0.2895 nm), the nearer distance between calcium ions and oxygen atoms, and the larger partial charge on the oxygen (- 0.8476 e), the electrostatic attraction between oxygen atoms and calcium ion is stronger and more energetically

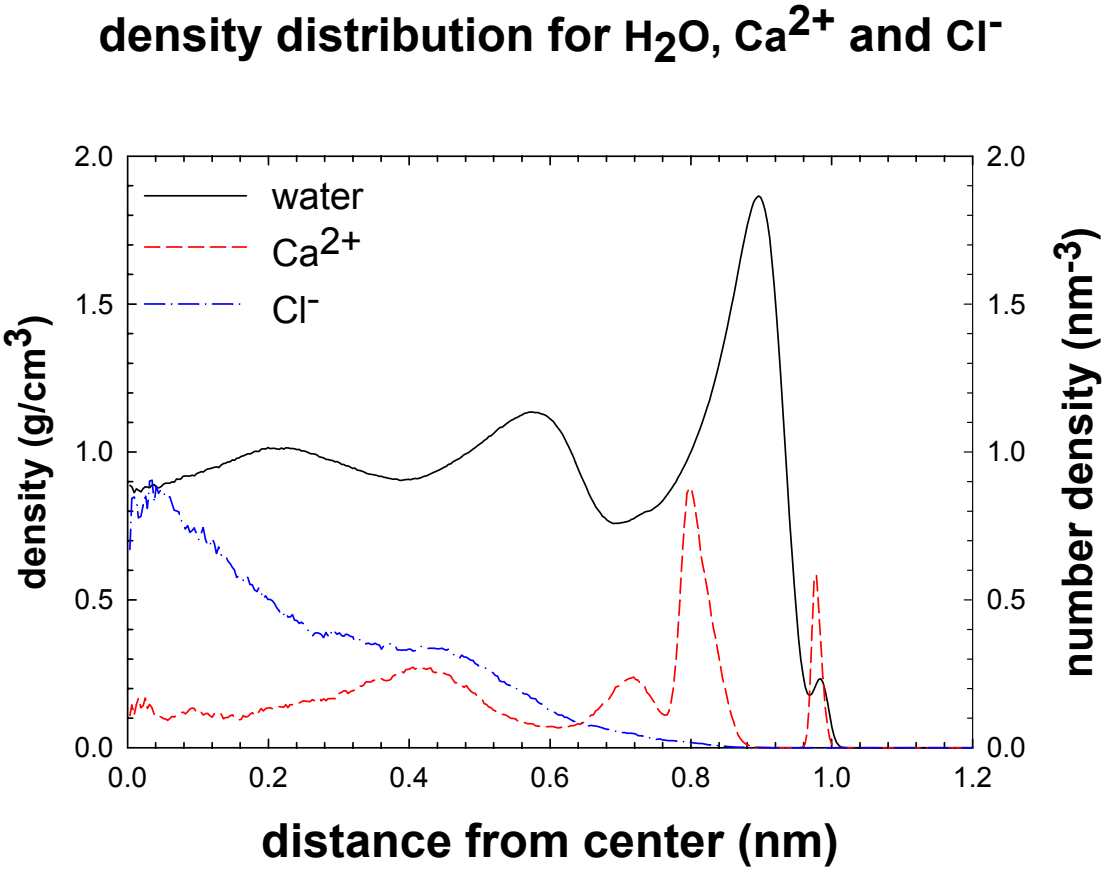

Figure 17: Density distribution for the water molecules denoted by oxygen atoms (water center), calcium ions and chloride ions in 1.2 nm nanochannel. Note that the water density distribution is plotted with the left axis and the ions density distribution is plotted with the right axis.

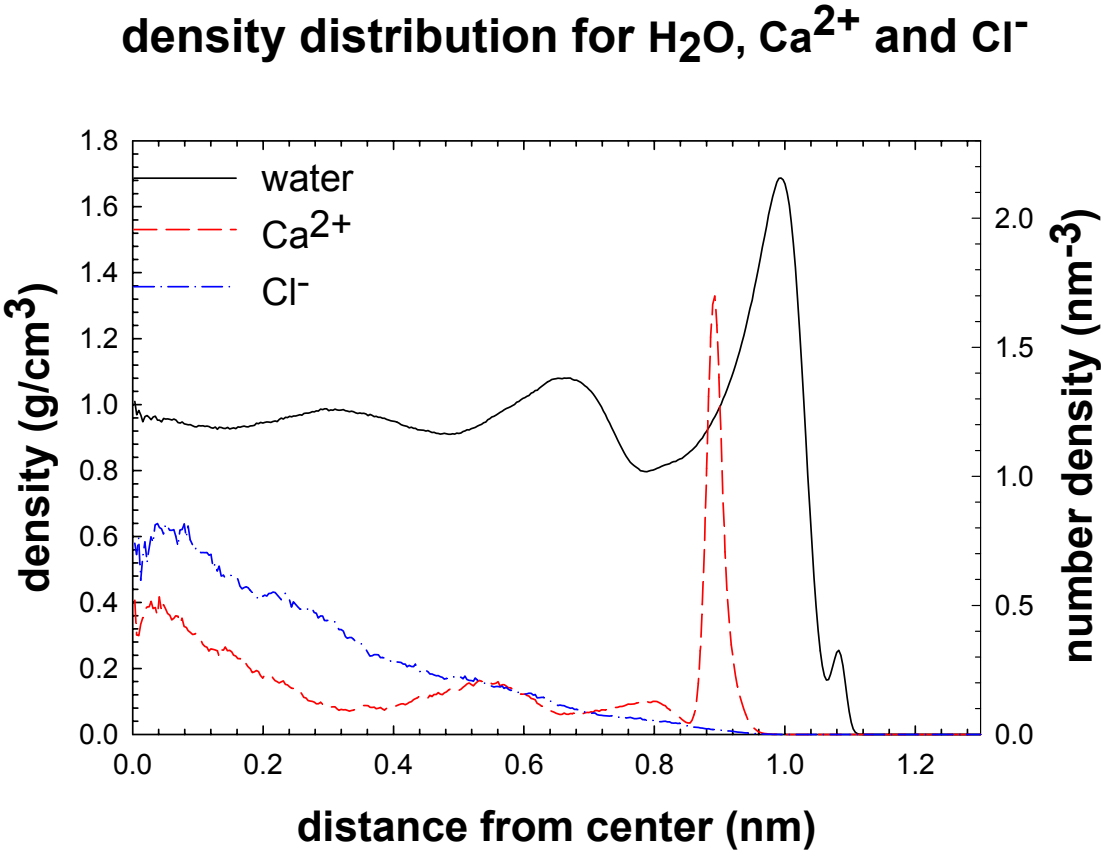

Figure 18: Density distribution for the water molecules denoted by oxygen atoms (water center), calcium ions and chloride ions in 1.3 nm nanochannel. Note that the water density distribution is plotted with the left axis and the ions density distribution is plotted with the right axis.

favorable when calcium ions locate in the valleys between oxygen atoms. This phenomenon is not observed for the chloride ion density distribution. Due to the larger size of the chloride ions ($\sigma_{Cl\text{-}Cl}$ = 0.4401 nm) and the smaller partial charge on the hydrogen (+ 0.4238 e), the electrostatic attraction between chloride ions and hydrogen atoms is weaker.

3.2 Effects of channel radii in $CaCl_2$ aqueous electrolyte systems: self - diffusivity

The self-diffusivity of water molecules in the axial direction has been calculated, as shown in Figure 19 and Table 5. The self-diffusivity is calculated from the slope of the line. In general, self-diffusivity of water molecules tends to increase with the increase of the radius of nanochannel. If the increase of the radius can accommodate one new layer of water molecules, the self-diffusivity of water molecules increases. If the increase of radius is about half or one-and-a-half of the diameter of water molecules, the self-diffusivity just decreases. Self-diffusivity is calculated at approximately constant core water density of 1.0 g/cm^3. The self-diffusivity of water molecules in the axial direction is close to that of bulk water at ambient conditions. Self-diffusivity is also affected by pressure in the fluids. The pressure is not kept constant when radius varies at constant density. But pressure calculation in these inhomogeneous, quasi-one-dimensional systems is not straightforward[17]. In this research, the effect of pressure on the self-diffusivity is minimized by adjusting the number of water molecules in each system so that the central density of water in each nanochannel is consistent.

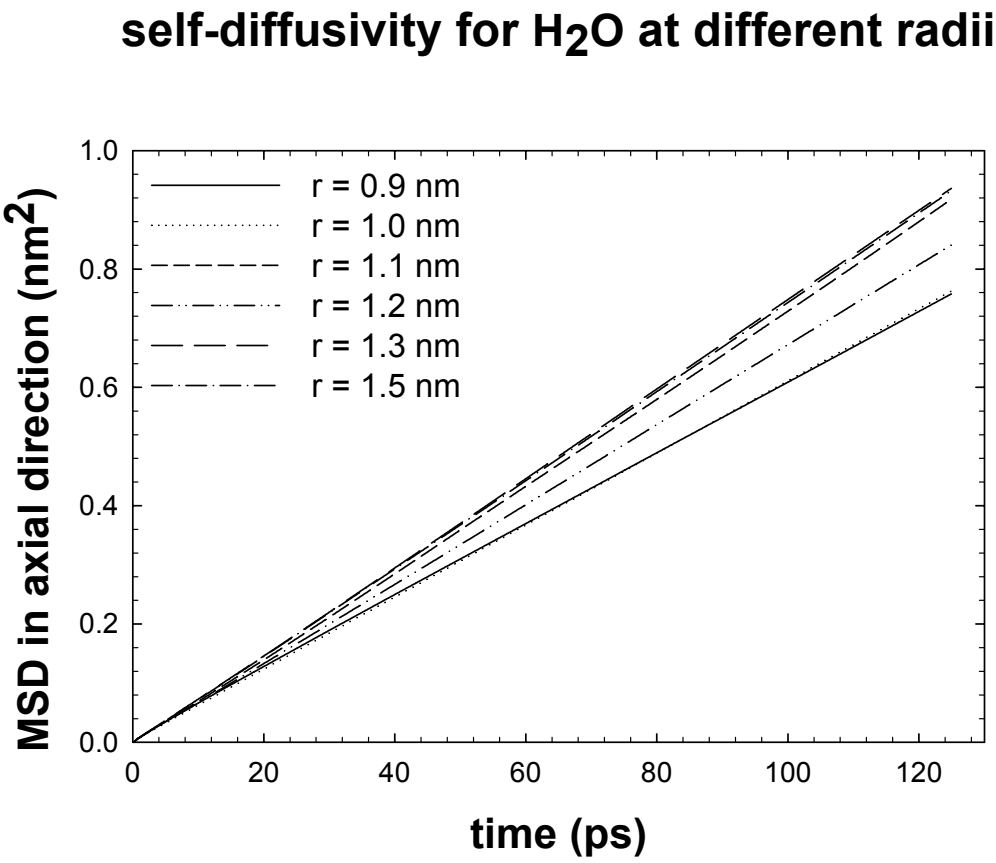

Figure 19: The mean square displacement (MSD) of water molecules in aqueous electrolyte solution system at different radii of nanochannel.

Table 5: Self-diffusivities of water molecules along axial direction of nanochannel at different radii

Radius (nm)	H_2O (1×10^{-5} cm^2/s)
0.9	3.008
1.0	3.046
1.1	3.456
1.2	3.367
1.3	3.596
1.5	3.738

Note: Standard deviations for self-diffusivities must be achieved by repeating simulations. So they are not included in this simulation.

The mean square displacement (MSD) of calcium ions is directly proportional to the square root of time. Figures of MSD vs. the square root of time are shown in Figures 20 through 26. The values of movement for Ca^{2+} (units of $length^2/time^{0.5}$) are very small. The small magnitude is likely the result of each Ca^{2+} spending most of the time adsorbed to a charged wall site. The one-half power of time might suggest single-file diffusion (SFD)[31]. SFD occurs when particles diffuse in a medium with restricted geometry in which molecules can not pass each other, therefore mainly move in one dimension[32]. Despite almost three decades of research, understanding of SFD is still far from complete. SFD should appear as the fluid molecular diameter approaches the effective

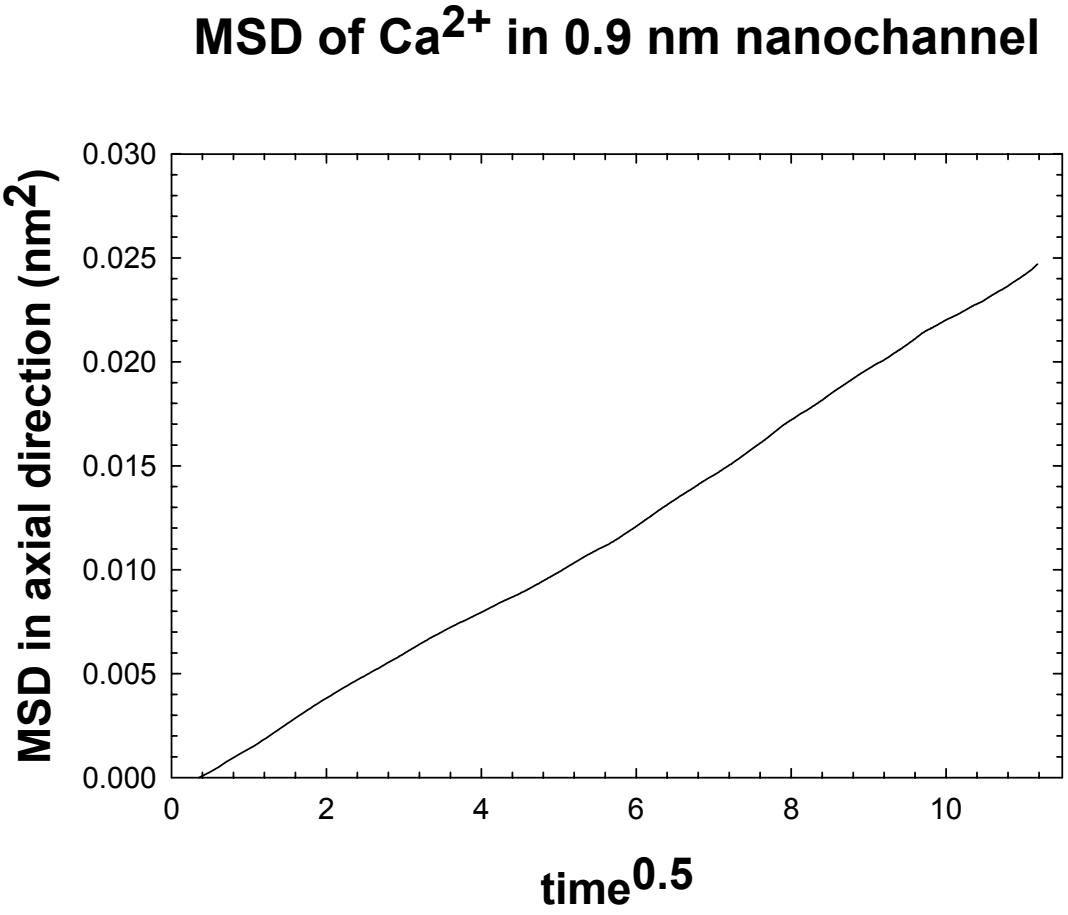

Figure 20: The mean square displacement (MSD) of calcium ions in silica nanochannel with radius = 0.9 nm. [MSD (nm^2) ~ $t^{0.5}$ ($ps^{0.5}$)]

Slope = 2.320×10^{-5} $cm^2/s^{0.5}$

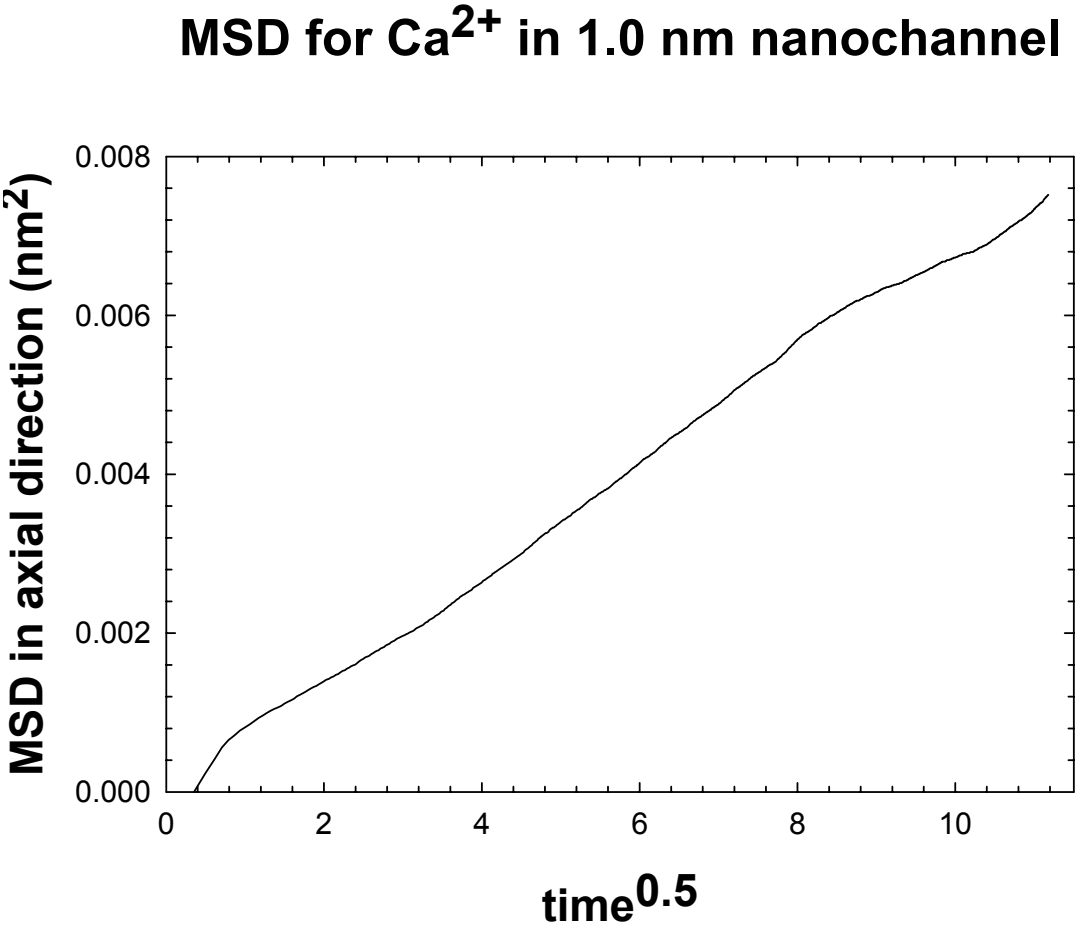

Figure 21: The mean square displacement (MSD) of calcium ions in silica nanochannel with radius = 1.0 nm. [MSD (nm^2) ~ $t^{0.5}$ ($ps^{0.5}$)]

Slope = 0.0675×10^{-5} $cm^2/s^{0.5}$

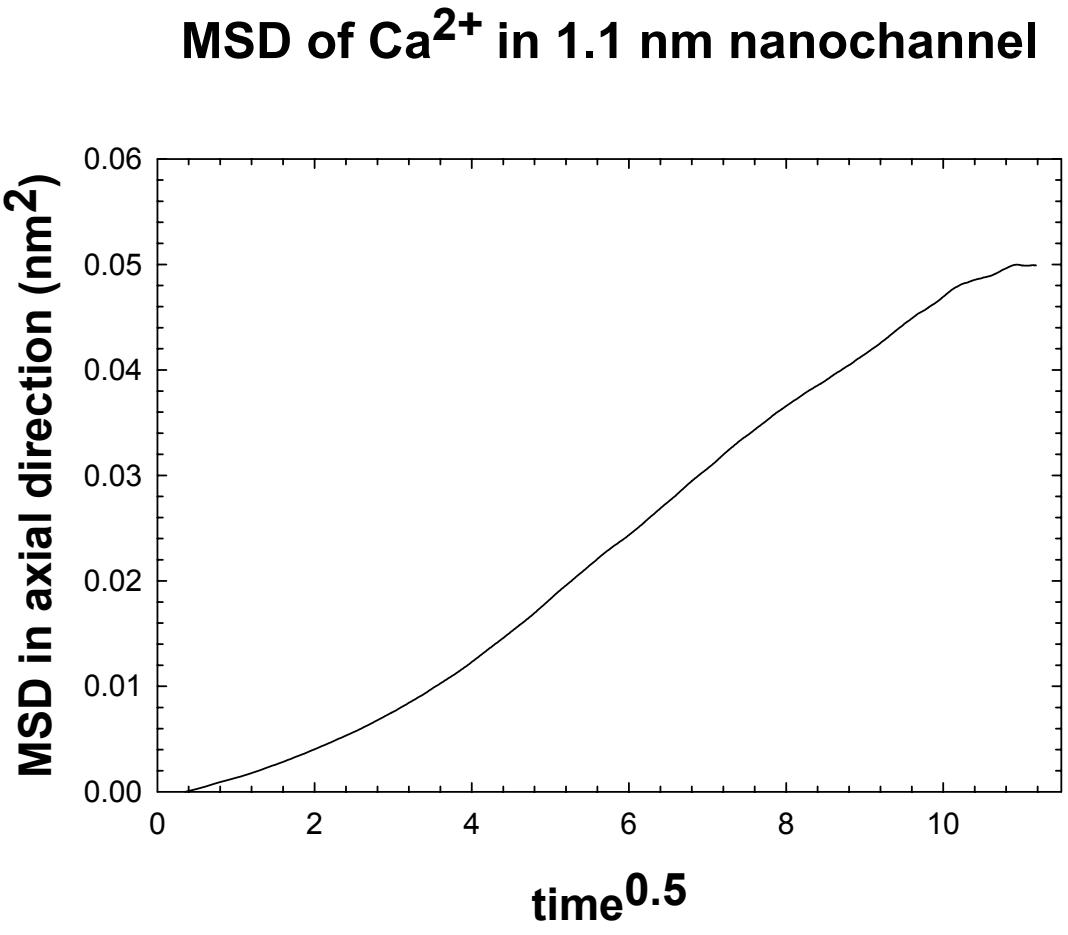

Figure 22: The mean square displacement (MSD) of calcium ions in silica nanochannel with radius = 1.1 nm. [MSD (nm^2) ~ $t^{0.5}$ ($ps^{0.5}$)]

Slope = 5.410×10^{-5} $cm^2/s^{0.5}$

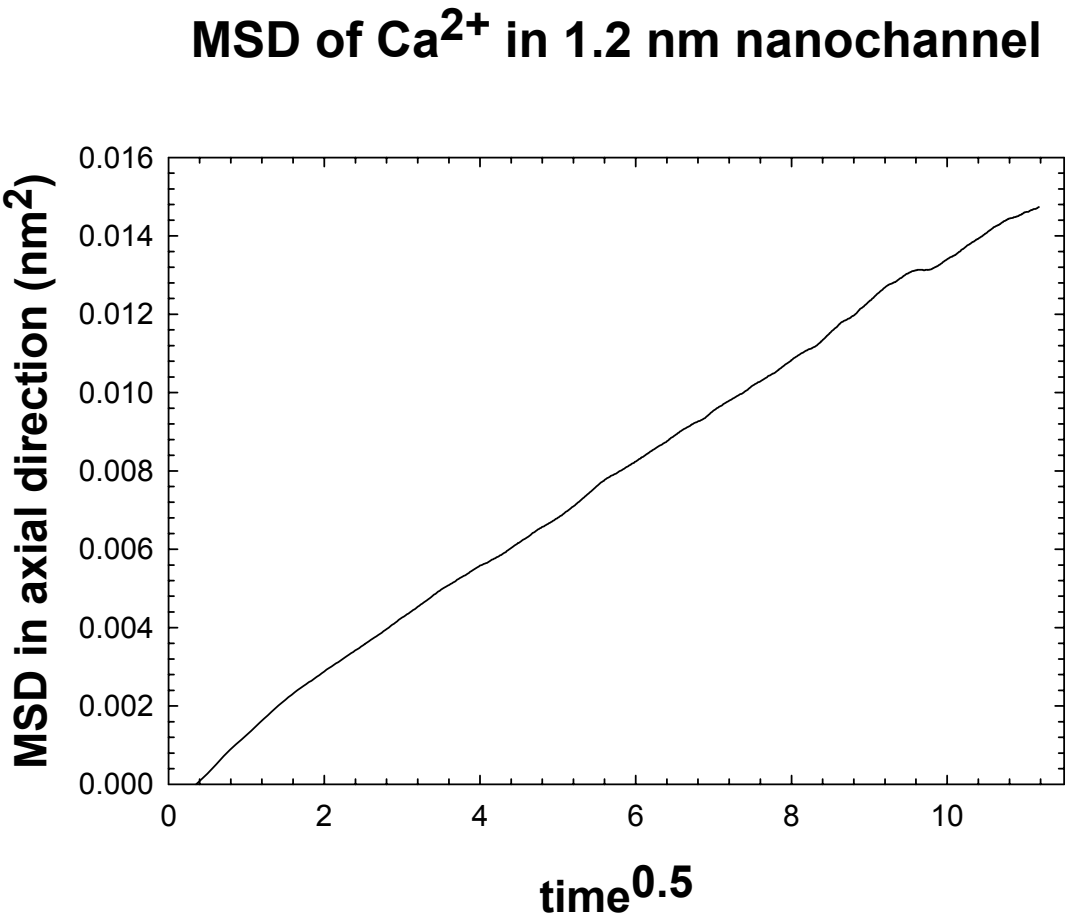

Figure 23: The mean square displacement (MSD) of calcium ions in silica nanochannel with radius = 1.2 nm. [MSD (nm^2) ~ $t^{0.5}$ ($ps^{0.5}$)]

Slope = 1.321×10^{-5} $cm^2/s^{0.5}$

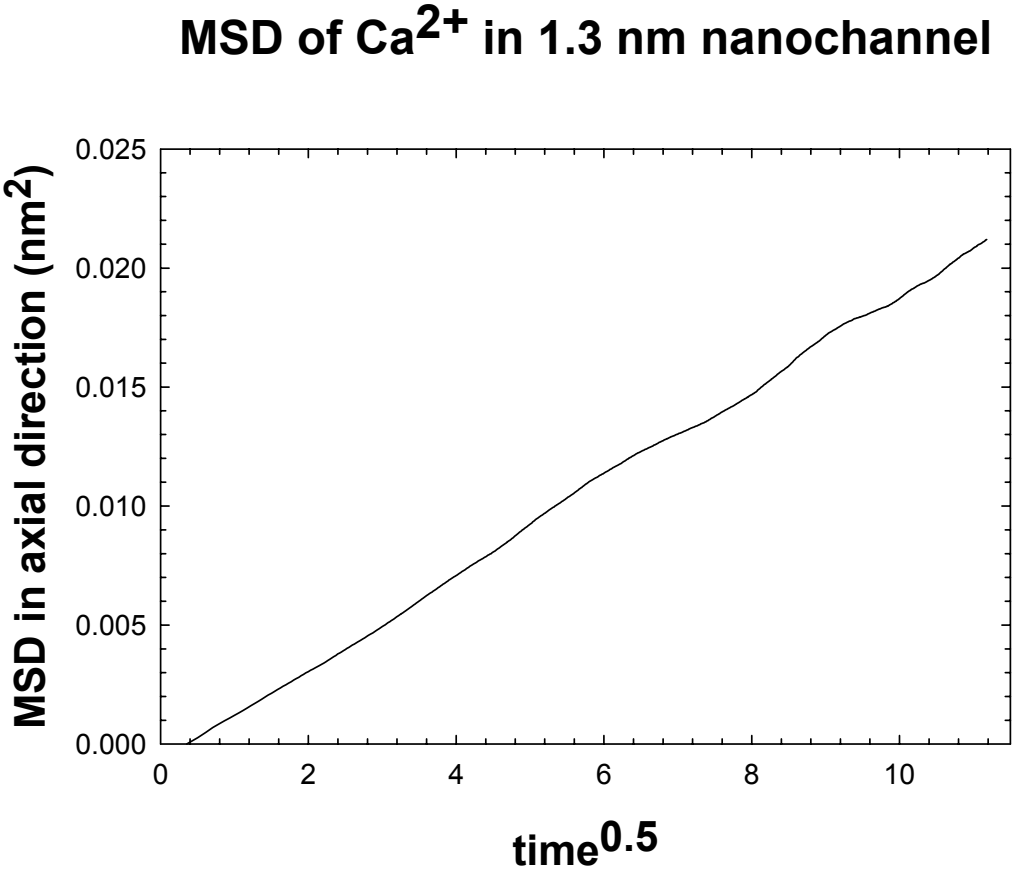

Figure 24: The mean square displacement (MSD) of calcium ion in silica nanochannel with radius = 1.3 nm. [MSD (nm^2) ~ $t^{0.5}$ ($ps^{0.5}$)]

Slope = 1.956×10^{-5} $cm^2/s^{0.5}$

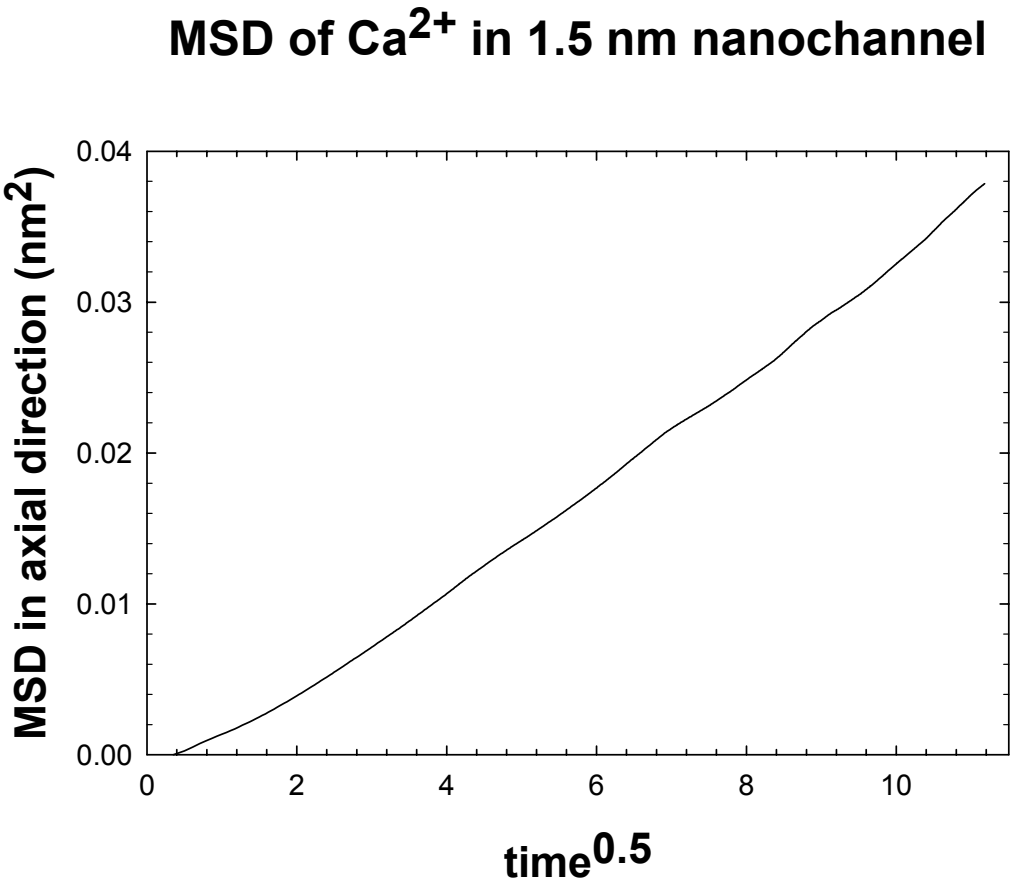

Figure 25: The mean square displacement (MSD) of calcium ions in silica nanochannel with radius = 1.5 nm. [MSD (nm^2) ~ $t^{0.5}$ ($ps^{0.5}$)]

Slope = 3.645×10^{-5} $cm^2/s^{0.5}$

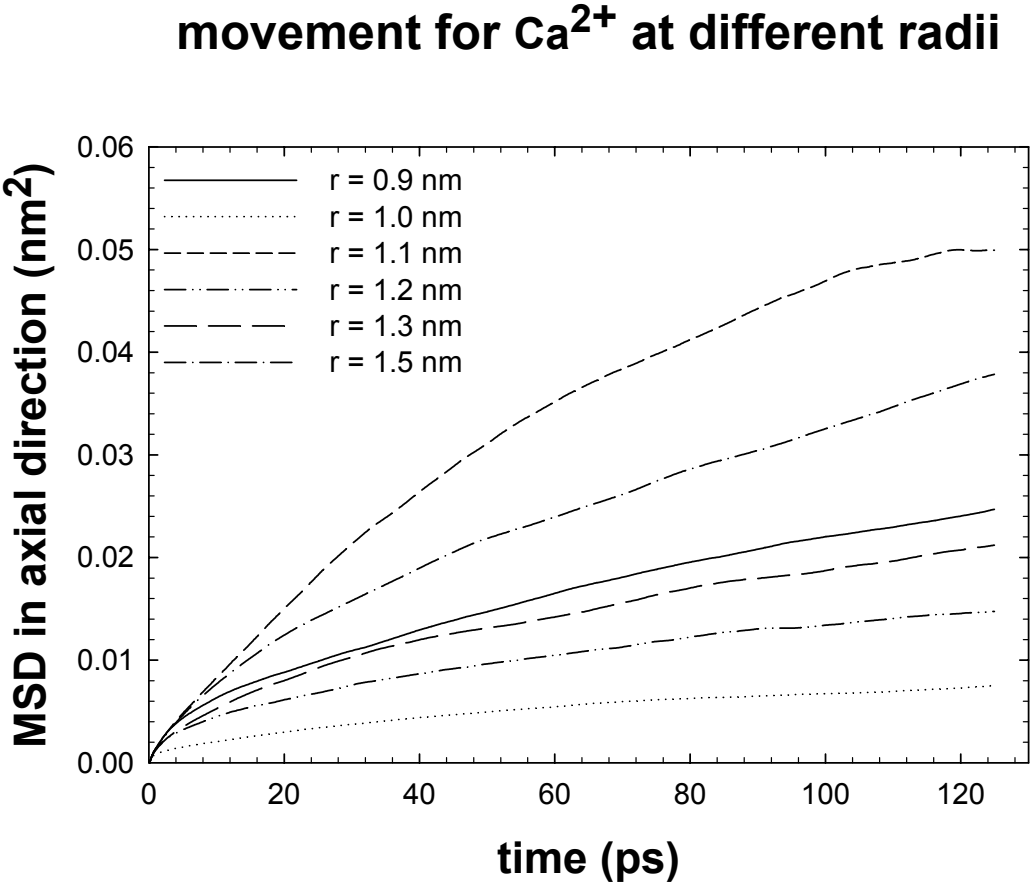

Figure 26: The mean square displacement (MSD) of calcium ions in aqueous electrolytes solution system at different nanochannel radii.

channel diameter, where fluid molecules are constrained so as not be able to pass each other, like the single-lane road where overtaking is not allowed[33]. However, in this research, the effective channel diameter is larger than any of the characteristic minimum length scales (Table 1). For instance, twice $\sigma_{Ca-Ca} = 0.579nm$ is still smaller than any nanochannel diameter designed, similarly to other parameters. So an ion (calcium or chloride) in the nanochannel should easily pass another ion (calcium or chloride) without overlap.

The implication is that the characteristic for calcium ions may not be the single-file diffusion (SFD). Tracking the mean square displacement of calcium ions (Figure 20-26), the MSD values are very small, which confirms again calcium ions in the electrolytes solutions do not move much (Figure 13 and 14) as mentioned before. For long periods of time Ca^{2+} ions remain fixed on the points where charges are set or just vibrate back and forth close to charges. This gives rise to "anomalous self-diffusion" of calcium ions. One additional thing needs to be pointed out: other monovalent cations like Na^{+}[17], Li^{+}, Rb^{+}, Cs^{+} exhibit ordinary self-diffusion along the channel axis, in which MSD is proportional to the observation time. This suggests divalent charges from calcium ions might lead to the anomalous self-diffusion, while calcium ions are strongly attracted to the charges and forbidden to move. But the exact explanation for calcium ions self-diffusion remains elusive. Perhaps, because of the similarity of random motion of Ca^{2+} around the surface charges to vibrational molecular motion in single file diffusion, the MSD of Ca^{2+} displays similarity to single-file diffusion in short time. The present simulations are not long enough to explore the long-time behavior (Table 6).

Table 6: Slopes of MSD vs. Time$^{0.5}$ at different nanochannel radii

($CaCl_2$ solutions)

Radius (nm)	Slopes (1×10^{-5} $cm^2/s^{0.5}$)
0.9	2.320
1.0	0.675
1.1	5.410
1.2	1.321
1.3	1.956
1.5	3.645

There is also good linearity of fit of the MSD vs. time for chloride ions in different radius nanochannels, as shown in Figure 27, demonstrating ordinary self-diffusion for chloride ions. The self-diffusivity values are shown in Table 7. Apparently, the calcium ions attracted to the wall charges present an obstacle so that chloride ions move somewhat slower than in bulk water.

3.3 Charged vs. uncharged surface at fixed channel radius of 1.0 nm

The radius of the silica nanochannel is 1.0 nm and length is 6.651nm. The fluids in the charged channel consist of 467 water molecules, 3 calcium ions, 2 chloride ions. 4 negative charges are distributed at the center of wall atoms. The fluid molecules in the uncharged channel consist of 474 water molecules, 0 calcium ions, 2 chloride ions. There are no charges on the wall of the nanochannel. The results are shown from Figure 28-30.

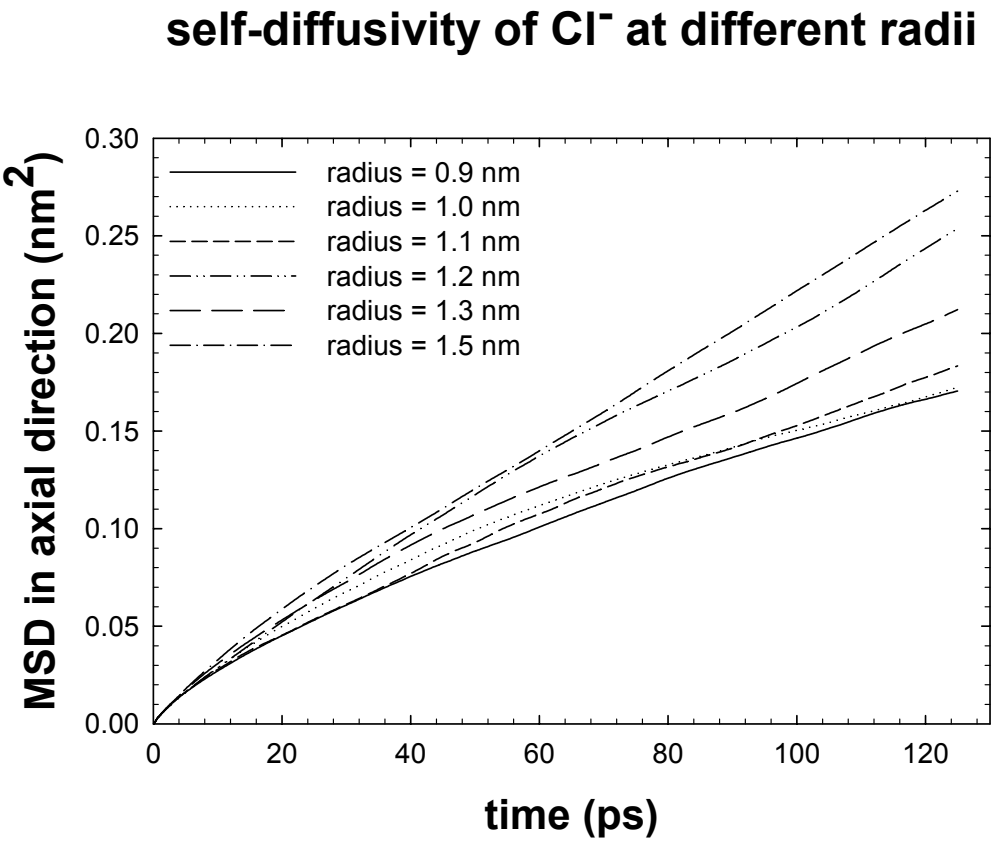

Figure 27: The mean square displacement (MSD) of chloride ions in aqueous electrolytes solution systems at different nanochannel radii.

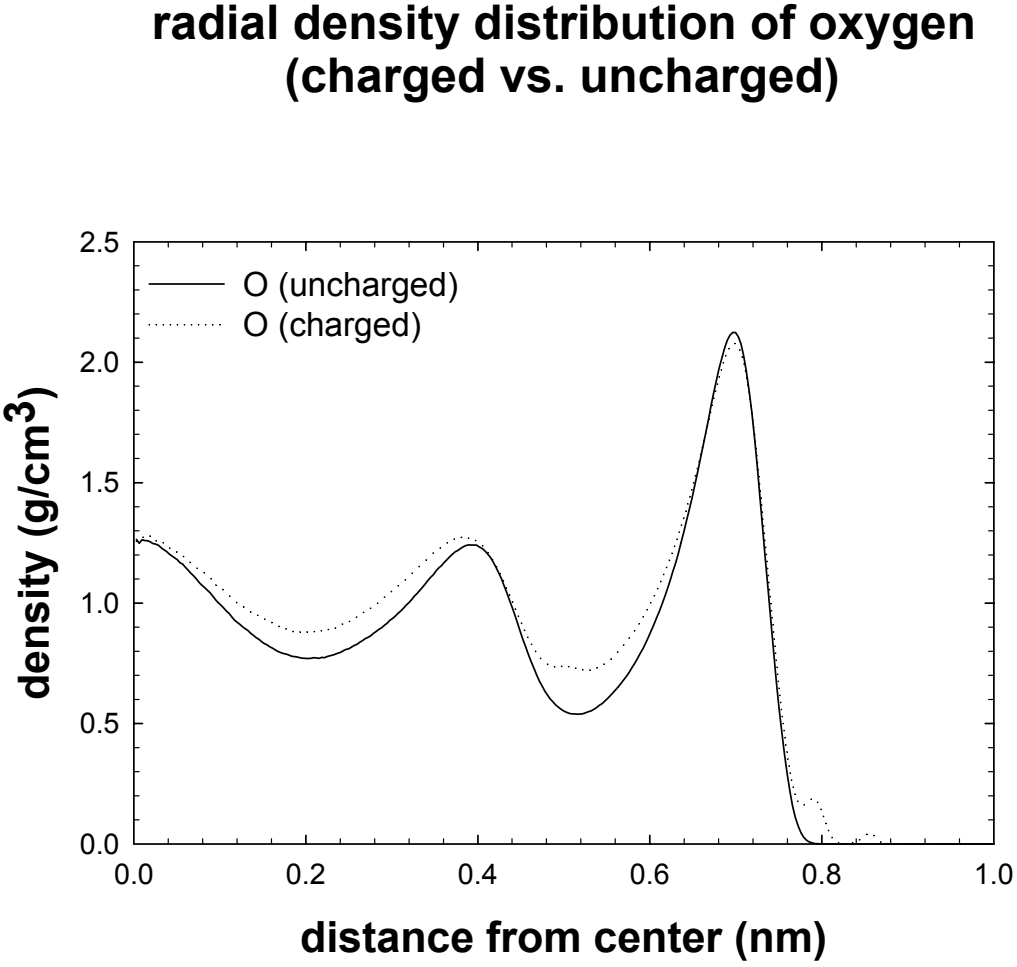

Figure 28: Radial density distribution of oxygen atoms in charged system vs. uncharged system. The radius of silica nanochannel length is 1.0 nm and length is 6.651nm. The fluid of the channel with charged wall consists of 467 water molecules, 3 calcium ions, 2 chloride ions. 4 negative charges are distributed on the center of wall atoms. The fluid in the channel with the uncharged wall consists of 474 water molecules, 0 calcium ions, 2 chloride ions. There are no charges on the wall of the nanochannel.

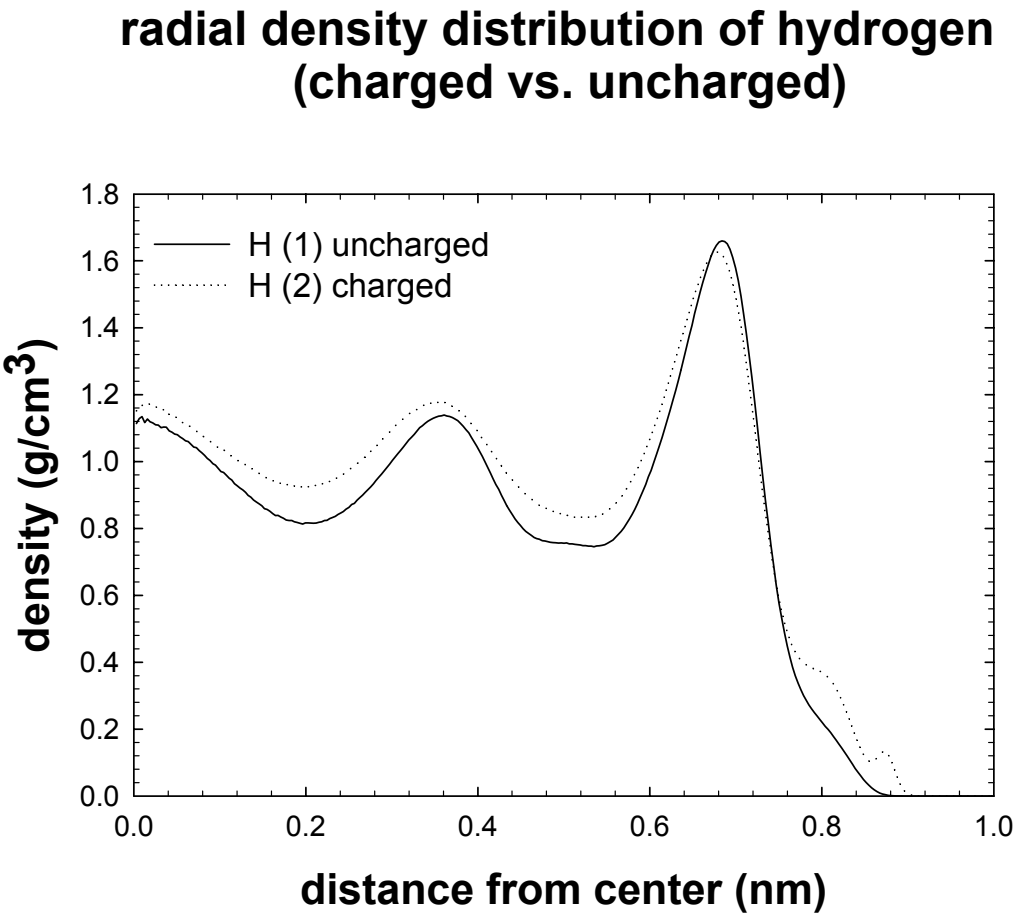

Figure 29: Radial density distribution of hydrogen atoms in charged system vs. uncharged system. The radius of silica nanochannel length is 1.0 nm and length is 6.651nm. The fluid of the channel with charged wall consists of 467 water molecules, 3 calcium ions, 2 chloride ions. 4 negative charges are distributed on the center of wall atoms. The fluid in the channel with the uncharged wall consists of 474 water molecules, 0 calcium ions, 2 chloride ions. There are no charges on the wall of the nanochannel.

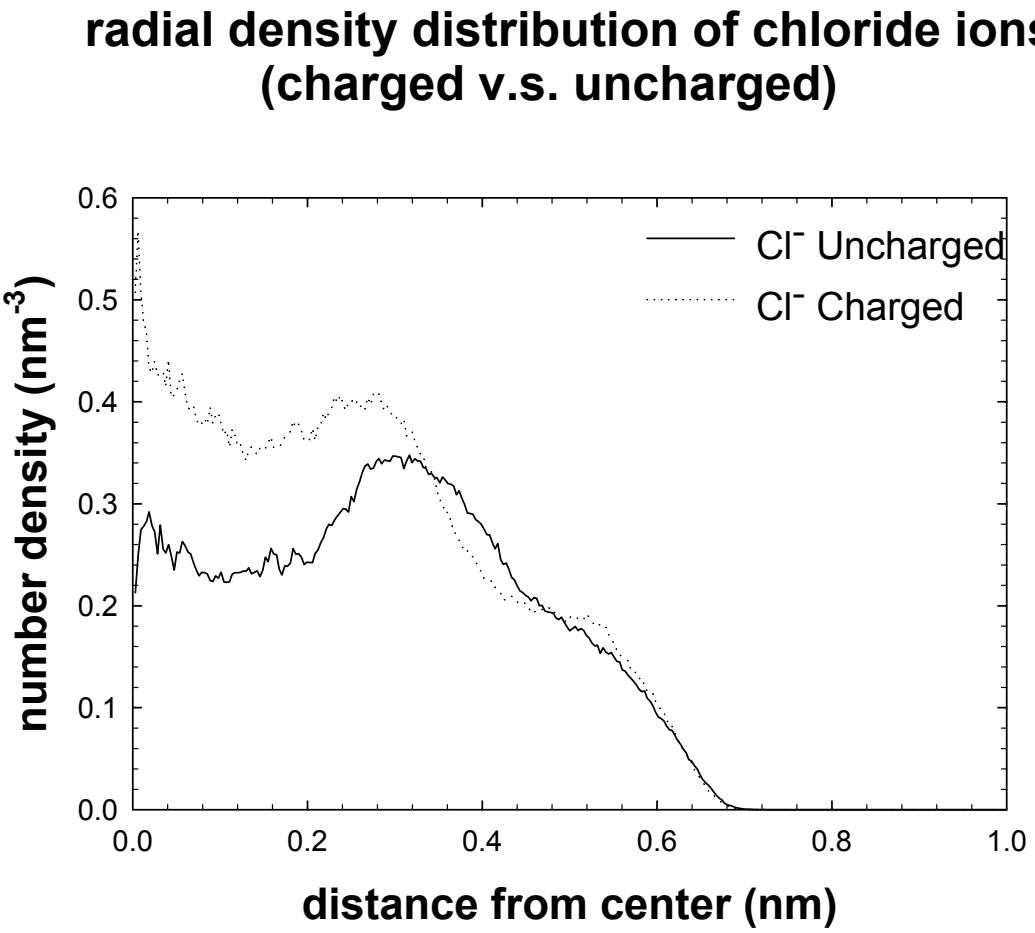

Figure 30: Radial density distribution of chloride ions in charged system vs. uncharged system. The radius of silica nanochannel length is 1.0 nm and length is 6.651nm. The fluid of the channel with charged wall consists of 467 water molecules, 3 calcium ions, 2 chloride ions. 4 negative charges were distributed on the center of wall atoms. The fluid in the channel with the uncharged wall consists of 474 water molecules, 0 calcium ions, 2 chloride ions. There are no charges on the wall of the nanochannel.

Table 7: Self-diffusivities of chloride ions along axial direction of nanochannel at different radii ($CaCl_2$ solution)

Radius (nm)	Cl^- (1×10^{-5} cm^2/s)
0.9	0.647
1.0	0.633
1.1	1.085
1.2	0.961
1.3	1.015
1.5	1.039

Note: Standard deviations for self-diffusivities must be achieved by repeating simulations. So they are not included in this simulation

Comparing the density distribution of oxygen atoms in the charged nanochannel with that in the uncharged nanochannel, the profiles show basically similar distribution except there are two small peaks near the wall surface in the charged nanochannel. As explained before, those two small peaks are caused by the interactions between wall atoms and water molecules in the valleys of wall atoms, under the effect of both L-J and electrostatic forces. Correspondingly, without the influence of charges, the two small peaks disappear, as shown in the profile of the uncharged channel. This evidence supports the earlier interpretation of the small peaks near the wall.

The density distributions of hydrogen atoms in charged and uncharged nanochannels are similar. There are three density shells in both distributions with same peak height at 0.70 nm, 0.38 nm and 0.00 nm from the center, and the distance between peaks is around the diameter of water molecules (0.30 nm).

The radial density distribution of chloride ions differs little in charged and uncharged channels, suggesting wall charges have little influence on chloride ions because of the screening effects on the wall charges by the adsorbed Ca^{2+} ions and their associated waters.

In comparison, the axial self-diffusivity of water molecules and chloride ions is decreased by 10.75 % and 68.80 % in the charged nanochannel. The values are compared and listed in Figure 31-32 and Table 8. Probably, this is attributable to the obstacle of calcium ions adsorbed on the wall charge sites.

Table 8 Comparison of self-diffusivity for charged and uncharged aqueous solutions

Radius (nm)	**Water molecules (1×10^{-5} cm^2/s)**	**Chloride ions (1×10^{-5} cm^2/s)**
1.0 (charged)	3.046	0.633
1.0 (uncharged)	3.413	2.029

Note: Standard deviations for self-diffusivities must be achieved by repeating simulations. So they are not included in this simulation.

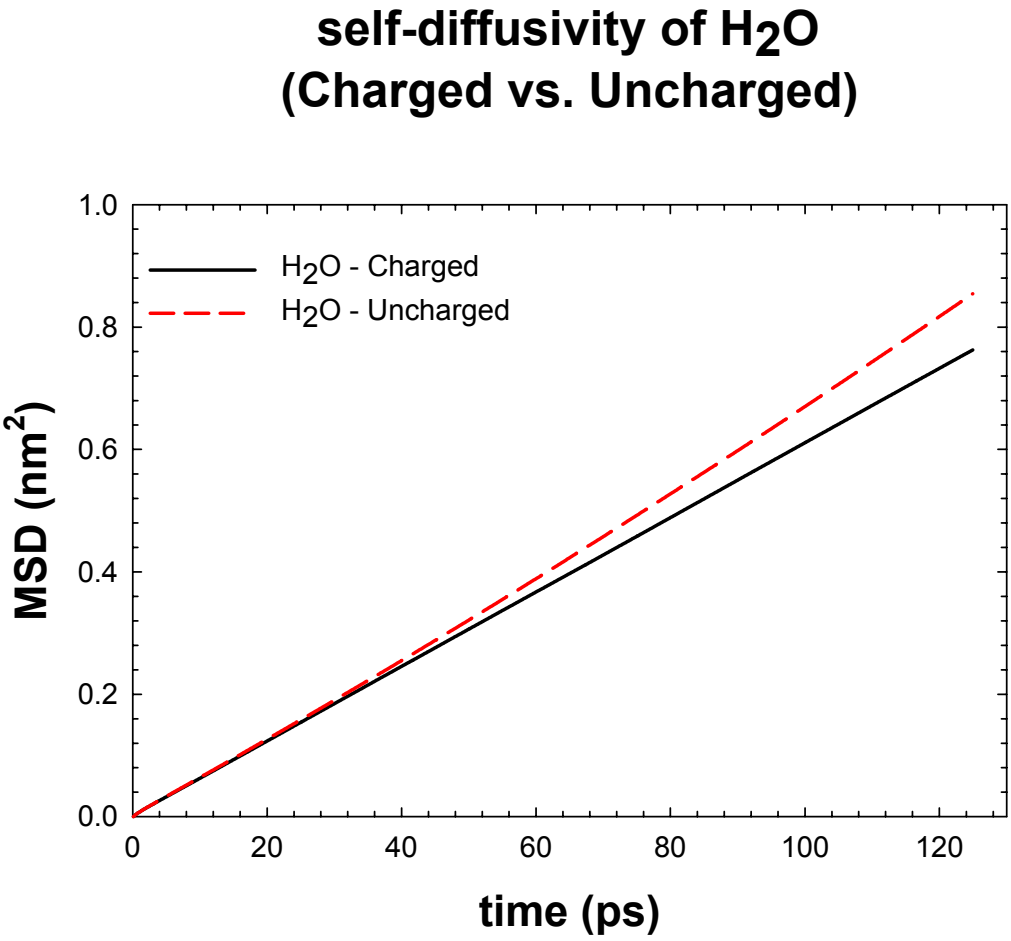

Figure 31: Self-diffusivity of water molecules ions in charged system vs. uncharged system. The radius of silica nanochannel length is 1.0 nm and length is 6.651nm. The fluid of the channel with charged wall consists of 467 water molecules, 3 calcium ions, 2 chloride ions. 4 negative charges are distributed on the center of wall atoms. The fluid in the channel with the uncharged wall consists of 474 water molecules, 0 calcium ions, 2 chloride ions. There are no charges on the wall of the nanochannel.

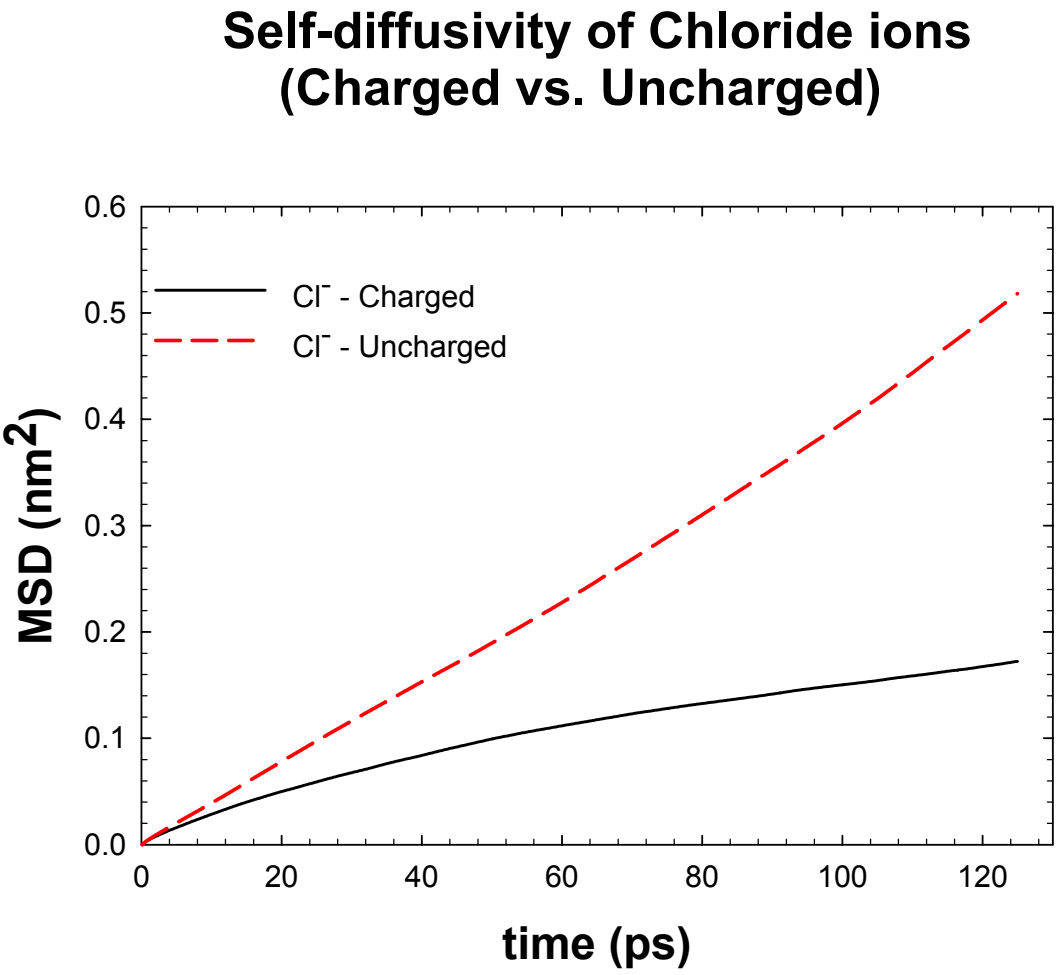

Figure 32: Self-diffusivity of chloride ions in charged system vs. uncharged system. The radius of silica nanochannel length is 1.0 nm and length is 6.651nm. The fluid of the channel with charged wall consists of 467 water molecules, 3 calcium ions, 2 chloride ions. 4 negative charges are distributed on the center of wall atoms. The fluid in the channel with the uncharged wall consists of 474 water molecules, 0 calcium ions, 2 chloride ions. There are no charges on the wall of the nanochannel.

3.4 Comparison of NaF, NaCl, NaBr, NaI in a 1.0 nm nanochannel

The behavior of anions F^-, Cl^-, Br^-, I^- has been investigated at a single radius of the nanochannel at 298K using SPC/E water model. For all the aqueous electrolytes solutions systems, the radius of the nanochannel is kept at 1.0 nm and length is 6.651 nm, where 470 water molecules, 6 sodium ions, and 2 anions are confined. 4 negative charges are distributed on the center of wall atoms. The concentration of anions ($0.132/nm^3$) and density of charges on the wall ($0.0957/nm^3$) are in accordance with $CaCl_2$ systems studied before. The core water density is fixed at 1.0 g/cm^3. The density distribution and self-diffusivities of water molecules, cations, and anions have been compared in these four aqueous solutions [(Na^+ and F^-), (Na^+ and Cl^-), (Na^+ and Br^-), (Na^+ and I^-)].

All ions are represented by a point charge centered in an L-J sphere. The potential parameters for ion-water, ion-ion, ion-wall, and water-wall interactions in these MD simulations, are listed in Tables 9-12. The radial density distribution of water molecules is displayed in Figures 33 through 36. The radial density distributions of sodium and anions are shown in Figures 39 through 42.

As seen from Figure 37 and Figure 38, the density distribution profiles for oxygen and hydrogen atoms are very similar in these four aqueous electrolytes systems, except that NaCl solutions exhibit a little bit lower density distribution. Water molecules form three distinctive layers when radial position varies from the channel center to the area close to the wall. The layer with highest probability is 0.30 nm from the wall; the second layer with less probability density is 0.61 nm from the wall, and in the center of nanochannel

Table 9 L-J parameters for NaF-H_2O-SiO_2

Pair	σ (nm)	ε / k_B (K)
Na-Na[32]	0.273	43.00
Na-F	0.2925	62.38
Na-O[15]	0.2876	62.73
O-O[16]	0.3166	78.168
F-F	0.312	90.50
F-O[15]	0.3143	84.11
Na-Wall	0.2865	99.45
F-Wall	0.306	144.27
Wall-Wall	0.3	230

Table 10 L-J parameters for NaCl-H_2O-SiO_2

Pair	σ (nm)	ε / k_B (K)
Na-Na[34]	0.273	43.00
Na-Cl	0.387	20.51
Na-O[15]	0.2876	62.73
O-O[18]	0.3166	78.168
Cl-Cl	0.486	20.19
Cl-O[15]	0.378	62.72
Na-Wall	0.2865	99.45
Cl-Wall	0.393	68.14
Wall-Wall	0.3	230

Table 11 L-J parameters for NaBr-H_2O-SiO_2

Pair	σ (nm)	ε / k_B (K)
Na-Na[34]	0.273	43.00
Na-Br	0.3636	46.53
Na-O[15]	0.2876	62.73
O-O[18]	0.3166	78.168
Br-Br[35]	0.4542	50.36
Br-O[15]	0.3854	62.74
Na-Wall	0.2865	99.45
Br-Wall	0.3771	107.62
Wall-Wall	0.3	230

Table 12 L-J parameters for NaI-H_2O-SiO_2

Pair	σ (nm)	ε / k_B (K)
Na-Na[34]	0.273	43.00
Na-I	0.395	46.53
Na-O[15]	0.2876	62.73
O-O[18]	0.3166	78.168
I-I[35]	0.517	50.36
I-O[15]	0.4168	62.74
Na-Wall	0.2865	99.45
I-Wall	0.4085	107.62
Wall-Wall	0.3	230

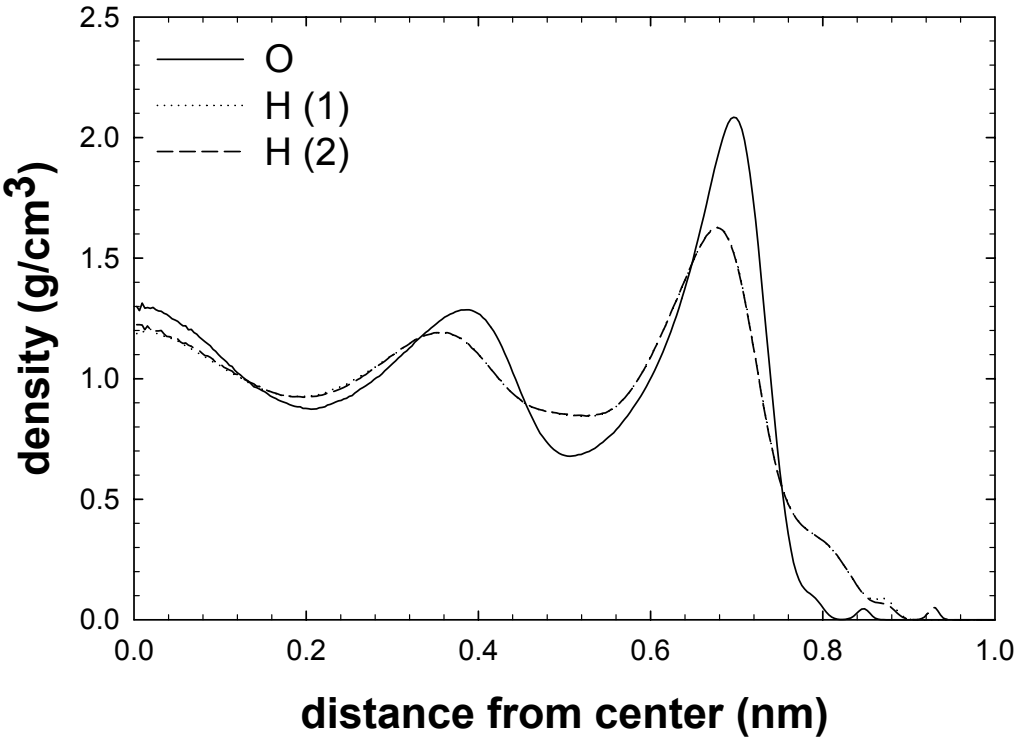

Figure 33: Radial density distribution of oxygen and hydrogen atoms when the radius of silica nanochannel is 1.0 nm (NaF). The system consists of 467 water molecules, 6 sodium ions, 2 chloride ions. 4 negative charges are distributed on the wall surface. The channel length is 6.651 nm, while the concentration of chloride ions ($0.132/nm^3$) and density of charges on the wall ($0.0957/nm^2$) are kept constant.

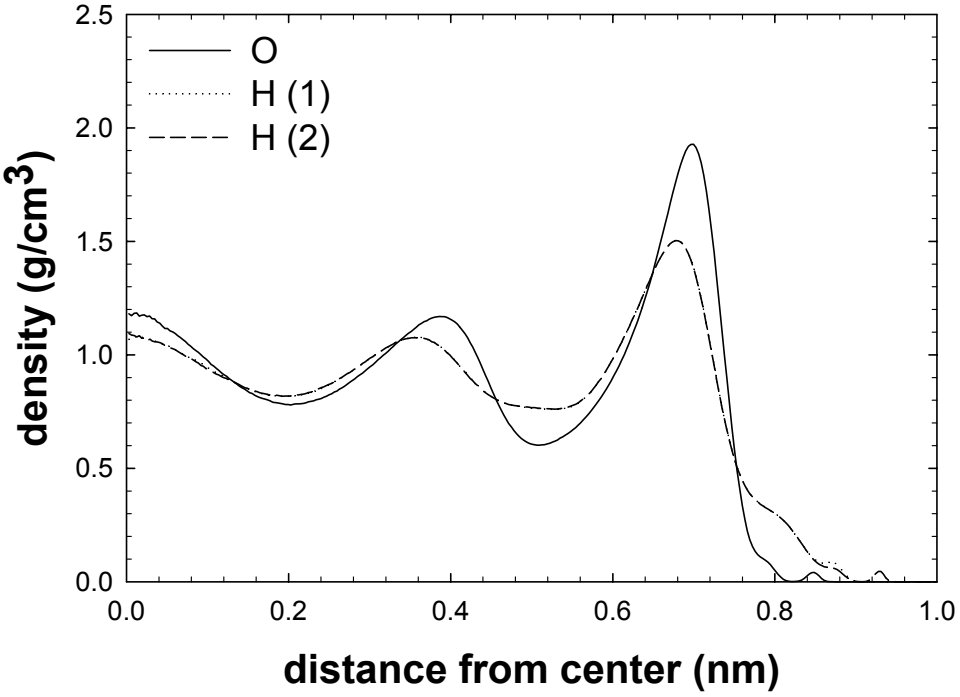

Figure 34: Radial density distribution of oxygen and hydrogen atoms when the radius of silica nanochannel is 1.0 nm (NaCl). The system consists of 467 water molecules, 6 sodium ions, 2 chloride ions. 4 negative charges are distributed on the wall surface. The channel length is 6.651 nm, while the concentration of chloride ions ($0.132/nm^3$) and density of charges on the wall ($0.0957/nm^2$) are kept constant.

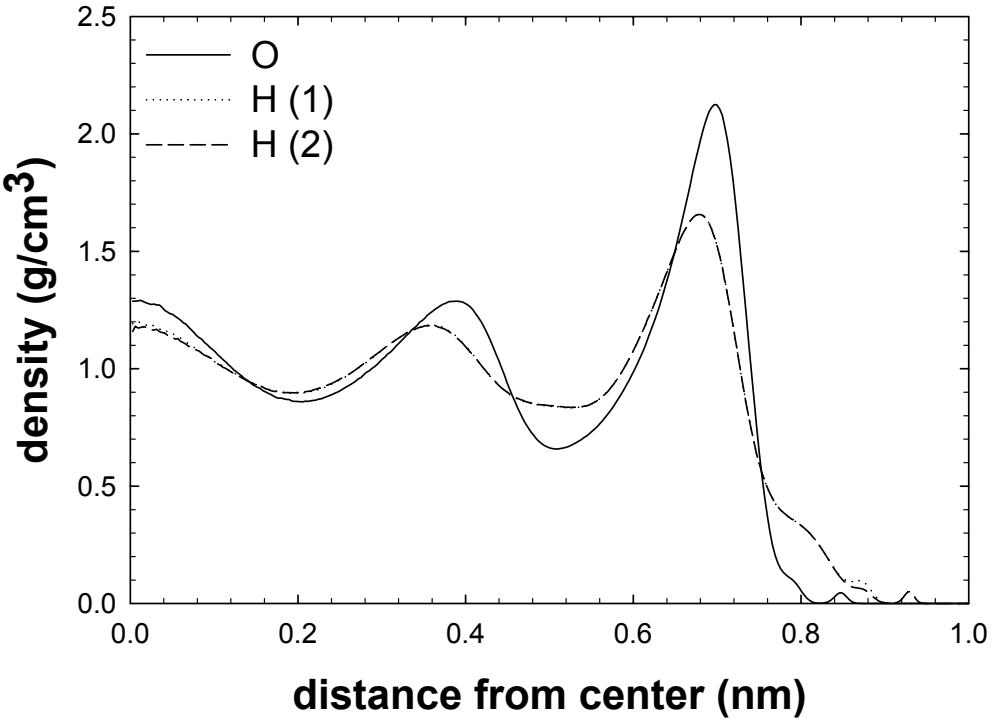

Figure 35: Radial density distribution of oxygen and hydrogen atoms when the radius of silica nanochannel is 1.0 nm (NaBr). The system consists of 467 water molecules, 6 sodium ions, 2 chloride ions. 4 negative charges are distributed on the wall surface. The channel length is 6.651 nm, while the concentration of chloride ions (0.132/nm^3) and density of charges on the wall (0.0957/nm^2) are kept constant.

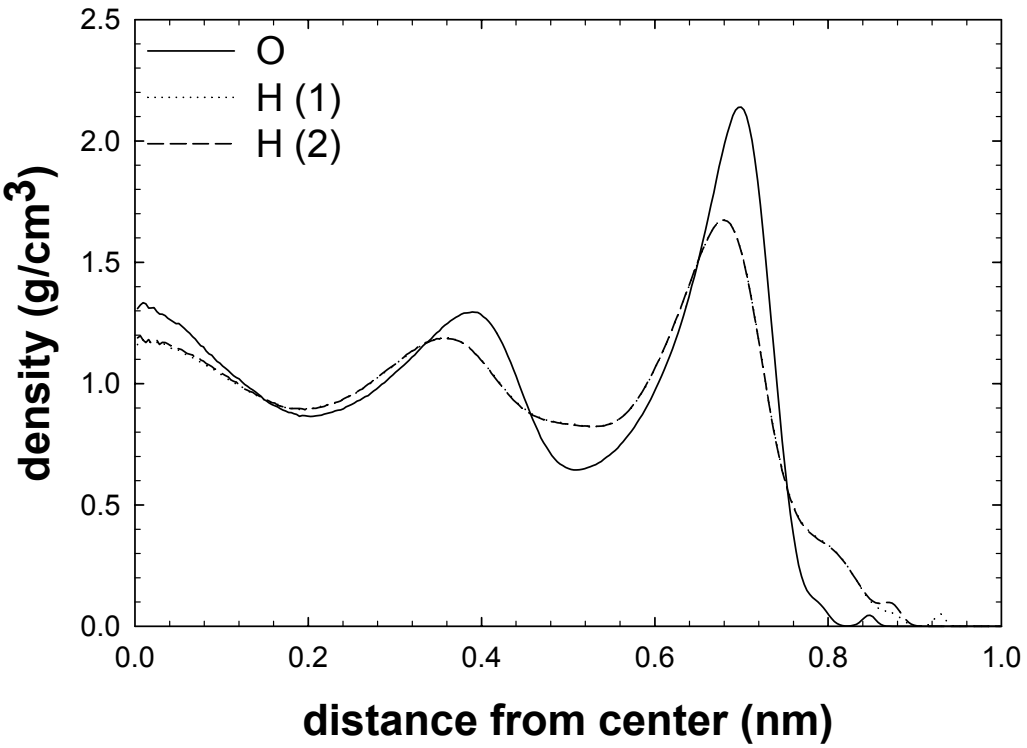

Figure 36: Radial density distribution of oxygen and hydrogen atoms when the radius of silica nanochannel is 1.0 nm (NaI). The system consists of 467 water molecules, 6 sodium ions, 2 chloride ions. 4 negative charges are distributed on the wall surface. The channel length is 6.651 nm, while the concentration of chloride ions (0.132/nm^3) and density of charges on the wall (0.0957/nm^2) are kept constant.

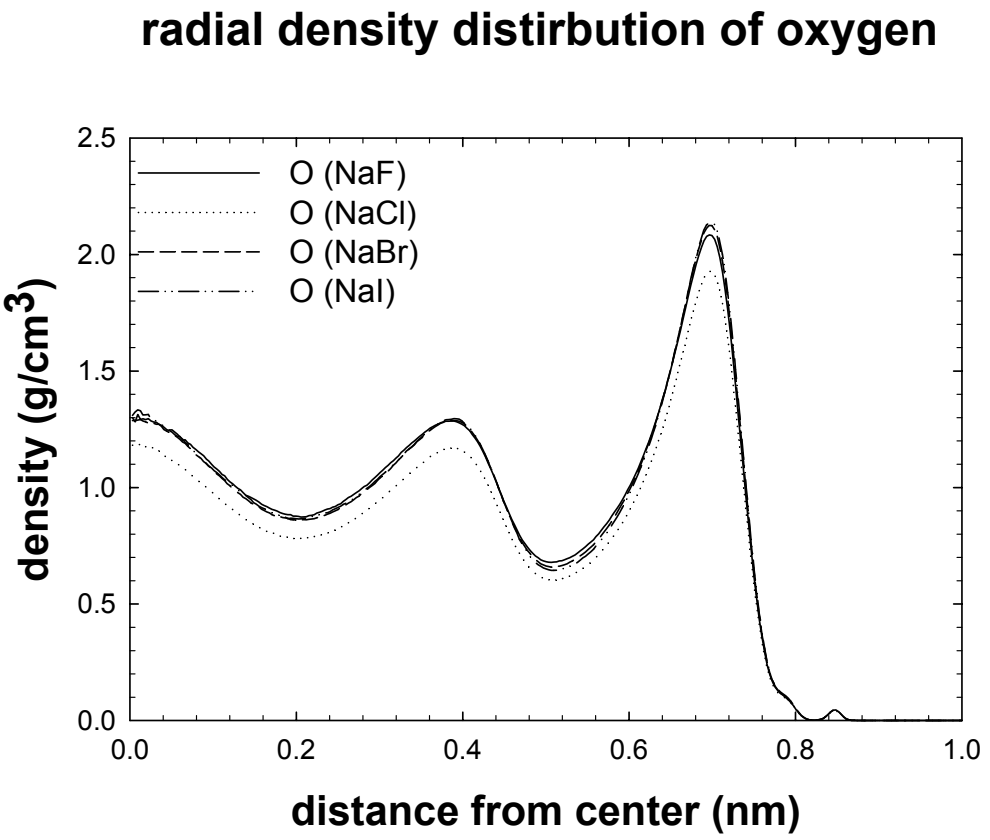

Figure 37: Radial density distribution of oxygen atoms in NaF, NaBr, NaCl, NaI aqueous solutions respectively. For every aqueous system, it consists of 467 water molecules, 6 cation ions, 2 chloride ions in the same size nanochannel with 1.0 nm radius and 6.651 nm cell length in the axial direction. 4 negative charges are distributed on the center of wall atoms nearest these charges. The concentration of anions ($0.132/nm^3$) and density of charges on the wall ($0.0957/nm^2$) are kept constant.

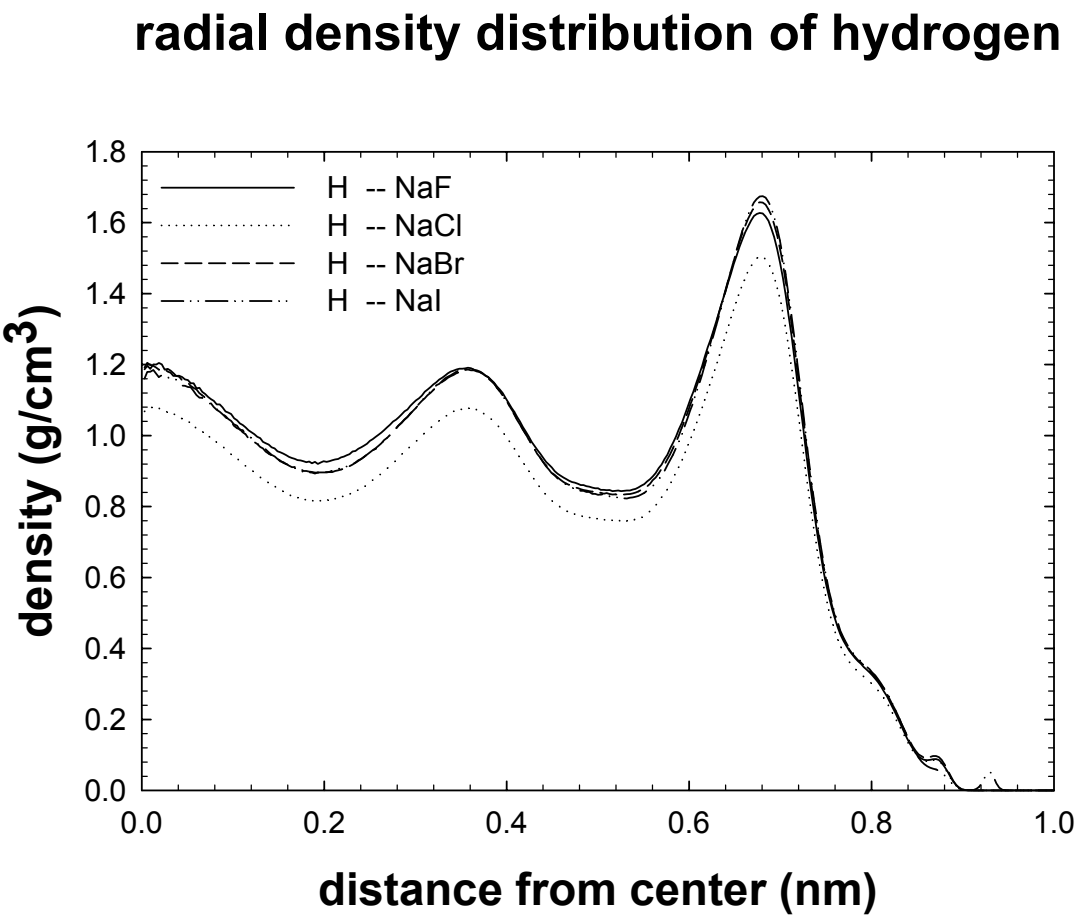

Figure 38: Radial density distribution of hydrogen atoms in NaF, NaBr, NaCl, NaI aqueous solutions respectively. For every aqueous system, it consists of 467 water molecules, 6 cation ions, 2 chloride ions in the same size nanochannel with 1.0 nm radius and 6.651 nm cell length in the axial direction. 4 negative charges are distributed on the center of wall atoms nearest these charges. The concentration of anions ($0.132/nm^3$) and density of charges on the wall ($0.0957/nm^2$) are kept constant.

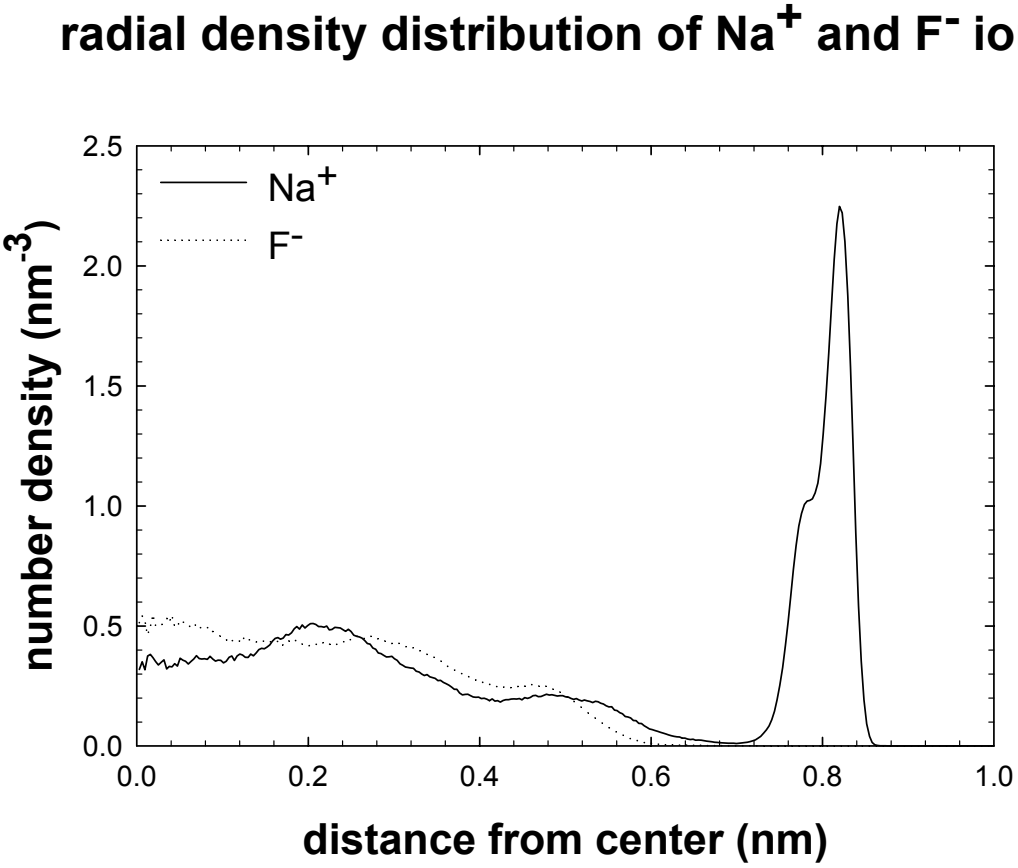

Figure 39: Radial density distribution of sodium and fluoride ions when the radius of silica nanochannel is 1.0 nm. The system consists of 467 water molecules, 6 sodium ions, 2 chloride ions. 4 negative charges are distributed on the wall surface. The channel length is 6.651 nm, while the concentration of chloride ions ($0.132/nm^3$) and density of charges on the wall ($0.0957/nm^2$) are kept constant.

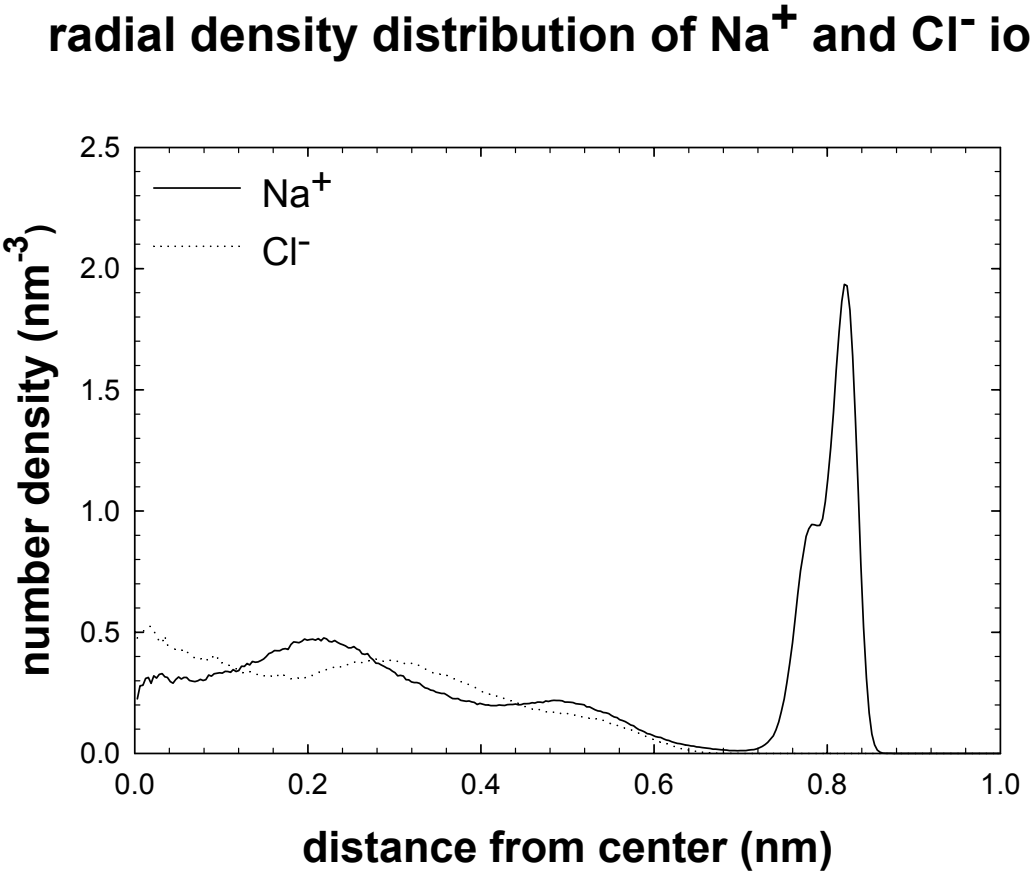

Figure 40: Radial density distribution of sodium and chloride ions when the radius of silica nanochannel is 1.0 nm. The system consists of 467 water molecules, 6 sodium ions, 2 chloride ions. 4 negative charges are distributed on the wall surface. The channel length is 6.651 nm, while the concentration of chloride ions (0.132/nm^3) and density of charges on the wall (0.0957/nm^2) are kept constant.

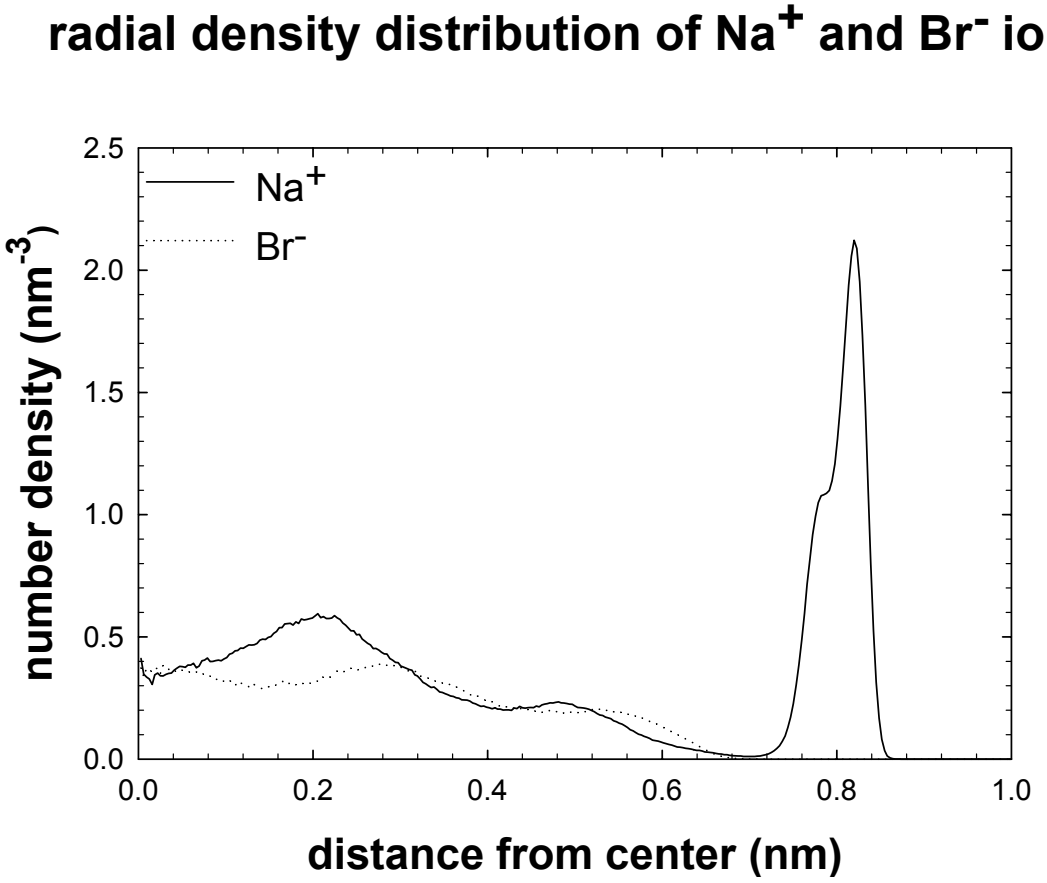

Figure 41: Radial density distribution of sodium and bromide ions when the radius of silica nanochannel is 1.0 nm. The system consists of 467 water molecules, 6 sodium ions, 2 chloride ions. 4 negative charges are distributed on the wall surface. The channel length is 6.651 nm, while the concentration of chloride ions (0.132/nm^3) and density of charges on the wall (0.0957/nm^2) are kept constant.

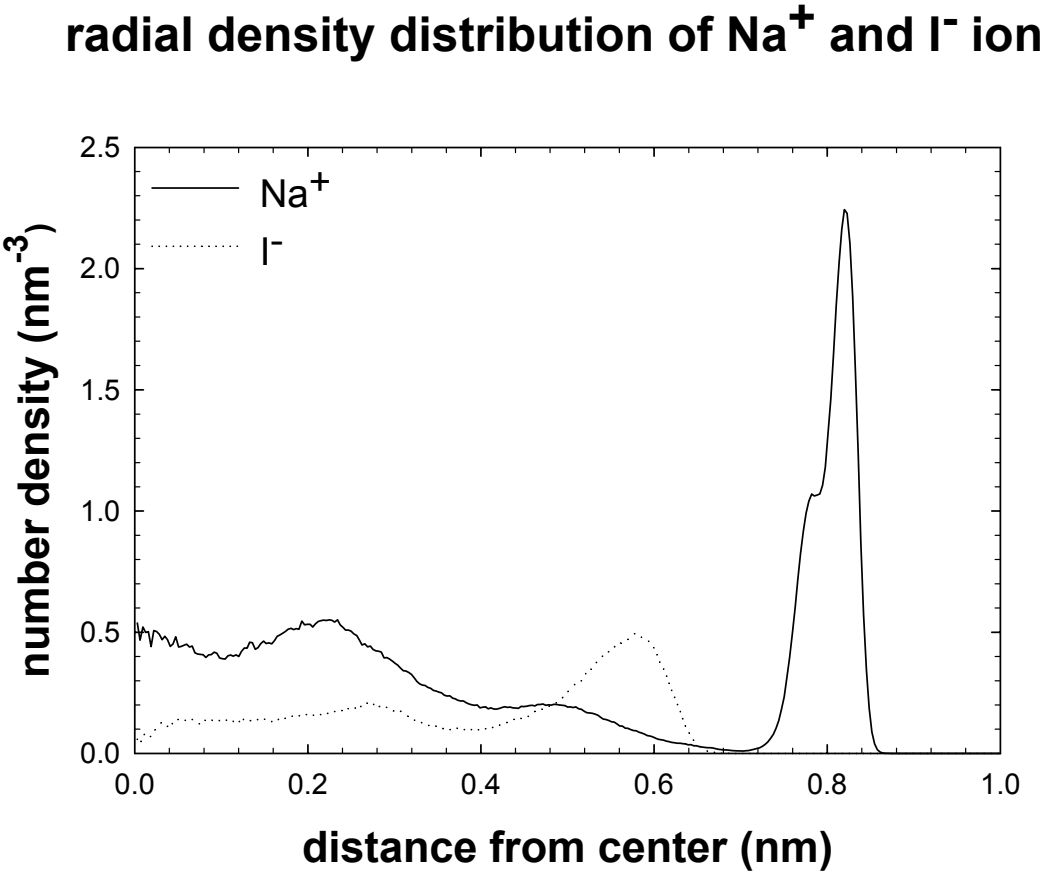

Figure 42: Radial density distribution of sodium and iodine ions when the radius of silica nanochannel is 1.0 nm. The system consists of 467 water molecules, 6 sodium ions, 2 chloride ions. 4 negative charges are distributed on the wall surface. The channel length is 6.651 nm, while the concentration of chloride ions (0.132/nm^3) and density of charges on the wall (0.0957/nm^2) are kept constant.

there is a third distinctive peak. Under the effect of charges distributed on the wall atoms, water structure is distributed in a way that hydrogen is closer to the wall than oxygen. There are also very small peaks adjacent to the wall, similarly to $CaCl_2$ aqueous systems, indicating again by sitting between the valleys of wall atoms, water molecules are subject to both electrostatic and L-J interactions from the wall charges. (See section 3.1 for discussion of these small peaks).

From Figure 43, the density distribution of sodium ions is very similar for every case. There is a distinct sharp peak of the sodium ions 0.2 nm from the wall, suggesting the adsorption of sodium ions to the charged sites. Unlike calcium ions, every sodium ion only has one positive charge, so when the negative unit charge on the surface captures a sodium ion there is little to hold the first shell of water molecules around the ion and the ion adsorbs directly to the surface charge site. As discussed earlier by Zhou[16], 4 sodium ions are attracted to the charge sites and other 2 sodium ions move freely in the system. The attachment of these 4 sodium ions neutralizes the wall charges so that the radial density distributions of other ions are hardly affected by the wall charges.

The radial density distribution of anions is shown in Figure 44. The height of peaks closest to the wall varies with the size of anions. As the size of the anion increases from F^-, Cl^-, Br^- to I^-, the height of peaks increases too. This order at first seems counterintuitive, but the anions carry the *same* charge as the wall atoms. So, the *repulsive*

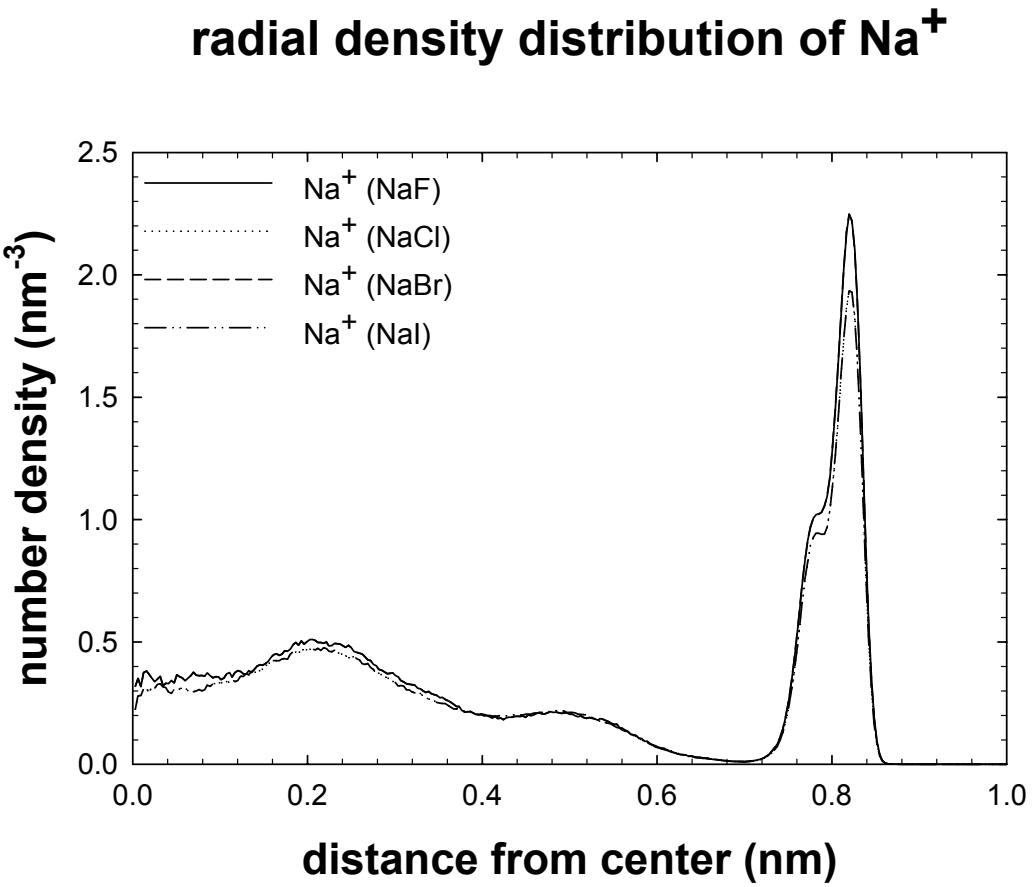

Figure 43: Radial density distribution of sodium ions in NaF, NaCl, NaBr, NaI aqueous solutions respectively. For every aqueous system, it consists of 467 water molecules, 6 cation ions, 2 chloride ions in the same size nanochannel with 1.0 nm radius and 6.651 nm cell length in the axial direction. 4 negative charges are distributed on the center of wall atoms nearest these charges. The concentration of anions ($0.132/nm^3$) and density of charges on the wall ($0.0957/nm^2$) are kept constant.

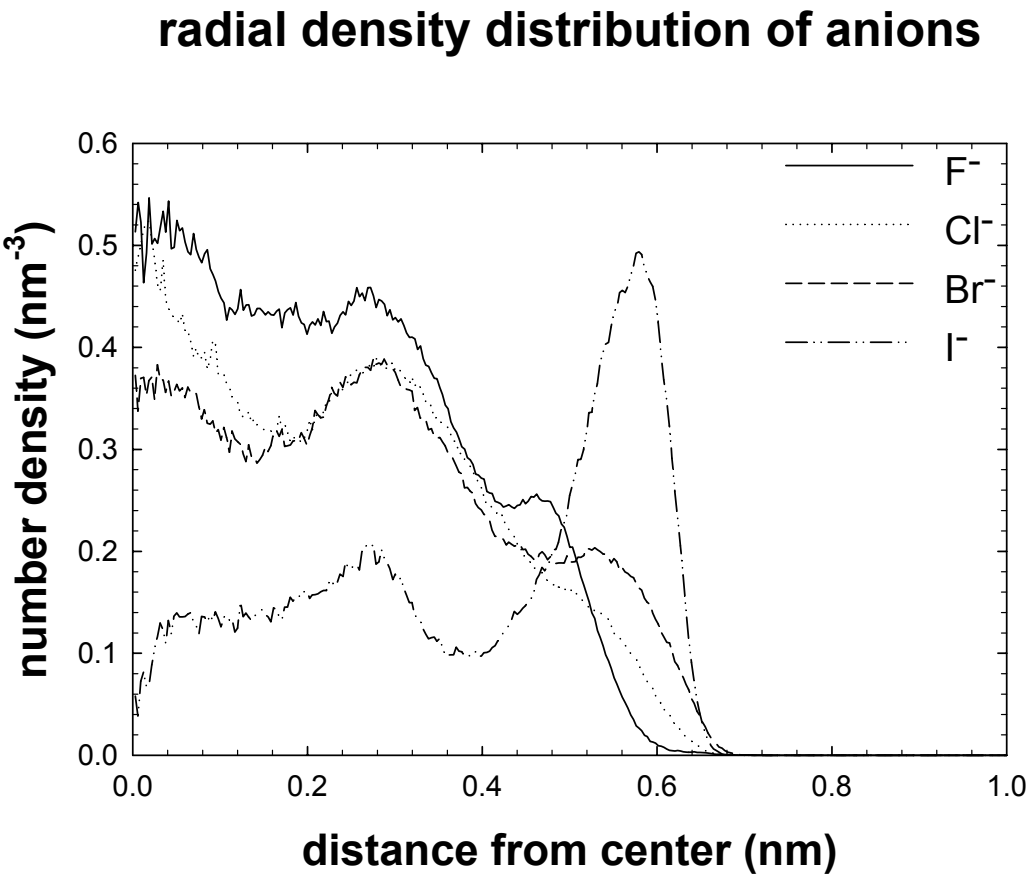

Figure 44: Radial density distribution of anions in NaF, NaCl, NaBr, NaI aqueous solutions respectively. For every aqueous system, it consists of 467 water molecules, 6 cation ions, 2 chloride ions in the same size nanochannel with 1.0 nm radius and 6.651 nm cell length in the axial direction. 4 negative charges are distributed on the center of wall atoms nearest these charges. The concentration of anions ($0.132/nm^3$) and density of charges on the wall ($0.0957/nm^2$) are kept constant.

force between wall charges and ions increases with decreasing ion size and the larger ions are repelled less strongly.

The self-diffusivities of water molecules, sodium ions, and anions all have an excellent fit of MSD vs. the observation time, as shown in Figure 45 to 47. The self-diffusivities for water, sodium ions, and anions are listed in Table 13. These values vary just slightly. Different anion sizes seem to have no effects on the determination of axial self-diffusivity of water or sodium. The anion self-diffusivity increases slightly with anion size. Compared with the published self-diffusivity values of F^-, Cl^-, Br^-, I^- at 298K in uncharged bulk water solutions[36], here, the self-diffusivity of F^-, Cl^-, Br^-, I^- is decreased by 25.23%, 38.84%, 43.76%, and 30.48 % respectively. That is because all the electrolytes simulated here are confined in the charged nanochannel. The sodium ions adsorbed to the wall charges present an obstacle, retarding the movement of anions and lowering their self-diffusivities.

Table 13: Self-diffusivities along axial direction of nanochannel in NaF, NaCl, NaBr, NaI aqueous electrolytes systems

Systems	H_2O (1×10^{-5} cm^2/s)	Na^+ (1×10^{-5} cm^2/s)	Anions (1×10^{-5} cm^2/s)
NaF	3.313	0.332	0.972
NaCl	3.124	0.372	1.058
NaBr	3.080	0.366	1.063
NaI	3.103	0.304	1.168

Note: Standard deviations for self-diffusivities must be achieved by repeating simulations. So they are not included in this simulation.

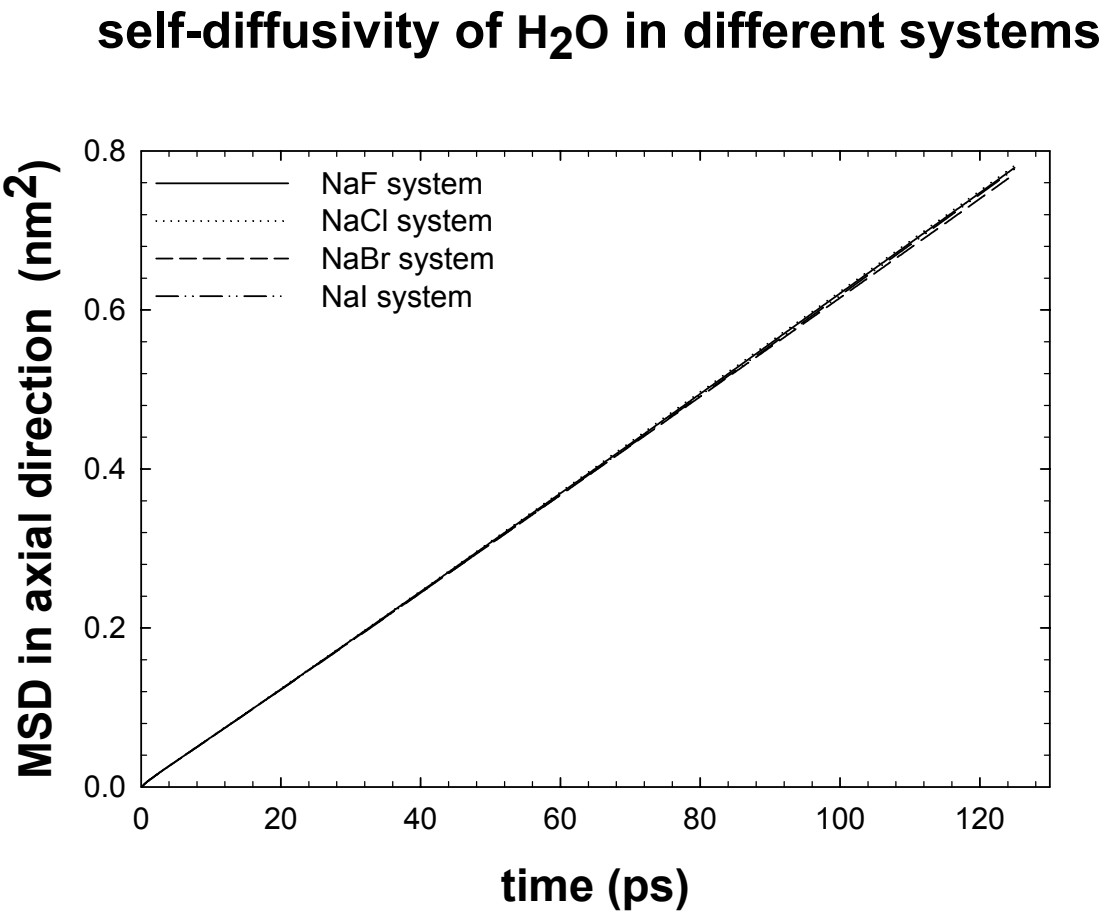

Figure 45: The mean square displacement (MSD) of water molecules versus time within silica nanochannel in NaF, NaCl, NaBr, NaI aqueous solutions. For every aqueous system, it consists of 467 water molecules, 6 cations, 2 chloride ions in the same size nanochannel with 1.0 nm radius and 6.651 nm cell length in the axial direction. 4 negative charges are distributed on the center of wall atoms nearest these charges. The concentration of anions ($0.132/nm^3$) and density of charges on the wall ($0.0957/nm^2$) are kept constant.

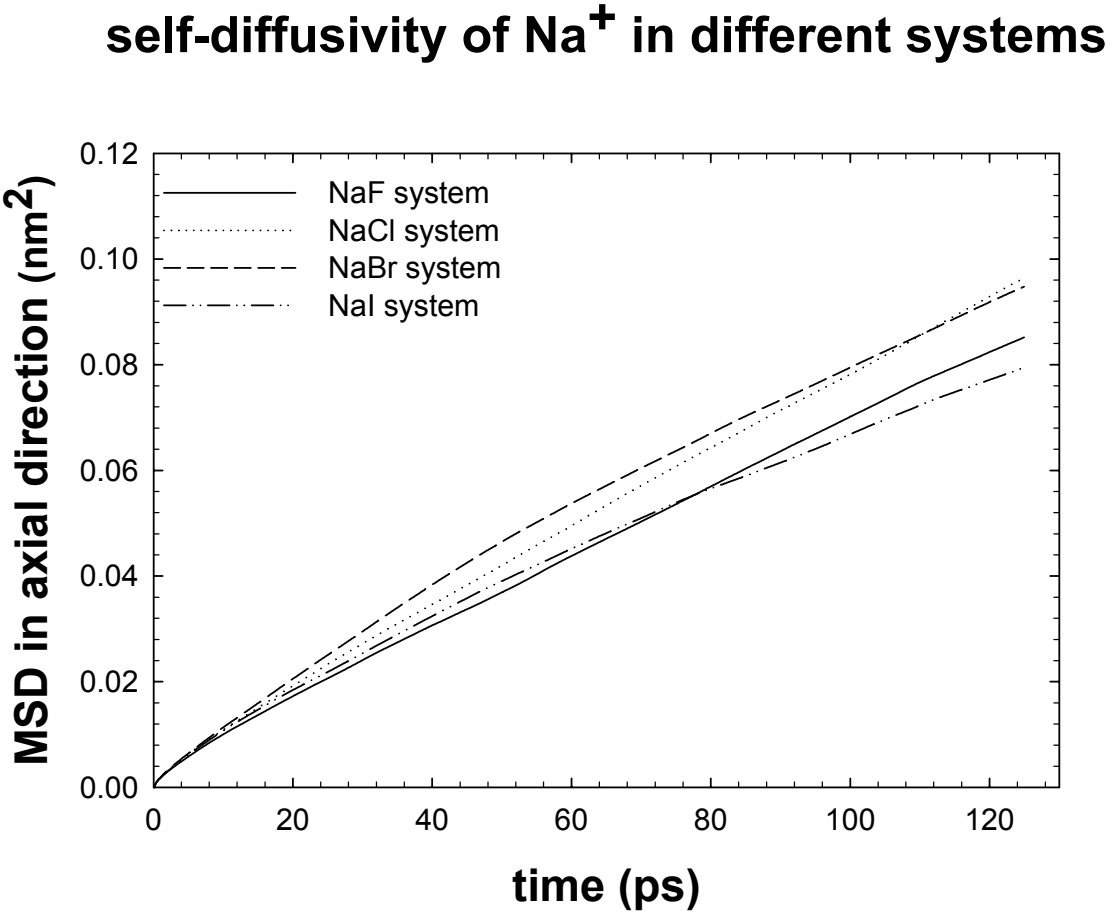

Figure 46: The mean square displacement (MSD) of sodium ions versus time within silica nanochannel in NaF, NaCl, NaBr, NaIl aqueous electrolytes solutions. For every aqueous system, it consists of 467 water molecules, 6 cations, 2 chloride ions in the same size nanochannel with 1.0 nm radius and 6.651 nm cell length in the axial direction. 4 negative charges are distributed on the center of wall atoms nearest these charges. The concentration of anions ($0.132/nm^3$) and density of charges on the wall ($0.0957/nm^2$) are kept constant.

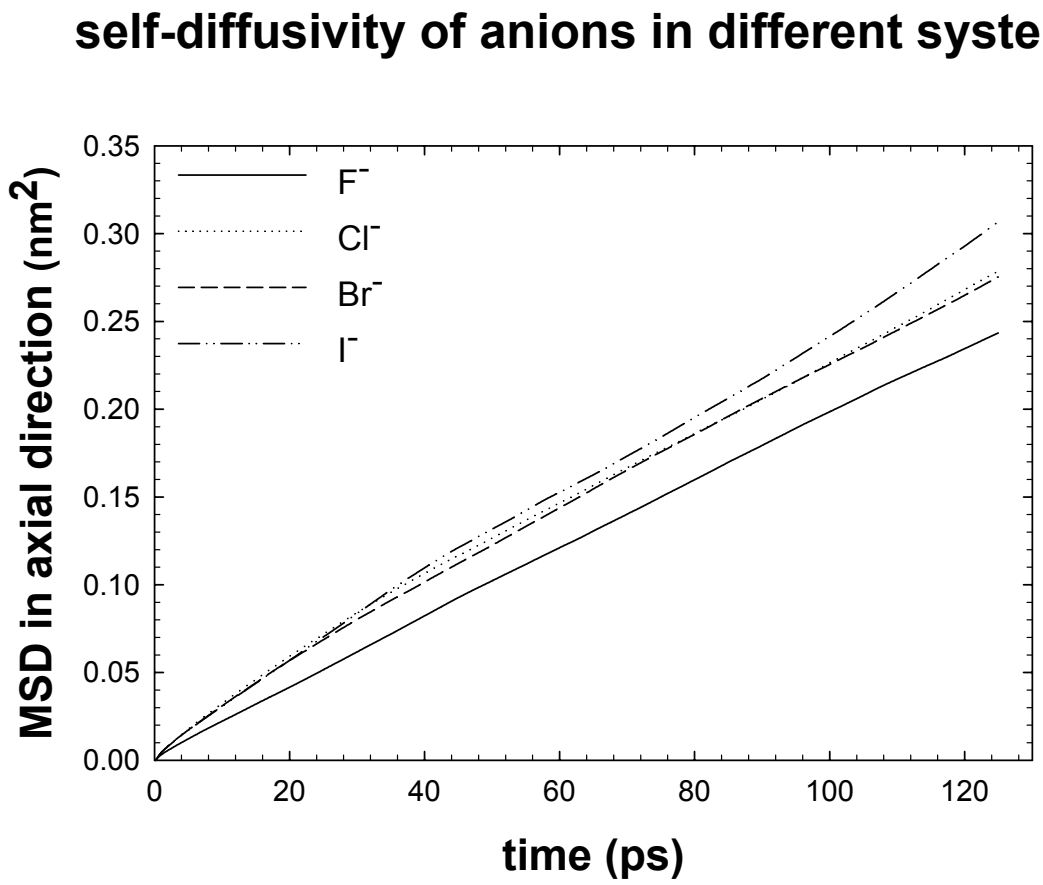

Figure 47: The mean square displacement (MSD) of anions versus time within silica nanochannel in NaF, NaCl, NaBr, NaI aqueous solutions. For every aqueous system, it consists of 467 water molecules, 6 cations, 2 chloride ions in the same size nanochannel with 1.0 nm radius and 6.651 nm cell length in the axial direction. 4 negative charges are distributed on the center of wall atoms nearest these charges. The concentration of anions ($0.132/nm^3$) and density of charges on the wall ($0.0957/nm^2$) are kept constant.

3.5 Comparison of NaCl, KCl, CsCl, RbCl in a 1.0 nm nanochannel

A series of molecular dynamics simulations of the alkali metal ions Na^+, K^+, Rb^+, Cs^+ has been implemented at a single radius of the nanochannel at 298K using the SPC/E water model. For all the aqueous electrolytes solutions, the radius of nanochannel is kept at 1.0 nm and length is 6.651 nm, where 470 water molecules, 6 cations, 2 chloride ions are confined. 4 negative charges are distributed on the center of wall atoms. The concentration of chloride ions ($0.132/nm^3$) and density of charges on the wall ($0.0957/nm^3$) are in accordance with $CaCl_2$ systems studied before. The core water density is fixed at 1.0 g/cm^3. The density distribution and self-diffusivities of water molecules, cations, and chloride ions have been compared in these four aqueous solutions [(Na^+ and Cl^-), (K^+ and Cl^-), (Cs^+ and Cl^-), (Rb^+ and Cl^-)].

The L-J potential parameters are listed in Table10, and Tables 14-16. The site charges are listed in Table 17. The radial density distribution of water molecules is displayed in Figures 48 through 51. The radial density distributions of cations and chloride are shown in Figures 54 through 57.

As seen in Figures 52 and 53, the density distributions or oxygen and hydrogen atoms are very similar in these four aqueous electrolytes systems. The RbCl distribution exhibits a little higher peak than others. Similarly to NaF, NaCl, NaBr, NaI systems, here water molecules form three distinctive layers when radial position varies from the channel center to the area close to the wall. The layer with highest probability is 0.30 nm from the

Table 14 L-J parameters for KCl-H_2O-SiO_2

Pair	**σ (nm)**	**ε / k_B (K)**
K-K	0.3334	50.34
K-Cl	0.3868	50.33
K-O[15]	0.3250	62.73
O-O[16]	0.3166	78.168
Cl-Cl[24]	0.4401	50.32
Cl-O[15]	0.3784	62.72
K-Wall	0.3167	107.60
Cl-Wall	0.3701	107.60
Wall-Wall	0.3	230

Table 15 L-J parameters for CsCl-H_2O-SiO_2

Pair	σ (nm)	ε / k_B (K)
Cs-Cs	0.3886	50.36
Cs-Cl	0.4144	50.34
Cs-O[31]	0.3526	62.74
O-O[16]	0.3166	78.168
Cl-Cl[24]	0.4401	50.32
Cl-O[15]	0.3784	62.72
Cs-Wall	0.3443	107.62
Cl-Wall	0.3701	107.6
Wall-Wall	0.3	230

Table 16 L-J parameters for RbCl-H_2O-SiO_2

Pair	σ (nm)	ε / k_B (K)
Rb-Rb	0.353	50.38
Rb-Cl	0.3965	50.35
Rb-O[31]	0.3348	62.756
O-O[16]	0.3166	78.168
Cl-Cl[24]	0.4401	50.32
Cl-O[15]	0.3784	62.72
Rb-Wall	0.3265	107.64
Cl-Wall	0.3701	107.6
Wall-Wall	0.3	230

Table 17 Site charges

Ions	Ca^{2+}	Cl^-	Na^+	K^+	Rb^+
Charge	+2	-1	+1	+1	+1
Ions	F^-	Br^-	I^-	O^{2-}	H^+
Charge	-1	-1	-1	-0.8476	+0.4238

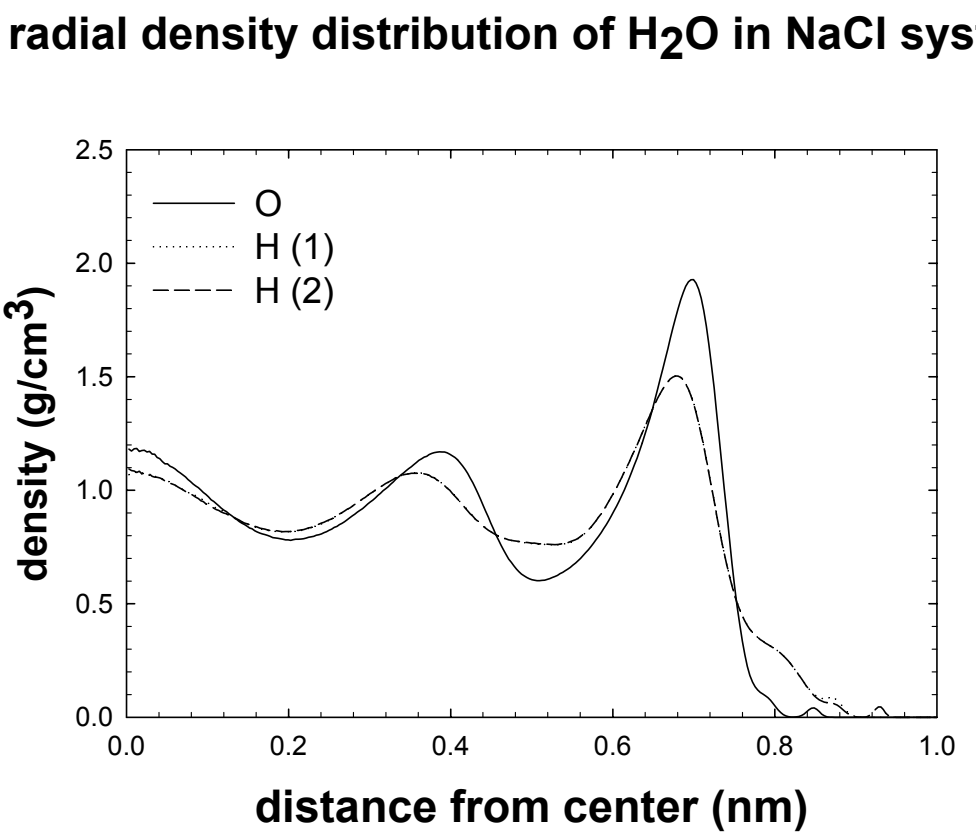

Figure 48: Radial density distribution of oxygen and hydrogen atoms when the radius of silica nanochannel is 1.0 nm (NaCl). The system consists of 467 water molecules, 6 sodium ions, 2 chloride ions. 4 negative charges are distributed on the wall surface. The channel length is 6.651 nm, while the concentration of chloride ions (0.132/nm^3) and density of charges on the wall (0.0957/nm^2) are kept constant.

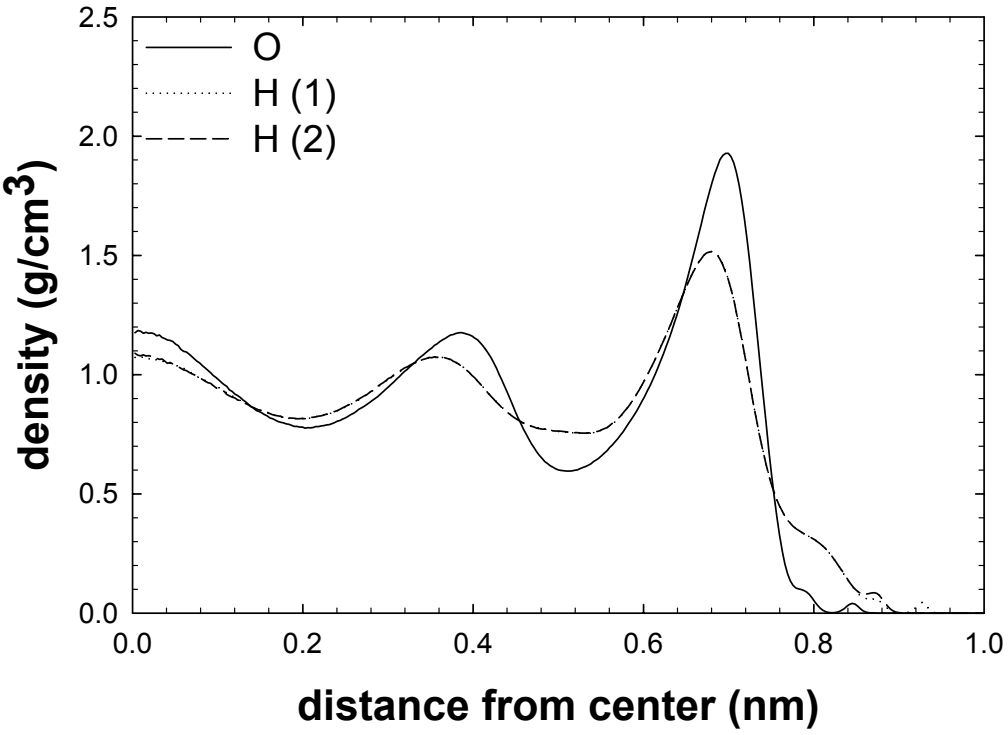

Figure 49: Radial density distribution of oxygen and hydrogen atoms when the radius of silica nanochannel is 1.0 nm (KCl). The system consists of 467 water molecules, 6 sodium ions, 2 chloride ions. 4 negative charges are distributed on the wall surface. The channel length is 6.651 nm, while the concentration of chloride ions (0.132/nm^3) and density of charges on the wall (0.0957/nm^2) are kept constant.

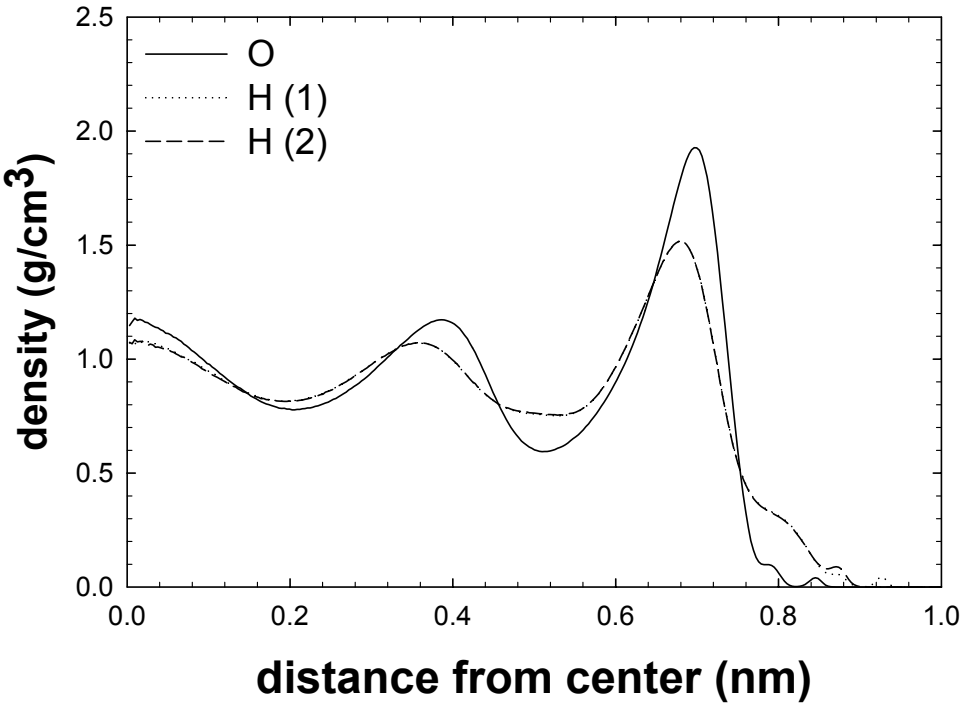

Figure 50: Radial density distribution of oxygen and hydrogen atoms when the radius of silica nanochannel is 1.0 nm (RbCl). The system consists of 467 water molecules, 6 sodium ions, 2 chloride ions. 4 negative charges are distributed on the wall surface. The channel length is 6.651 nm, while the concentration of chloride ions (0.132/nm^3) and density of charges on the wall (0.0957/nm^2) are kept constant.

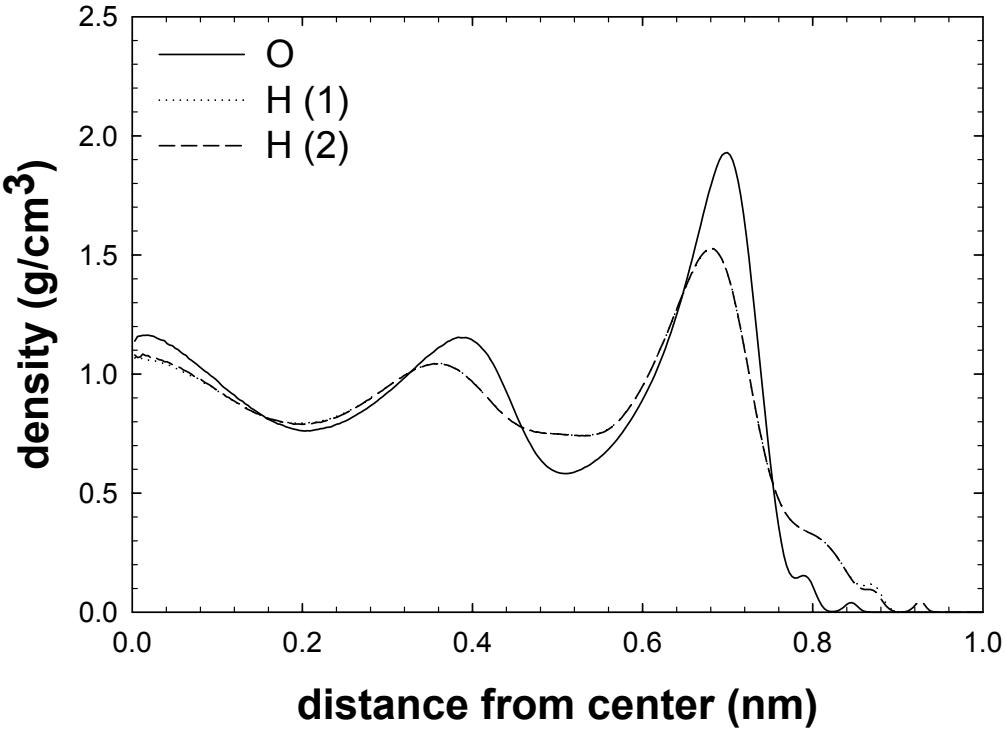

Figure 51: Radial density distribution of oxygen and hydrogen atoms when the radius of silica nanochannel is 1.0 nm (CsCl). The system consists of 467 water molecules, 6 sodium ions, 2 chloride ions. 4 negative charges are distributed on the wall surface. The channel length is 6.651 nm, while the concentration of chloride ions ($0.132/nm^3$) and density of charges on the wall ($0.0957/nm^2$) are kept constant.

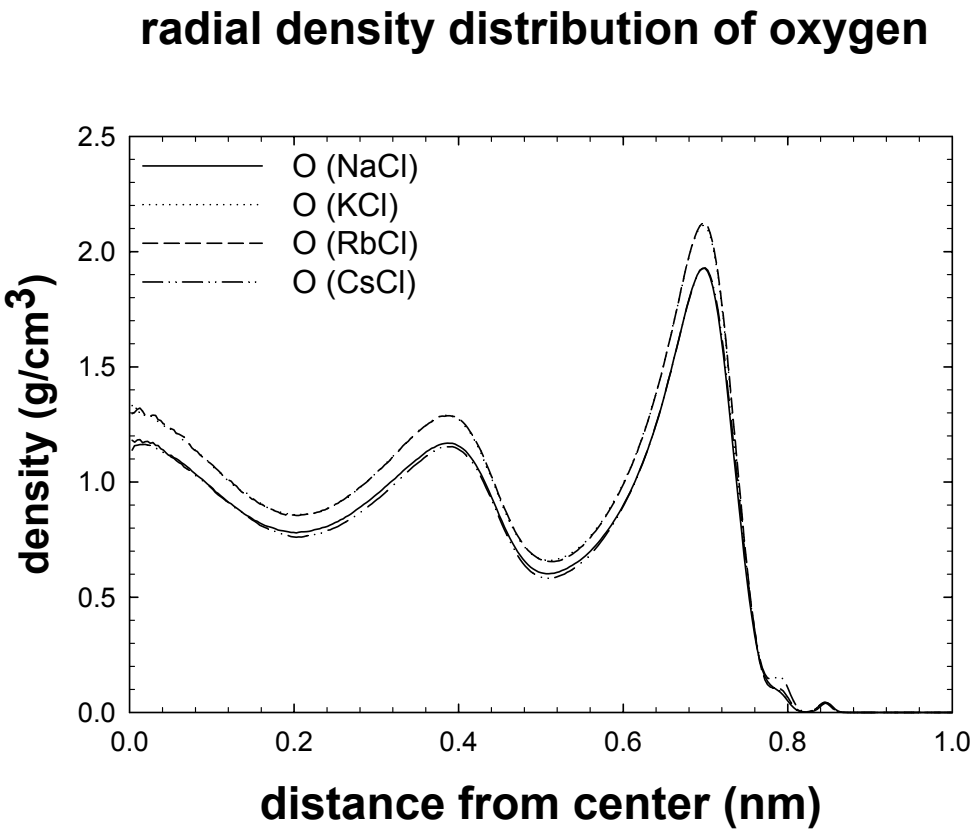

Figure 52: Radial density distribution of oxygen atoms in NaCl, KCl, RbCl, CsCl aqueous solutions respectively. For every aqueous system, it consists of 467 water molecules, 6 cations, 2 chloride ions in the same size nanochannel with 1.0 nm radius and 6.651 nm cell length in the axial direction. 4 negative charges are distributed on the center of wall atoms nearest these charges. The concentration of anions ($0.132/nm^3$) and density of charges on the wall ($0.0957/nm^2$) are kept constant.

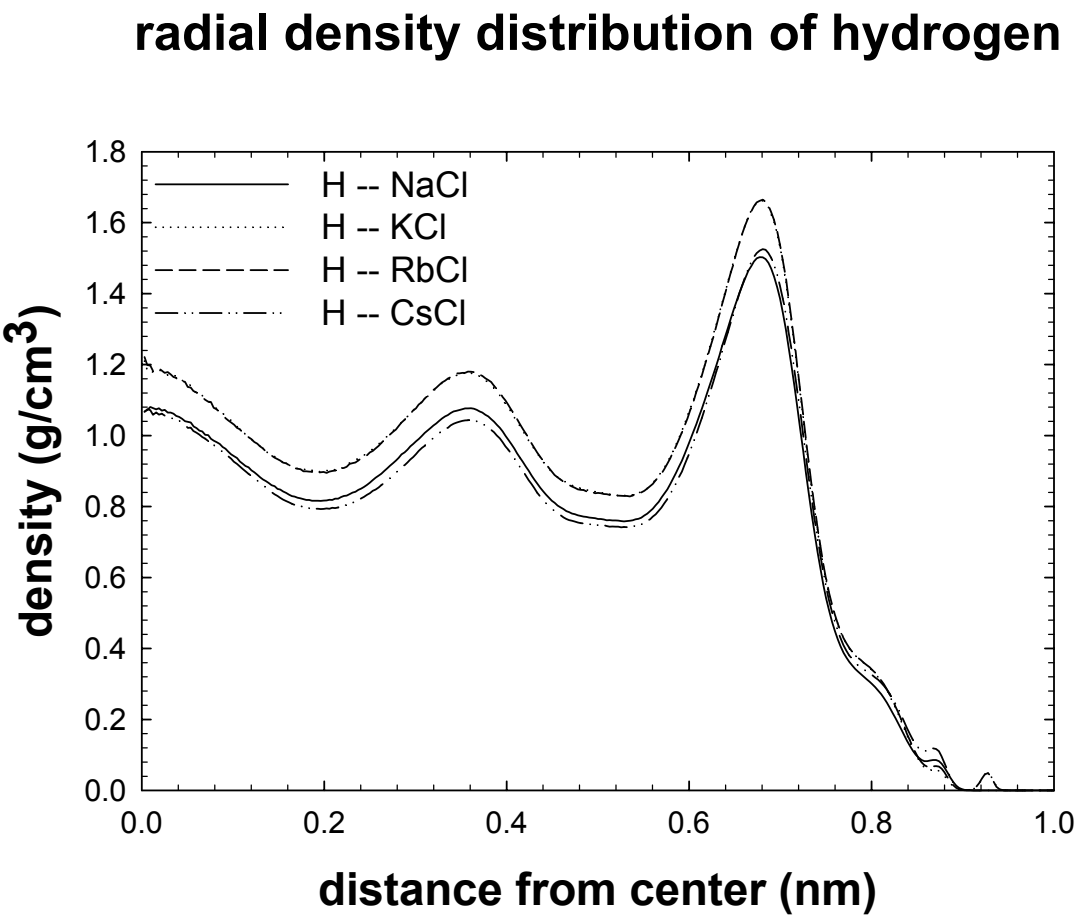

Figure 53: Radial density distribution of hydrogen atoms in NaCl, KCl, RbCl, CsCl aqueous solutions respectively. For every aqueous system, it consists of 467 water molecules, 6 cations, 2 chloride ions in the same size nanochannel with 1.0 nm radius and 6.651 nm cell length in the axial direction. 4 negative charges are distributed on the center of wall atoms nearest these charges. The concentration of anions ($0.132/nm^3$) and density of charges on the wall ($0.0957/nm^2$) are kept constant.

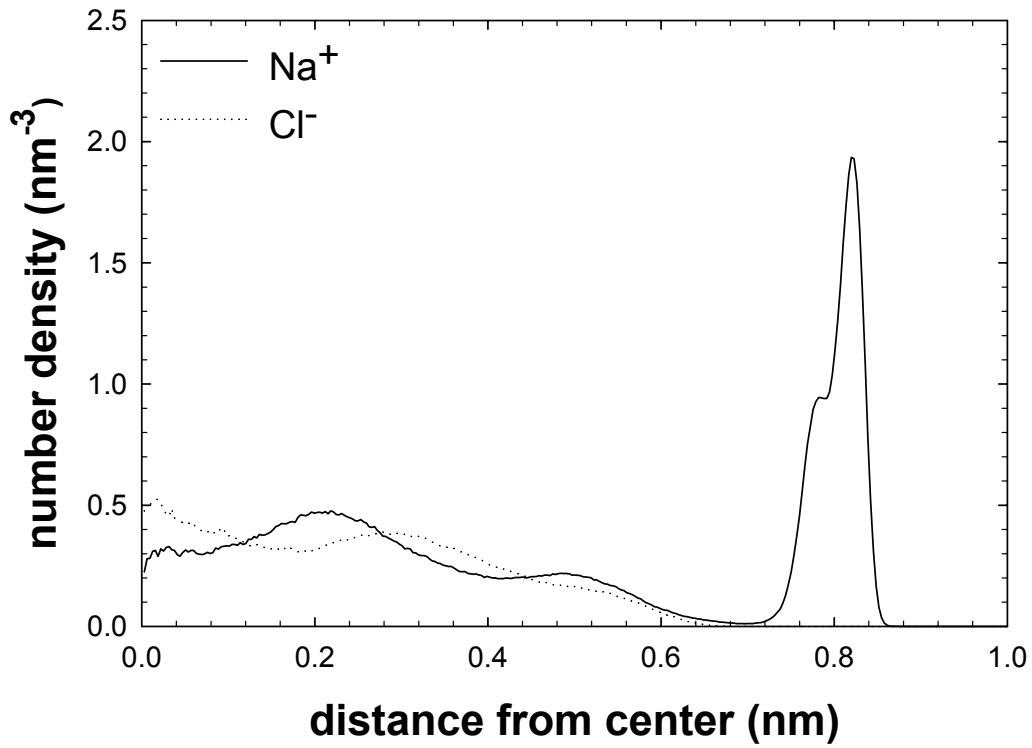

Figure 54: Radial density distribution of sodium and chloride ions when the radius of silica nanochannel is 1.0 nm. The system consists of 467 water molecules, 6 sodium ions, 2 chloride ions. 4 negative charges are distributed on the wall surface. The channel length is 6.651 nm, while the concentration of chloride ions ($0.132/nm^3$) and density of charges on the wall ($0.0957/nm^2$) are kept constant.

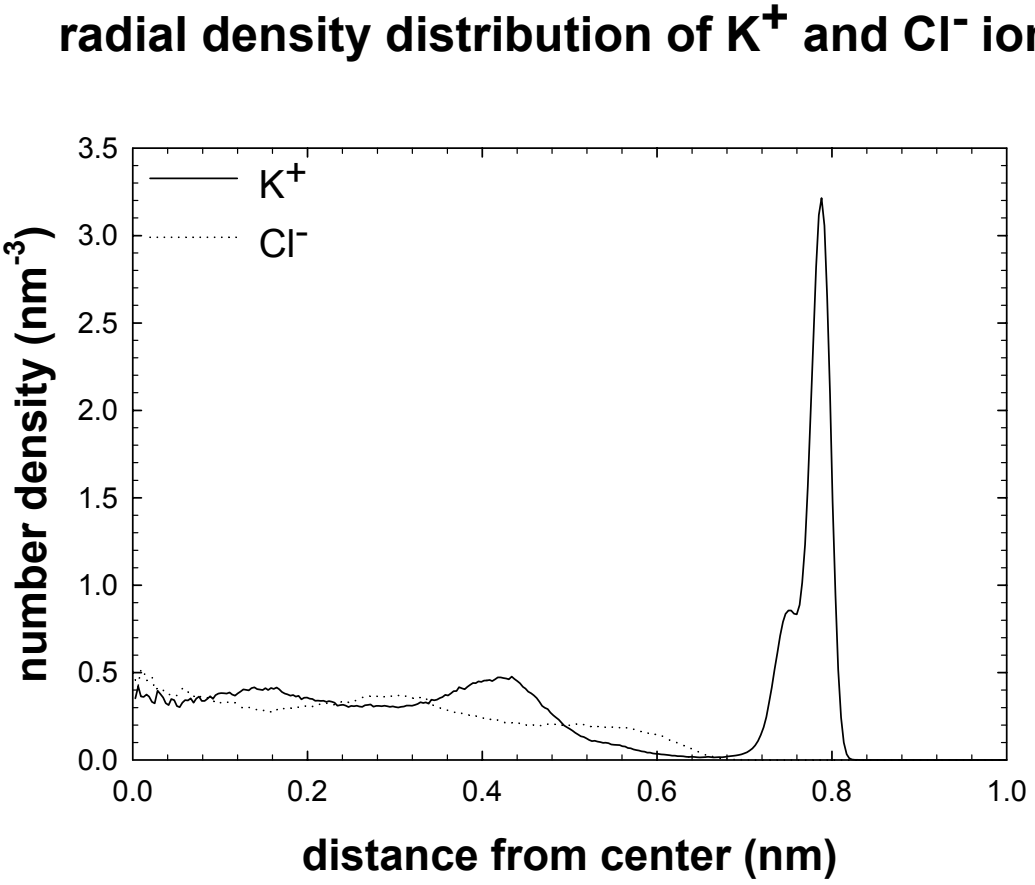

Figure 55: Radial density distribution of potassium and chloride ions when the radius of silica nanochannel is 1.0 nm. The system consists of 467 water molecules, 6 sodium ions, 2 chloride ions. 4 negative charges are distributed on the wall surface. The channel length is 6.651 nm, while the concentration of chloride ions ($0.132/nm^3$) and density of charges on the wall ($0.0957/nm^2$) are kept constant.

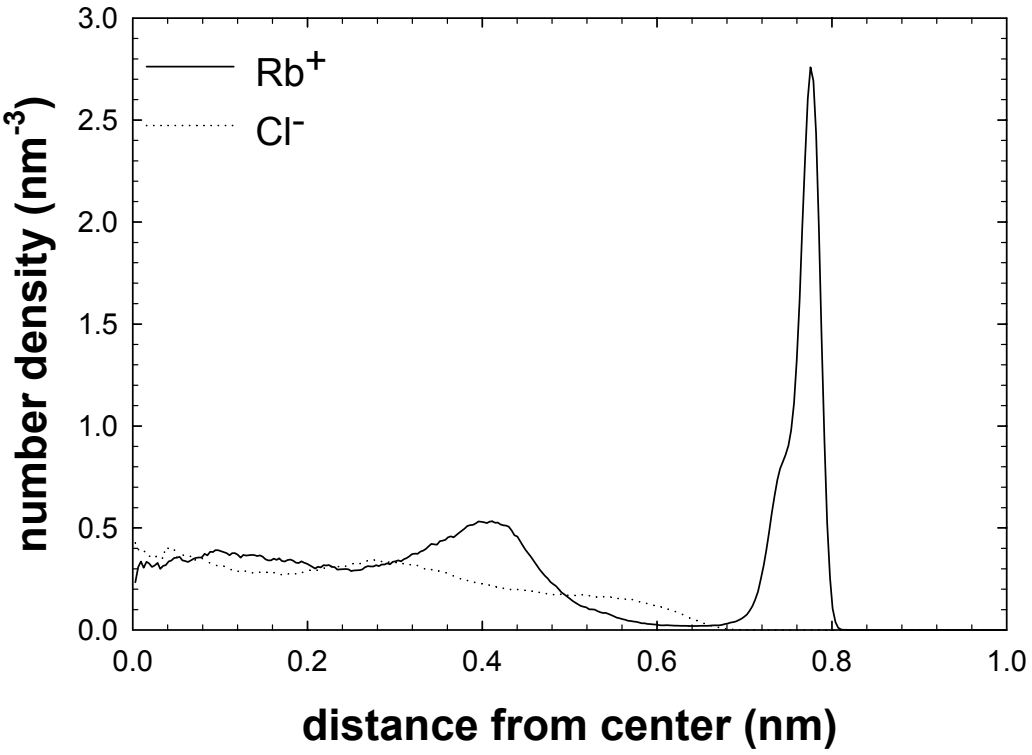

Figure 56: Radial density distribution of rubidium and chloride ions when the radius of silica nanochannel is 1.0 nm. The system consists of 467 water molecules, 6 sodium ions, 2 chloride ions. 4 negative charges are distributed on the wall surface. The channel length is 6.651 nm, while the concentration of chloride ions ($0.132/nm^3$) and density of charges on the wall ($0.0957/nm^2$) are kept constant.

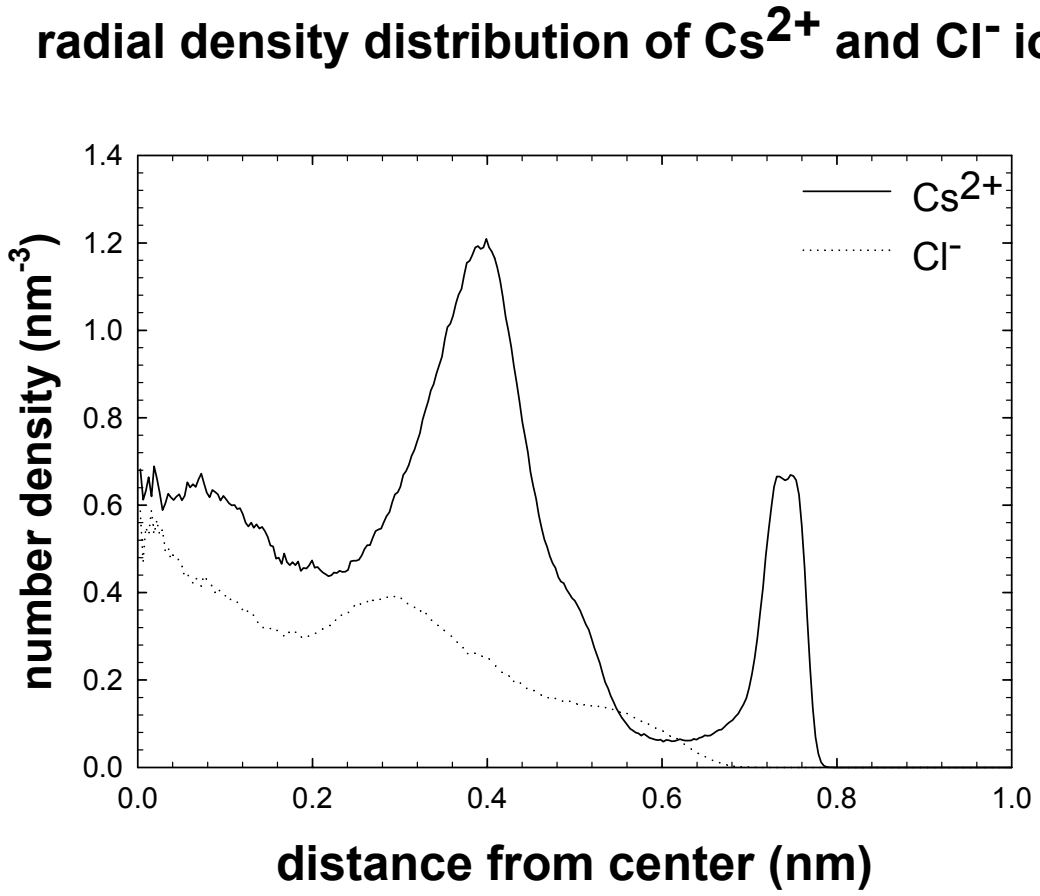

Figure 57: Radial density distribution of cesium and chloride ions when the radius of silica nanochannel is 1.0 nm. The system consists of 467 water molecules, 6 sodium ions, 2 chloride ions. 4 negative charges are distributed on the wall surface. The channel length is 6.651 nm, while the concentration of chloride ions (0.132/nm^3) and density of charges on the wall (0.0957/nm^2) are kept constant.

wall; the second layer with less probability density is 0.61 nm from the wall, and in the center of nanochannel there is a distinctive third peak. There are also very small peaks adjacent to the wall, similarly to $CaCl_2$ aqueous systems, indicating again by sitting in the valleys between wall atoms, water molecules are subject to both electrostatic and L-J interactions from the wall charges.

As shown in Figure 58, the density distribution of cations is worthy of notice. Although there is a distinct sharp peak close to the wall for every cation's distribution, which is the adsorption of cations to the wall charges, the position of adsorption peak varies with the size of cations. The smaller of the cation's size, the closer of the adsorption peak to the wall. Due to the smaller-nearest principle, when the size of ions is smaller, the electrostatic attraction between cations and charges is stronger, thus the adsorption peak is closer to the wall. Within these four cations, sodium has the minimum diameter and it is closest to the wall. In contrast, cesium adsorption peak is the farthest from the wall with maximum size. The data are shown in Table 18. The radial distributions of chloride are similar for every system, as shown in Figure 59.

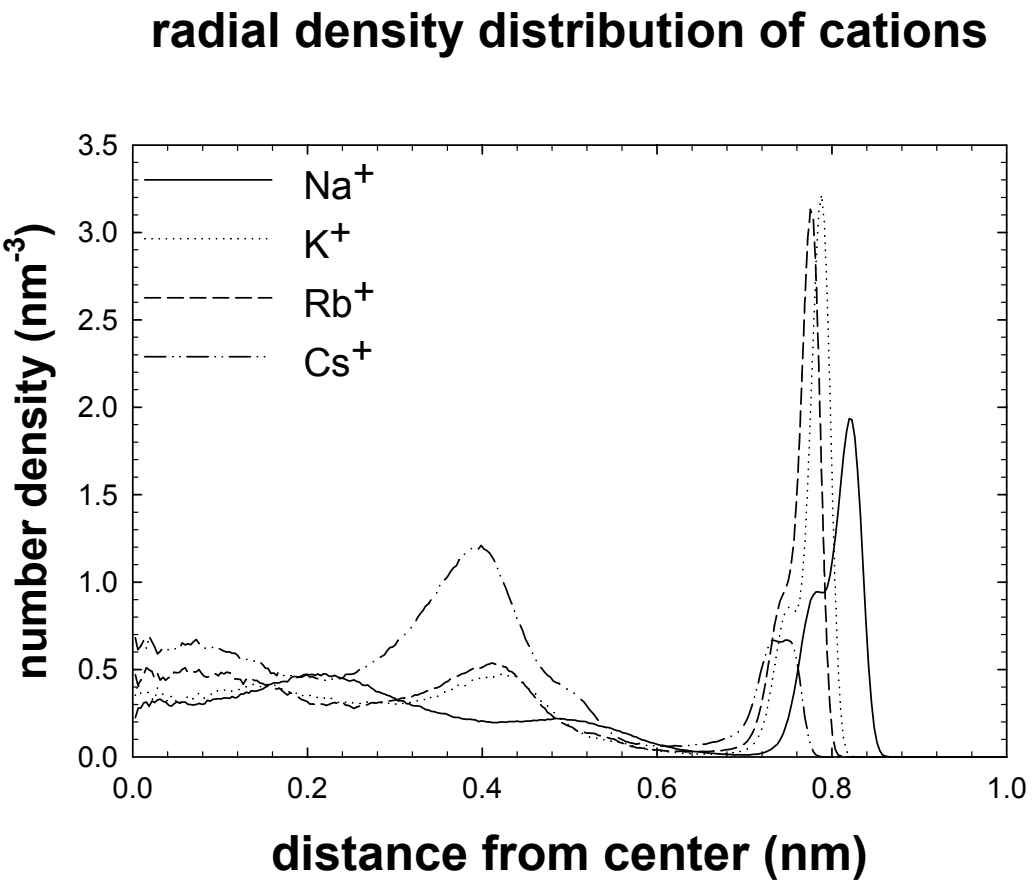

Figure 58: Radial density distribution of cations in NaCl, KCl, RbCl, CsCl aqueous solutions respectively. For every aqueous system, it consists of 467 water molecules, 6 cations, 2 chloride ions in the same size nanochannel with 1.0 nm radius and 6.651 nm cell length in the axial direction. 4 negative charges are distributed on the center of wall atoms nearest these charges. The concentration of anions ($0.132/nm^3$) and density of charges on the wall ($0.0957/nm^2$) are kept constant.

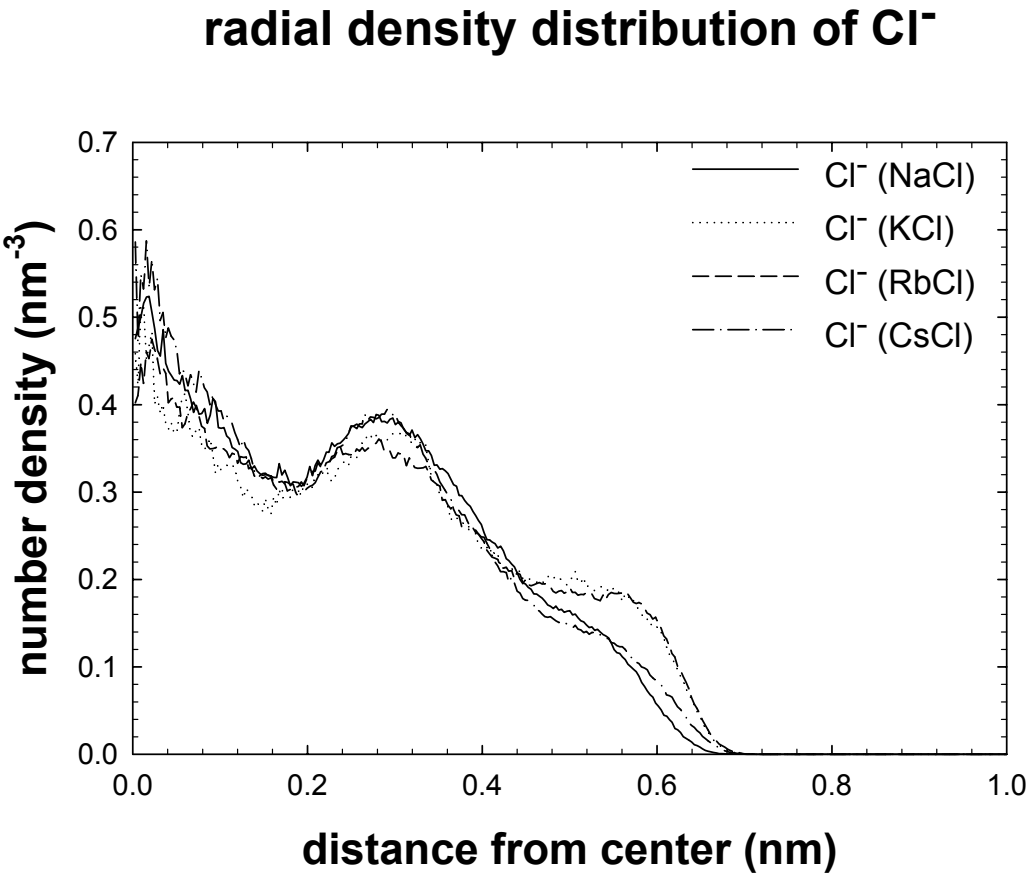

Figure 59: Radial density distribution of chloride ions in NaCl, KCl, RbCl, CsCl aqueous solutions respectively. For every aqueous system, it consists of 467 water molecules, 6 cations, 2 chloride ions in the same size nanochannel with 1.0 nm radius and 6.651 nm cell length in the axial direction. 4 negative charges are distributed on the center of wall atoms nearest these charges. The concentration of anions ($0.132/nm^3$) and density of charges on the wall ($0.0957/nm^2$) are kept constant.

Table 18 Distance between adsorption peak and the wall

for different sizes of cations (Na^+, K^+, Cs^+, Rb^+)

cations	diameter (nm)	the distance adsorption peak from the wall(nm)
Na^+	0.273	0.18
K^+	0.3334	0.21
Rb^+	0.353	0.23
Cs^+	0.3886	0.26

The self-diffusivities of water molecules, cations, and chloride all have an excellent fit of MSD vs. the observation time, as shown in Figures 60 to 62. The self-diffusivities for water, sodium ions, and anions are listed in Table 19. These values vary a little but in a certain range. Different cation sizes seem to have no effect on the determination of axial self-diffusivity. Compared with the published self-diffusivity value of Na^+, K^+, Rb^+, and Cs^+ at 298K in uncharged bulk water systems[36], here the self-diffusivity of Na^+, K^+, Rb^+, and Cs^+ is decreased by 69.51%, 76.58%, 78.01%, 49.85 % respectively. Because there are 4 negative charges distributed on the wall surfaces, monovalent cations are attracted to the wall charges and do not move freely (4 ions are fixed to the wall charges and 2 ions move freely), restraining the movement of unadsorbed cations.

Table 19: Self-diffusivities along axial direction of nanochannel in NaCl, KCl, RbCl, CsCl aqueous electrolytes systems

Systems	H_2O (1×10^{-5} cm^2/s)	Cations (1×10^{-5} cm^2/s)	Cl^- (1×10^{-5} cm^2/s)
NaCl	3.124	0.372	1.058
KCl	3.165	0.473	0.9187
RbCl	3.165	0.464	1.107
CsCl	3.160	1.003	1.116

Note: Standard deviations for self-diffusivities must be achieved by repeating simulations. So they are not included in this simulation.

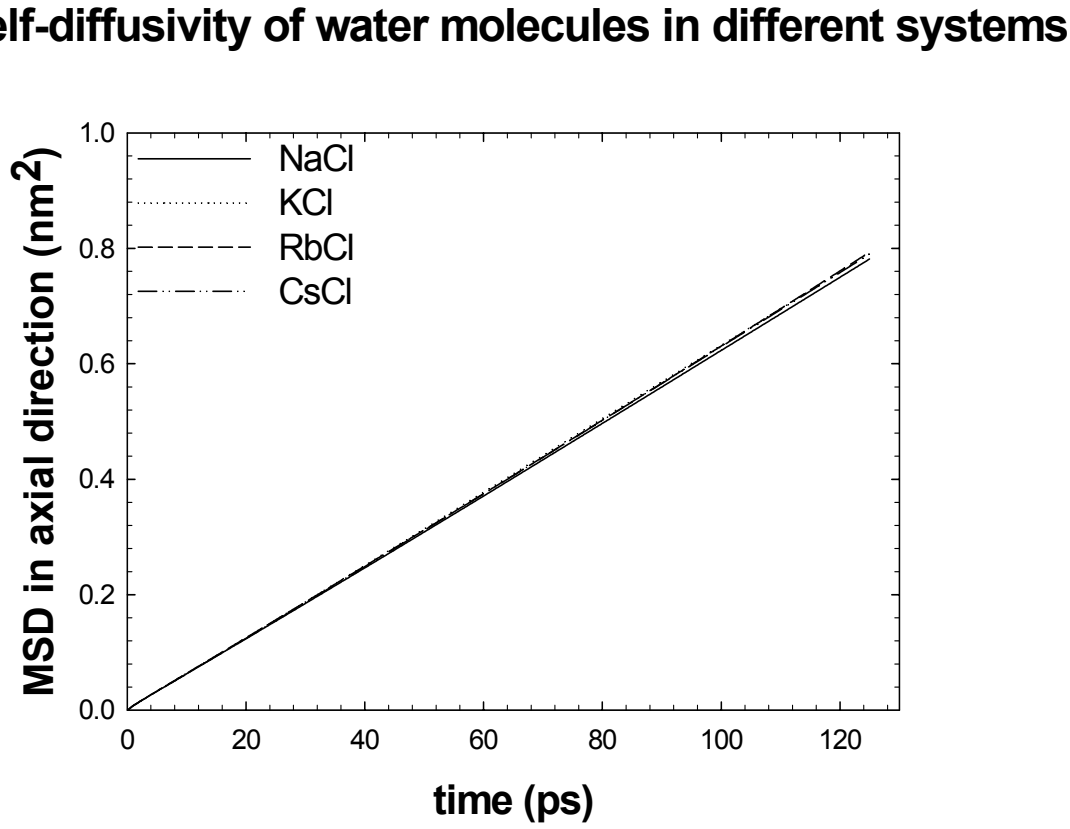

Figure 60: The mean square displacement (MSD) of water molecules versus time within silica nanochannel in NaCl, KCl, RbCl, CsCl aqueous solutions respectively. For every aqueous system, it consists of 467 water molecules, 6 cations, 2 chloride ions in the same size nanochannel with 1.0 nm radius and 6.651 nm cell length in the axial direction. 4 negative charges are distributed on the center of wall atoms nearest these charges. The concentration of anions ($0.132/nm^3$) and density of charges on the wall ($0.0957/nm^2$) are kept constant.

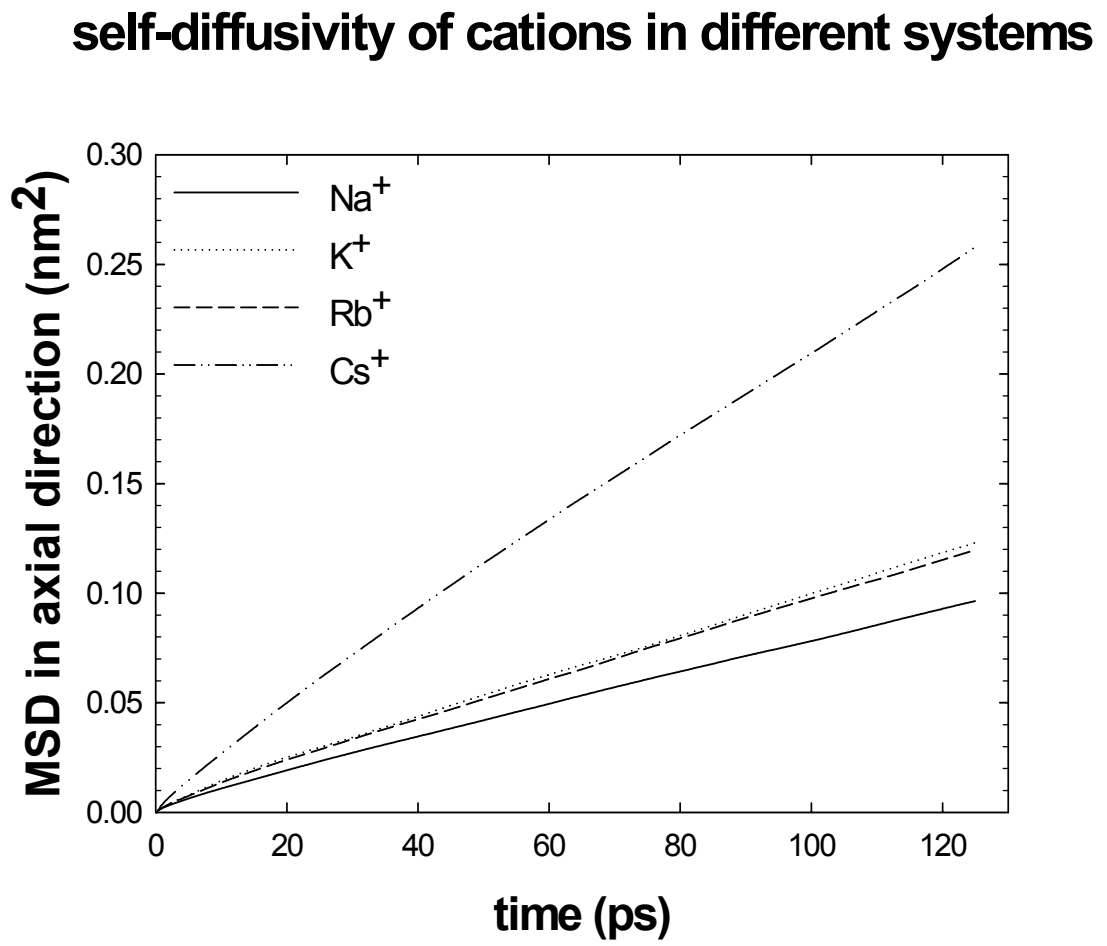

Figure 61:The mean square displacement (MSD) of cations versus time within silica nanochannel in NaCl, KCl, RbCl, CsCl aqueous solutions respectively. For every aqueous system, it consists of 467 water molecules, 6 cations, 2 chloride ions in the same size nanochannel with 1.0 nm radius and 6.651 nm cell length in the axial direction. 4 negative charges are distributed on the center of wall atoms nearest these charges. The concentration of anions ($0.132/nm^3$) and density of charges on the wall ($0.0957/nm^2$) are kept constant.

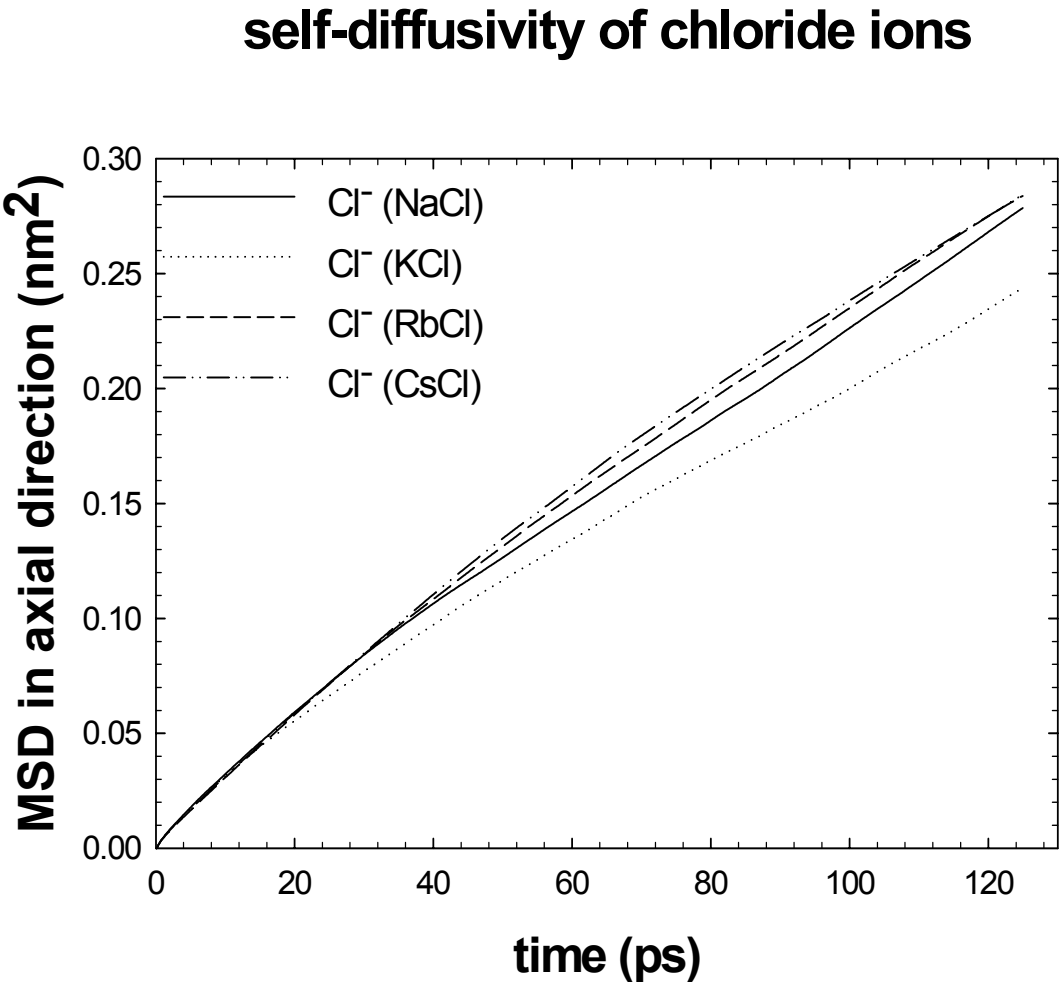

Figure 62: The mean square displacement (MSD) of chloride ions versus time within silica nanochannel in NaCl, KCl, RbCl, CsCl aqueous solutions respectively. For every aqueous system, it consists of 467 water molecules, 6 cations, 2 chloride ions in the same size nanochannel with 1.0 nm radius and 6.651 nm cell length in the axial direction. 4 negative charges are distributed on the center of wall atoms nearest these charges. The concentration of anions ($0.132/nm^3$) and density of charges on the wall ($0.0957/nm^2$) are kept constant.

4. Conclusions

This thesis helps improve our understanding of aqueous electrolytes in nanochannel. The properties of density distribution and self-diffusitivity of $CaCl_2$, NaF, NaCl, NaBr, NaI, KCl, RbCl, CsCl have been investigated. Since ions are used to buffer and disentangle DNA, and a charged wall enable ssDNA to move into nanochannel electrokinetically, therefore, this research advances progress toward nanochannel method for ssDNA sequencing.

For $CaCl_2$ aqueous electrolytes, in nanochannels with radii ranging from 0.9nm to 1.5nm, water molecules exhibit density oscillations within 0.35 nm from the wall and become bulk-like near the center. Water molecules form different layers. In general, with the radius increasing, the fluids' self-diffusivities tend to increase too. However, when the increment of radius is not large enough to hold one new layer of molecules, the self-diffusivities tend to decrease. The small peaks closest to the wall seen in the density distribution of water molecules, are attributable to the interactions between hydrogen atoms and charges set on the wall atoms, when water sits in the valleys between wall atoms.

Except near surface charges, ions seem to avoid the region near the wall, which is preferentially occupied by orderly layered water molecules. Calcium ions are attracted to the wall charges so that they do not move freely or just vibrate back and forth. For calcium ions, a sharp density peak occurs 0.22 nm from the wall is attributed to the direct adsorption of counter-ions at the charge sites. Another high peak 0.4nm from the wall

shown in some calcium density distributions is attributed to adsorption of hydrated calcium ions. The calcium density distribution displays peaks that coincide with the valleys of the water density distribution. By sitting in the valleys between two peaks of the oxygen distribution, calcium ions increase their hydration number of water molecules and thus are energetically favorable.

The mean square displacement (MSD) of calcium ions is directly proportional to the square root of time. It is not certain whether or not this results are from single-file diffusion, because there is enough spatial room for calcium ions to pass each other in the nanochannel diameter. Subject to the attraction from wall charges, calcium ions diffuse much more slowly than in bulk water at ambient conditions. Water molecules and chloride ions display ordinary diffusion.

Calcium ions attracted to the wall charges present an obstacle inside the nanochannel, retarding the movement of fluids. The self-diffusivities of fluids in a charged nanochannel are smaller than those in an uncharged nanochannel.

For four aqueous solutions [(Na^+ and F^-), (Na^+ and Cl^-), (Na^+ and Br^-), (Na^+ and I^-)], the density distributions of water molecules are very similar. Water molecules form three distinctive layers when radial position varies from the channel center to the area close to the wall. The distinct sharp peak of the sodium ions, which is 0.2 nm from the wall, is the adsorption of sodium ions to the charged sites. Different anion sizes seem to have no

effects on the axial self-diffusivity of water or sodium. The anion self-diffusivity increases slightly with anion size.

For four aqueous solutions [(Na^+ and Cl^-), (K^+ and Cl^-), (Cs^+ and Cl^-), (Rb^+ and Cl^-)], the smaller the cation's size, the closer of the adsorption peak of cations to the wall. Due to the smaller-nearest principle, when the size of ions is smaller, the electrostatic attraction between cations and charges is stronger, thus the adsorption peak is closer to the wall. Different cation sizes seem to have no effect on the determination of axial self-diffusivity.

5 Further Research

The understanding of self-diffusion of Ca^{2+} in a charged nanochannel is still incomplete, because the current simulation has not been running for a long enough period. It is recommended to perform long-time simulation to explore more precisely the behavior of Ca^{2+} in the future.

References

1. Sanger, F. and A.R. Coulson, *Rapid Method for Determining Sequences in DNA by Primed Synthesis with DNA-Polymerase.* Journal of Molecular Biology, 1975. **94**(3): p. 441-&.

2. Maxam, A.M. and W. Gilbert, *New Method for Sequencing DNA.* Proceedings of the National Academy of Sciences of the United States of America, 1977. **74**(2): p. 560-564.

3. Sanger, F., S. Nicklen, and A.R. Coulson, *DNA Sequencing with Chain-Terminating Inhibitors.* Proceedings of the National Academy of Sciences of the United States of America, 1977. **74**(12): p. 5463-5467.

4. Deamer, D.W. and M. Akeson, *Nanopores and nucleic acids: prospects for ultrarapid sequencing.* Trends in Biotechnology, 2000. **18**(4): p. 147-151.

5. Nakane, J.J., M. Akeson, and A. Marziali, *Nanopore sensors for nucleic acid analysis.* Journal of Physics-Condensed Matter, 2003. **15**(32): p. R1365-R1393.

6. Chen, C.M. and E.H. Peng, *Nanopore sequencing of polynucleotides assisted by a rotating electric field.* Applied Physics Letters, 2003. **82**(8): p. 1308-1310.

7. Kasianowicz, J.J., et al., *Characterization of individual polynucleotide molecules using a membrane channel.* Proceedings of the National Academy of Sciences of the United States of America, 1996. **93**(24): p. 13770-13773.

8. Li, J., et al., *Ion-beam sculpting at nanometre length scales.* Nature, 2001. **412**(6843): p. 166-169.

9. Saleh, O.A. and L.L. Sohn, *An artificial nanopore for molecular sensing.* Nano Letters, 2003. **3**(1): p. 37-38.

10. Bokhsti, S.H.e.a. in *computer society bionformatics conference (Los Alamitos, CA: IEEE computer society press)*. 2002.

11. Tegenfeldt, J.O., et al., *Near-field scanner for moving molecules.* Physical Review Letters, 2001. **86**(7): p. 1378-1381.

12. Marti, J. and M.C. Gordillo, *Temperature effects on the static and dynamic properties of liquid water inside nanotubes.* Physical Review E, 2001. **6402**(2): p. -.

13. Brodka, A. and T.W. Zerda, *Properties of liquid acetone in silica pores: Molecular dynamics simulation.* Journal of Chemical Physics, 1996. **104**(16): p. 6319-6326.

14. Lo, W.Y., K.Y. Chan, and K.L. Mok, *Molecular-Dynamics Simulation of Ions in Charged Capillaries.* Journal of Physics-Condensed Matter, 1994. **6**: p. A145-A149.

15. LyndenBell, R.M. and J.C. Rasaiah, *Mobility and solvation of ions in channels.* Journal of Chemical Physics, 1996. **105**(20): p. 9266-9280.

16. Zhou, J.D., *Molecular simulation of aqueous electrolytes in silica nanochannels*, in *Chemical Engineering*. 2002, University of Tennessee: Knoxville.

17. Zhou, J.D., S.T. Cui, and H.D. Cochran, *Molecular simulation of aqueous electrolytes in model silica nanochannels.* Molecular Physics, 2003. **101**(8): p. 1089-1094.

18. Berendsen, H.J.C., J.R. Grigera, and T.P. Straatsma, *The Missing Term in Effective Pair Potentials.* Journal of Physical Chemistry, 1987. **91**(24): p. 6269-6271.

19. Lee, S.H. and P.T. Cummings, *Molecular dynamics simulation of limiting conductances for LiCl, NaBr, and CsBr in supercritical water.* Journal of Chemical Physics, 2000. **112**(2): p. 864-869.

20. Koneshan, S., J.C. Rasaiah, and L.X. Dang, *Computer simulation studies of aqueous solutions at ambient and supercritical conditions using effective pair potential and polarizable potential models for water.* Journal of Chemical Physics, 2001. **114**(17): p. 7544-7555.

21. Tsuneyuki, S., et al., *1st-Principles Interatomic Potential of Silica Applied to Molecular-Dynamics.* Physical Review Letters, 1988. **61**(7): p. 869-872.

22. Feuston, B.P. and S.H. Garofalini, *Empirical 3-Body Potential for Vitreous Silica.* Journal of Chemical Physics, 1988. **89**(9): p. 5818-5824.

23. Vanbeest, B.W.H., G.J. Kramer, and R.A. Vansanten, *Force-Fields for Silicas and Aluminophosphates Based on Abinitio Calculations.* Physical Review Letters, 1990. **64**(16): p. 1955-1958.

24. Steele, W.A., *Physical Interaction of Gases with Crystalline Solids .1. Gas-Solid Energies and Properties of Isolated Adsorbed Atoms.* Surface Science, 1973. **36**(1): p. 317-352.

25. Cui, S.T., *Molecular dynamics study of single-stranded DNA in aqueous solution confined in a nanopore.* Molecular Physics, 2004. **102**(2): p. 139-146.

26. Lai, S.K., et al., *anomalous diffusivity and electric conductivity for low concentration electrolytes in nanopores.* Physical Review E, 2004. **69**(051203).

27. Allen, M.P. and D.J. Tildesley, *Computer Simulation of Liquids*. 1987, Oxford.

28. Berendsen, H.J.C., et al., *Molecular-Dynamics with Coupling to an External Bath.* Journal of Chemical Physics, 1984. **81**(8): p. 3684-3690.

29. Andersen, H.C., *Rattle - a Velocity Version of the Shake Algorithm for Molecular-Dynamics Calculations.* Journal of Computational Physics, 1983. **52**(1): p. 24-34.

30. Cui, S.T. and H.D. Cochran, *Molecular dynamics simulation of interfacial electrolyte behaviors in nanoscale cylindrical pores.* Journal of Chemical Physics, 2002. **117**(12): p. 5850-5854.

31. Keffer, D., A.V. McCormick, and H.T. Davis, *Unidirectional and single-file diffusion in AlPO4-5: Molecular dynamics investigations.* Molecular Physics, 1996. **87**(2): p. 367-387.

32. Sastre, G. and A. Corma, *Ordinary diffusion and single file diffusion in zeolites with monodimensional channels. Benzene and n-butane in ITQ-4 and L zeolites.* Topics in Catalysis, 2003. **24**(1-4): p. 7-12.

33. Mon, K.K. and J.K. Percus, *Self-diffusion of fluids in narrow cylindrical pores.* Journal of Chemical Physics, 2002. **117**(5): p. 2289-2292.

34. Crozier, P.S., et al., *Model channel ion currents in NaCl-extended simple point charge water solution with applied-field molecular dynamics.* Biophysical Journal, 2001. **81**(6): p. 3077-3089.

35. Dang, L.X. and D.E. Smith, *Mean Force Potential for the Calcium-Chloride Ion-Pair in Water - Comment.* Journal of Chemical Physics, 1995. **102**(8): p. 3483-3484.

36. Lee, S.H. and J.C. Rasaiah, *Molecular dynamics simulation of ion mobility .2. Alkali metal and halide ions using the SPC/E model for water at 25 degrees C.* Journal of Physical Chemistry, 1996. **100**(4): p. 1420-1425.

Appendices

Appendix 1.

FORTRAN code to remove the charges to the center of wall atoms nearest charges

```
      subroutine nearest
      include 'water.inc'
      integer jatm_min,i,j
      double precision dist(20,1000), distan(20,1000), dmin, dmin_old

      open (7,file='nearest.fmt', form='formatted', status='unknown')

      do 120 i=1,nqsurf
      dmin = cube
      dmin_old = cube

      do 150 j=1, nsfmol
      dist(i,j)=(xq(i)-xsf(j))**2+(yq(i)-ysf(j))**2+(zq(i)-zsf(j))**2
      distan(i,j) = sqrt(dist(i,j))

      dmin = min(distan(i,j),dmin)

      if (dmin .lt. dmin_old) then
      jatm_min = j
      dmin_old = dmin
      endif
150   continue


      xq(i) = xsf(jatm_min)
      yq(i) = ysf(jatm_min)
      zq(i) = zsf(jatm_min)
      write(7,*) 'for i=',i,'j=',jatm_min
      write(7,*) 'xsf=', xsf(jatm_min)
      write(7,*) 'ysf=', ysf(jatm_min)
      write(7,*) 'zsf=', zsf(jatm_min)
      write(7,*) 'xq =', xq(i)
      write(7,*) 'yq =', yq(i)
      write(7,*) 'zq =', zq(i)

120   continue
      close(7)

      return
      end
```

Appendix 2

FORTRAN code to track the activities of calcium ions in aqueous electrolytes solution system

```
      subroutine location

      include 'water.inc'

      integer i,M,im

      if (kb.gt.5030000) then
      if (mod(kb,50).eq.0) then
      M = M +1
      if (M.gt.401) stop

      im = 1

      do 20 i=1,natom

      write(6,100)im,M,x0(i,im),y0(i,im),z0(i,im)
100   format(1x,i6,1x,i6,3(1x,f10.4))

20    continue

      endif
      endif
      return
      end
```

Appendix 3.

FORTRAN code to construct the spatial configuration between charge, calcium ion nearest charge and oxygen atoms within $1.2\sigma_{Ca\text{-}Ca}$ distance with calcium ion

```
      subroutine cawater
      include 'water.inc'

      integer i,j,jm,N,k,jatm_min
      double precision rx,ry,rz,rsq,rxx,ryy,rzz,rsqq
      double precision dmin, dmin_old,rsqx
      double precision rxl,ryl,rzl,rsql,interim,ang

      N= N+1

      open(unit=7,file='cawater.fmt',form='formatted',status='unknown')
      rewind (unit=7)

      do 20 i=1,npion

      do 40 jm=1,nm
      rx = x0(1,i) - xo(1,jm)
      ry = y0(1,i) - yo(1,jm)
      rz = z0(1,i) - zo(1,jm)
      rz = rz - cubez*nint(rz/cubez)
      rsq = rx*rx + ry*ry + rz*rz

      if ((sqrt(rsq) .lt. 1.0973).and.(N .eq. 1))  then

      write (7,200) i, jm

200   format(///,1x, 'ca2+=', i6,
     &   /, 1x, 'water=', i6)

      write (7,300) x0(1,i),y0(1,i),z0(1,i),xo(1,jm),yo(1,jm),
     &          zo(1,jm), sqrt(rsq)

300   format ( 1x, 'ca(x)= ', f14.4, 8x, 'ca(y)= ', f14.4,
     &      /, 1x, 'ca(z)= ', f14.4, 8x, 'water(x)= ', f14.4,
     &      /, 1x, 'water(y)= ', f14.4, 5x, 'water(z)= ', f14.4
     &      //, 1x, 'dis_Ca_O= ', f14.4)

      write(7,270)
270   format()

      dmin = cube
      dmin_old = cube

      do 50 k=1, nqsurf
      rxx = xq(k) - xo(1,jm)
```

```
      ryy = yq(k) - yo(1,jm)
      rzz = zq(k) - zo(1,jm)
      rzz = rzz - cubez*nint(rzz/cubez)
      rsqq = rxx*rxx + ryy*ryy + rzz*rzz
      rsqx = sqrt(rsqq)


      dmin = min(dmin, rsqx)

      if (dmin .lt. dmin_old) then

      jatm_min = k
      dmin_old = dmin

      endif

50    continue


      write (7,400) dmin, jatm_min
400   format(1x, 'min_dis_O_charge=', f14.4,
     &    /,1x, 'this charge is #', i6)

      write (7,450) xq(jatm_min), yq(jatm_min), zq(jatm_min)

450   format(/,1x,'charge(x)= ',f14.4,
     &     /,1x,'charge(y)= ',f14.4,
     &     /,1x,'charge(z)= ',f14.4)


      rxl = x0(1,i) - xq(jatm_min)
      ryl = y0(1,i) - yq(jatm_min)
      rzl = z0(1,i) - zq(jatm_min)
      rsql = rxl*rxl + ryl*ryl + rzl*rzl
      write(7,500) sqrt(rsql)
500   format(/,1x,'dis_ca_charge=', f14.4)

      interim = dmin*dmin + (sqrt(rsql))*(sqrt(rsql))
     &        - (sqrt(rsq))*(sqrt(rsq))
      interim = interim/(2*dmin*sqrt(rsql))
      ang = acos(interim)
      ang = 180*ang/pi


      write (7,510) ang
```

```
510     format(/,1x,'angle_O_charge_ca=', f14.4,1x,'degree')

        endif

40      continue

20      continue
        close (unit=7)
        return

        end
```

Appendix 4.

FORTRAN code to construct three dimensions and two dimensions profiles between calcium ions and wall charges

```
      subroutine  dis3D
      include 'water.inc'

      integer i, j, jm, ir

      double precision grfac, smpfac, denfac, rsq, rx, ry, rz


      do 10 i =1, nqsurf
      do 20 j =1, natom
      do 30 jm =1, npion
      rx = xq(i) - x0(j,jm)
      ry = yq(i) - y0(j,jm)
      rz = zq(i) -  z0(j,jm)
      rz = rz - cubez* nint(rz/cubez)
      rsq =  rx*rx + ry*ry + rz*rz
      ir = nint(sqrt(rsq)*100) + 1
      if ( ir .le. maxcnt ) then
      grsion(1, j, ir) =  grsion(1, j, ir) + 1.0d0
      endif
30    continue
20    continue
10    continue


      do 15 i =1, nqsurf
      do 25 j =1, natom
      do 35 jm =1, npion
      rx = xq(i) - x0(j,jm)
      ry = yq(i) - y0(j,jm)
      rsq =  rx*rx + ry*ry
      ir = nint(sqrt(rsq)*100) + 1
      if ( ir .le. maxcnt ) then
      grsion(2, j, ir) =  grsion(2, j, ir) + 1.0d0
      endif
35    continue
25    continue
15    continue

      igcnt = igcnt + 1

      if (mod(kb, kproc) .eq. 0) then
      open (unit=7,file='dis3D.fmt',form='formatted',status='unknown')
      rewind (unit=7)
```

```
      do 40 ir =1, maxcnt
      smpfac = float(igcnt)
      denfac = cubez*pi*0.01**2
      denfac = denfac * (ir**2 - (ir-1)**2)
      grfac = smpfac*denfac

      write(7,100) ir, grsion (1,1,ir), grsion (1,1,ir)/grfac,
     &             grsion (2,1,ir), grsion (2,1,ir)/grfac
40    continue
      close (unit=7)
      endif
100   format(1x, i6, 4(1x, f10.4))
      return
      end
```

Vita

Lingchen Liao was born in Nanjing, Jiangsu Province, China on July 1978. She joined the department of biochemical engineering at Nanjing University of Chemical Technology where she received her Bachelor degree in biochemical engineering in 2000. Subsequently, she studied in the Master program at the same department for two years. In August 2002, she pursued studies in the Department of Chemical Engineering at the University of Tennessee, Knoxville. She has served as a graduate research assistant at Oak Ridge National Laboratory, TN (ORNL). She gained her Master of Science degree in Chemical Engineering with Minor degree in Statistics in August 2004.